THE PROCEEDINGS OF
THE PHYSICAL SOCIETY

Section B

Vol. 65, Part 9 1 September 1952 No. 393 B

The Load Dependence of Rubber Friction

By A. SCHALLAMACH

The British Rubber Producers' Research Association, Welwyn Garden City, Herts.

MS. received 8th May 1952

ABSTRACT. It is shown experimentally that the load dependence of rubber friction can be explained as being due to the load dependence of the true area of contact between rubber and track if the surface asperities of the rubber are assumed to be hemispherical.

§1. INTRODUCTION

It has been known for some time that the friction of rubber does not obey the classical laws of solid friction, but it appears that only two investigations have been reported in the literature in which this subject was treated systematically. Roth, Driscoll and Holt (1942), working with rubber compounds of the tyre tread type, investigated the velocity dependence, and Thirion (1946), working mainly with non-loaded vulcanizates of rubber, studied the influence of the normal load on rubber friction. The results may be summarized by saying that the coefficient of rubber friction on glass (i) increases with increasing velocity, and (ii) decreases with increasing normal load.

In this paper, we shall present experimental evidence that the load dependence of rubber friction can be satisfactorily explained by the assumption that the frictional force is proportional to the true area of contact between rubber and track.

§2. THE AREA OF CONTACT

(i) *Theoretical*

In the case of ordinary solids (Bowden and Tabor 1950), the irregularities of the surfaces make the true area of contact between contiguous bodies smaller than the apparent area where they touch. The same assumption will be made with regard to the true area of contact between rubber and a hard track which is, however, assumed to be ideally plane. The specimen will then be supported on its surface asperities which will be increasingly compressed with increasing load, and the accompanying squeezing out of the asperities on the track will increase the true area of contact. We shall deduce the load dependence of the true area of contact by assuming the surface asperities to be hemispherical.

Let each hemisphere cover an area A of the base, and let its true area of contact under the load W be a. Since the elastic behaviour of rubber at small deformations can be adequately described in terms of a single modulus M, we can write, from dimensional considerations, $a/A=f(W/MA)$ in order to have dimensionless quantities on both sides of the equation. That is to say, the ratio a/A depends only on the pressure W/A; if furthermore the number of hemispheres per unit area is inversely proportional to A, the total area of contact contributed by all the hemispheres is independent of their size and depends only on the normal load. It will be seen therefore that the relation between the area of contact and the normal load can be found experimentally by carrying out model experiments with hemispheres of a convenient size.

(ii) *Experimental*

The hemispheres employed by us for this purpose had a diameter of 3·8 cm; they were compressed with a transparent plate which had a scale engraved on it for the measurement of the diameter of the circle of contact.

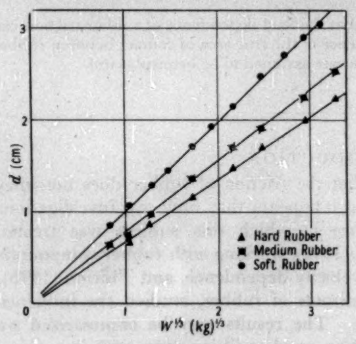

Fig. 1. Diameter of the circle of contact d plotted against $W^{1/3}$.

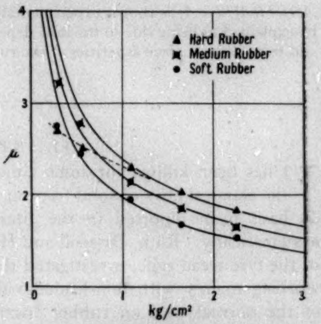

Fig. 3. Coefficient of friction μ plotted against normal apparent pressure. Full lines, theoretical curves calculated as: hard rubber, $2{\cdot}39p^{-1/3}$; medium rubber, $2{\cdot}20p^{-1/3}$; soft rubber, $1{\cdot}90p^{-1/3}$. Dotted line, experimental points for the hard rubber.

We experimented with three different unloaded vulcanizates of natural rubber compounded to give samples of different hardness, and we shall refer to them briefly as hard, medium and soft rubbers. Details of the compounding formulae and conditions of cure are given in the Appendix. Following technological convention, we specify the hardness of the rubbers by the value of the stress, referred to the original cross section, necessary to elongate a test piece by 300% and call this quantity M_{300}. The values of M_{300} were 50, 21, 6·4 kg/cm² for hard, medium and soft rubber respectively.

The results of the model experiments are shown in fig. 1 in which the diameter of the circle of contact d is plotted against the cube root of the load W. It will be seen that the graphs of fig. 1 are straight lines so that we have the empirical result

$$d \propto W^{1/3}. \qquad \ldots\ldots(1)$$

It will be remembered that in classical elasticity theory Hertz's formula for the *small* deformation of a soft sphere by a hard plane is given by $d = 2{\cdot}2(Wr/2E)^{1/3}$ where r is the radius, and E is Young's modulus of the sphere. It is noteworthy that an equation of this form should still hold in the case of the large deformations encountered here.

§ 3. THE COEFFICIENT OF FRICTION

If the area of contact is given as a function of the load W and if, according to our assumption, the frictional force is proportional to it, then the coefficient of friction μ is, by definition

$$\mu = c'a/W, \qquad \ldots\ldots(2)$$

where c' is an unknown factor. Taking into account the results of fig. 1 we substitute eqn. (1) in eqn. (2), introduce a new factor c, and have

$$\mu = cW^{-1/3}, \qquad \ldots\ldots(3)$$

where c has to be determined by experiment for any one velocity.

The velocity dependence of rubber friction makes it very difficult to measure the static coefficient of friction, for it is almost impossible to determine the exact value of the tangential stress under which the sample begins to move. We decided therefore to measure the dynamic coefficient of friction. The experiments were carried out with equipment very similar to that of Roth, Driscoll and Holt but in our case the track was supported on vertical cantilever springs by the deflection of which the frictional force was measured. The track was covered with plate glass which was carefully cleaned with acetone by a standard technique after each run. The samples had an area of about 3·4 cm^2 and had the form shown in fig. 2, which is a perspective view of the sample as seen from underneath.

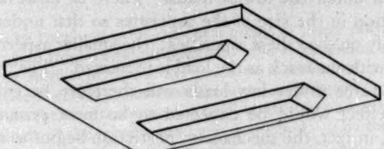

Fig. 2. View of the sample.

The surface has been divided into two runners in order to produce as broad a supporting area for the weights constituting the normal load as was possible in the circumstances.

When the sample moves it is strained in simple shear by the frictional force and if no precautions are taken the rear edge of the sample will trail behind and be under a lower pressure than the rest of the surface, the pressure on which increases correspondingly. To obviate this source of error the ends of the samples were chamfered as shown in fig. 2. The heights of the runners and of the supporting plate were each $\frac{1}{16}$ in. In order to obtain a standard rugosity of the rubber surface the samples were moulded against a ground glass plate, as was done by Roth, Driscoll and Holt.

The velocity at which the measurements were made was in all cases $2{\cdot}16 \times 10^{-3}$ cm/sec. It had to have a comparatively low value if vibrations and stick–slip phenomena were to be rigidly excluded.

It is invariably found that during the course of an experiment the frictional force increases as the sample travels along the track. The force increases, however, at a diminishing rate and becomes sensibly constant after the sample has traversed about 10 cm. Nevertheless it is not always easy to say whether the force has in fact become constant; fortunately, the final value is reached progressively earlier in successive experiments, and we repeated our measurements in rotation until the results became reproducible.

The results are shown in fig. 3 where the full lines are the expected curves calculated by means of eqn. (3), with a factor c chosen to give the best fit.

§4. DISCUSSION

The two softer compounds fit the theoretical curves of fig. 3 reasonably well, considering that there is only one arbitrary constant by which the adjustment has been effected. This agreement is good evidence that in the case of soft rubbers, and within the range of normal loads employed here, the frictional force is proportional to the true area of contact. There is therefore a formal analogy between the friction of rubber and of metals (Bowden and Tabor 1950). The load dependence of rubber friction can be described by eqn. (3) which is based on Hertz's equation for the deformation of spheres and it should be mentioned that such a relation was suggested by Bowden for rubber during the recent International Conference on Abrasion and Wear at Delft (1951). It is interesting to note that the friction of diamond (Bowden and Young 1951) obeys a similar law.

The departure of the hard rubber from the theoretical curve is most pronounced at lower loads, and is most probably due to the following cause. It has been assumed that all surface asperities are identical and are all in contact with the track even under the lowest loads. There is, however, certain to be a statistical distribution in the size of the asperities so that under a small load the sample will rest only on the tallest asperities; the smaller asperities will gradually come into contact with the track as the load is increased. The true area of contact and the frictional force under low loads will therefore be smaller than in the ideal case. The effect would be expected to be most pronounced with hard compounds where, in fact, the mechanism of friction begins to resemble ordinary solid friction with a constant coefficient of friction.

Our results cannot be compared directly with those of Thirion who worked at higher normal loads. The load dependence of the coefficient of friction above, say 3 kg/cm^2 is, according to Thirion, given by $1/\mu = a + bp$ where a and b are constants. It will be seen immediately that at sufficiently high loads the frictional force becomes essentially constant. This is understandable from our point of view because the deformation of the surface asperities cannot continue indefinitely at the rate given by eqn. (1) but the area of contact must eventually reach a limiting value.

ACKNOWLEDGMENT

This work forms part of the research programme undertaken by the Board of the British Rubber Producers' Research Association.

APPENDIX

The samples contained the following ingredients expressed as parts per 100 parts of rubber; all samples were vulcanized at a temperature of 140° c.

	Hard rubber	Medium rubber	Soft rubber
Sulphur	4·0	2·5	—
Accelerator	Mercapto benzthiazole, 0·5 Diphenyl guanidine, 1·0	Santocure, 0·6	Tetramethyl thiuram disulphide, 1·5
Zinc oxide	5·0	5·0	2·25
Anti-oxidant	Nonox S, 1·0	Phenyl-β-naphthylamine, 1·0	—
Stearic acid	1·0	1·0	0·1875
Time of cure (min)	40	50	60

REFERENCES

Bowden, F. P., and Tabor, D., 1950, *The Friction and Lubrication of Solids* (Oxford University Press).

Bowden, F. P., and Young, J. E., 1951, *Proc. Roy. Soc.* A, **208,** 444.

International Conference on Abrasion and Wear, 1951, *Engineering*, **172,** 724.

Roth, F. L., Driscoll, R. L., and Holt, W. L., 1942, *J. Res. Nat. Bur. Stand., Wash.*, **28,** 439.

Thirion, P., 1946, *Rev. Gén. Caoutch.*, **23,** 101.

The Frictional Properties of Plastics

By K. V. SHOOTER and D. TABOR

Research Laboratory for the Physics and Chemistry of Surfaces, Department of Physical Chemistry, Cambridge

MS. received 12*th March* 1952

ABSTRACT. The frictional properties of a group of linear polymers have been investigated at loads ranging from a few milligrams to several kilograms at slow speeds of sliding. At light loads the coefficient of friction tends to increase but at loads above 100 g the coefficient of friction is generally constant and is almost independent of the size and shape of the surfaces. From the results obtained at loads above 100 g a tentative theory to explain the origin and magnitude of the friction has been developed. The theory is similar to that of Bowden and Tabor for the friction of metals. When a plastic slides on a harder metal strong adhesion occurs between the surfaces and shearing takes place within the bulk of the plastic rather than at the interface. The frictional force is essentially equal to the product of the area of contact and the bulk shear strength of the plastic. The experiments also show that the area of contact is proportional to the applied load so that the plastic behaves as if it possesses an effective yield pressure which is constant. The coefficient of friction is thus primarily determined by the bulk properties of the plastic and is equal to the ratio of the shear strength to the effective yield pressure of the plastic. When a plastic slides on a softer metal shearing occurs within the metal and the friction is primarily determined by the bulk properties of the metal itself rather than those of the plastic. Examination of the surface damage produced during sliding shows marked transfer of the softer to the harder material.

The frictional behaviour of polytetrafluoroethylene differs from that of the other plastics in that the adhesion during sliding is small and shearing apparently takes place preferentially at the interface. However, when this plastic slides on a sufficiently soft metal marked adhesion and transfer of the metal to the plastic occurs.

§ 1. INTRODUCTION

In the study of non-metallic friction, plastics provide a family of materials of particular interest. They are widely used for a variety of industrial and technological purposes so that their frictional and wear characteristics are important. In addition their chemical composition and physical properties can be varied over a wide range and for this reason they are well suited to an investigation of the basic mechanism of friction. The only systematic work so far recorded in this field has been restricted to synthetic fibres (Gralén and Olofsson 1947, Gralén and Lindberg 1948). The work of Gralén and his co-workers has indeed yielded results of considerable value but they have not yet led to a definite theory of friction. This is partly because of the small range of loads over which measurements can be made and partly because of the difficulty of determining the nature of the surface layers.

The present paper describes an investigation of the frictional properties of a group of linear polymers (including nylon, perspex and substituted polyethylenes) over a range of loads from 0·04 to 10 000 g.

§ 2. EXPERIMENTAL

Three different types of apparatus have been used to measure the friction, Whitehead's apparatus (1950) for loads from 0·04 to 140 g, Eldredge's (to be published) for loads from 100 g to 5 kg and the Bowden–Leben apparatus (1939) for loads from 1 kg to 10 kg. Over their common load ranges the same coefficients of friction were obtained. With each apparatus the friction was measured between a hemispherically ended slider and a flat plate. A constant sliding speed of 0·01 cm/sec was used for all experiments.

Several methods of cleaning the plastic specimens were tried: washing with organic solvents, cutting away the surface with a degreased cutting tool, vigorous rubbing with degreased cloth and abrasion on 600 grade emery paper under a stream of water. No marked differences in frictional behaviour were produced by the different methods of cleaning. After the preliminary experiments the abrasion technique was adopted as standard. With careful cleaning no particles of abrasive were picked up by the plastic. The metal specimens were cleaned using the method given by Tingle (1950).

The Area of Contact and the Shearing Process during Sliding

In order to determine the mechanism of friction it is necessary to know the area of contact between the sliding surfaces. Bowden and Tabor (1939) have shown that the real area of contact between a metal sphere and flat is very nearly equal to the apparent area of contact calculated from the diameter of the indentation left on the flat. The square of the width of the groove left by a steel slider on a block of plastic can therefore be taken as a measure of the real projected area of contact between the sliding surfaces. Measurements of the diameter d of the groove left by a 3·2 mm radius steel slider on the different plastics have been made at loads W ranging from 1 to 10 kg. When d^2 is plotted against W as in fig. 1 it is found that there is a linear relationship between them. We may therefore write $W = Ap$ where A is the area of contact and is proportional to d^2. It is found that with sliders of different radii of curvature the same type of relation holds and that, if the diameter of the groove is not too large, p is to a first approximation independent of the curvature of the slider. By analogy with the similar equation given by Bowden and Tabor (1939) for metals the constant p can be termed the 'effective yield pressure' of the plastic. These results show that the deformation process simulates the properties of a plastic deformation. The shallowing of the groove with time indicates that the deformation is of the retarded elastic type rather than plastic.

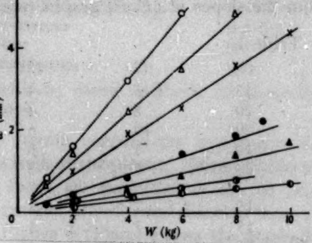

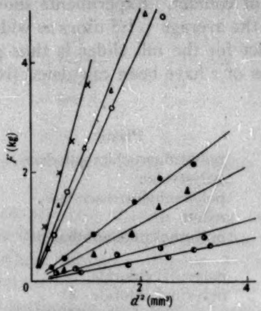

Fig. 1. The relationship between the area of contact and the applied load for a steel slider (6·35 mm radius) sliding on a block of plastic.

Fig. 2. The relationship between the frictional force and the area of contact for a steel slider (6·35 mm radius) sliding on a block of plastic.

In fig. 2 the frictional force F is plotted against the square of the diameter of the groove left by the steel slider on the plastic; it is seen that F is proportional to the area of contact: $F=As$. A similar equation has been found to apply to the friction of metals (Bowden, Moore and Tabor 1943). When the metal specimens slide together cold welding occurs at the areas of intimate contact and the frictional force is the force required to shear these welded junctions. The constant s is thus the shear strength of the junctions. A similar process may be considered to occur when steel and a plastic slide together. If the surfaces adhere together strongly during sliding shearing will take place within the bulk of the plastic rather than at the interface. If the sliding process is of this nature the constant s will be equal to the shear strength of the plastic. To test this hypothesis the bulk shear strengths of the plastic have been measured and compared with the values of s calculated from the friction data.

Calculation of s

The area of contact over which shearing occurs will depend upon the extent to which the deformation of the plastic is reversible, i.e. on the extent to which the load is supported over the rear half of the steel slider. If there is no recovery of the groove the slider will be in contact with the plastic over a semicircle of diameter d where d is the diameter of the groove. In this case $A=\pi d^2/8$. On the other hand if recovery is rapid and complete the slider will make contact over a full circle of diameter d. Here $A=\pi d^2/4$. It has been found that some recovery of the groove occurs. The extent to which this recovery helps to support the load over the rear half of the slider has been estimated by making measurements with sliders from which the rear half has been ground away.

If the full slider makes contact over a semicircle of diameter d the 'half' slider will give a groove of the same diameter. On the other hand, if the recovery of the groove is complete and the full slider makes contact over a circle of diameter d then since the area of contact is proportional to the load the 'half' slider will have to make a groove $\sqrt{2}$ times as wide in order to achieve the same area of contact. Experiments show that the groove made by the 'half' slider is on the average $\sqrt{1\cdot5}$ times as wide as the groove of the full slider. The area of contact for the full slider is thus given by $A=1\cdot5\pi d^2/8$. Using this equation values of s have been calculated from the slopes of (F, d^2) graphs (see table 1).

Table 1

Plastic		(1)	(2)	(3)
polytrifluorochloroethylene		13	5	4
polystyrene		20	8	4
polymethylmethacrylate		20	10	6
nylon		10	5	6
polyethyleneterephthalate		20	5	5
polyvinyl chloride		15	7	5
polyvinyl chloride	8*	15	7	5
	12*	14	6	4
	16*	14	5	4
	22*	10	3	3
	30*	4	1	2
polyethylene	1†	2	0·8	1·4
	2	—	0·7	1
	3	1·7	0·7	0·8
	4	—	0·6	0·6
	5	1·5	0·2	0·2

(1) Approx. Vickers pyramid hardness (kg/mm²), (2) shearing force per unit area of contact during sliding (kg/mm²), (3) bulk shear strength (kg/mm²).

* Parts of plasticizer, dioctylphthalate per 100 parts of plastic.

† Molecular weight decreases in the order 1 . . . 5.

The Bulk Shear Strengths of the Plastics

The shear strengths of the plastics have been measured at a shearing speed of 0·01 cm/sec. A cylinder of plastic was pressed into holes in two brass blocks attached to the arms of a Hounsfield tensometer. The axis of the cylinder was at right angles to the direction of pull. The brass blocks were pulled over one another at a speed of 0·01 cm/sec to produce a shear in the plastic cylinder and the stress–strain curve recorded. The shear strength was calculated from the maximum tension achieved and the initial area of cross section of the plastic cylinder. Repeat experiments agreed to within 5%. The values obtained (given in table 1) agree with the calculated values of s to within a factor of two. This suggests that the coefficient of friction is primarily determined by the properties of the plastic:

$$\mu=\frac{s}{p}=\frac{\text{shear strength of plastic}}{\text{`effective yield pressure' of plastic}}.$$

This is supported by the following additional experiments.

For the two other sliding combinations, a hemispherical plastic slider on itself or on a plate of steel, the area of contact will again be given by $W=Ap$;

provided the adhesion between the sliding surfaces is sufficiently strong the frictional force will again be given by $F = As$. The coefficient of friction should therefore be the same as that for a steel slider sliding on plastic. The figures in table 2 show that essentially the same coefficient of friction is obtained for all the sliding combinations.

Table 2

Plastic	(1)	(2)	(3)
polyvinyl chloride	0·4–0·45	0·4–0·45	0·35–0·4
polymethylmethacrylate	0·45–0·5	0·4–0·6	0·5
polystyrene	0·4–0·5	0·4–0·5	0·4–0·5
nylon	0·3	0·3	0·25
polyethylene 1	0·3	0·25	0·25

(1) Steel slider sliding on plastic, (2) plastic slider sliding on plastic, (3) plastic slider sliding on steel.

These results confirm the hypothesis that shearing during sliding occurs within the bulk of the plastic. Direct evidence for this shearing process has been obtained from an examination of the surface damage. Figure 3 (Plate) shows fragments of polyvinyl chloride that remain adhering to a steel plate after sliding. Figure 4 (Plate) shows the marked surface damage that occurs when polyvinyl chloride slides on itself.

Table 3

Plastic slider	Steel VPH 150	Copper VPH 105	Silver VPH 45	Glass —	Polymethylmethacrylate VPH 20
polymethylmethacrylate VPH 20	0·5	0·5	—	0·5	0·5
polythylene VPH 2	0·25	0·2	0·2	0·2	0·2
polyvinyl chloride VPH 15	0·35–0·4	0·35	0·45	0·35–0·4	0·35–0·4
nylon VPH 10	0·25	0·25	0·2	0·25	—

VPH : Vickers pyramid hardness (kg/mm²)

From this general picture it follows that for a plastic sliding on any material that is harder and has a higher shear strength than itself the coefficient of friction should be the same as that found for steel and plastic sliding together. The results given in table 3 show that this is so. Essentially the same coefficient of friction is obtained for plastic sliding on steel, copper, silver, glass or a harder plastic. If, however, the second sliding specimen is softer than the plastic, the coefficient of friction should be determined by the properties of the second specimen rather than those of the plastic. Some experiments have been performed using the very soft metal indium. The coefficient of friction differs from that for steel sliding on the plastic and approaches the value obtained for indium sliding on steel ($\mu \simeq 1{\cdot}0$) as shown in table 4.

Table 4

Plastic	Steel sliding on plastic	Indium sliding on plastic
polyethyleneterephthalate	0·1–0·2	0·75
polyvinyl chloride	0·35–0·45	0·75
polymethylmethacrylate	0·45–0·5	1·0

Examination of the track left by the indium slider on the plastics clearly shows that shearing has occurred within the softer indium. Figure 5 (Plate), for example, shows the indium left on polyethyleneterephthalate after sliding.

Friction and Apparent Area of Contact

The friction of several flat blocks of polyvinyl chloride and polyethylene of different sizes sliding on a large flat block of the same plastic has been measured. At loads from 100–5 000 g the same coefficient of friction was obtained for apparent areas of contact ranging from a few square millimetres to 100 cm^2 and these values were the same as for curved sliders (polyvinyl chloride $\mu = 0{\cdot}35$–$0{\cdot}45$, polyethylene $\mu = 0{\cdot}25$–$0{\cdot}3$). These experiments show that the frictional force is determined solely by the total load and not by the size or shape of the surfaces.

The Ploughing Term

Bowden, Moore and Tabor (1943) have suggested that the frictional force F can be regarded as the sum of two terms: $F = S + P$ where S the shearing term is equal to As and P the ploughing term is the force required to groove the surfaces during sliding. For a hard hemispherical slider P is proportional to d^3. Except at very heavy loads the ploughing term is relatively small and to a first approximation $F = As$. Where the ploughing term contributes appreciably to the frictional force F will increase more rapidly than A (or d^2) and the coefficient of friction will increase as the load is further increased. It is evident from geometrical considerations that the ploughing term will be most important for the curved steel slider sliding on a block of plastic. For a given width of groove the smaller the radius of curvature of the slider the greater will be the amount of plastic displaced. Experiments show that with the softer plastics (polyethylene, plasticized polyvinyl chloride, polytetrafluoroethylene) the ploughing term is an appreciable part of the frictional force for steel sliders of small radius of curvature. The curves in fig. 6 illustrate this effect for steel sliding on plasticized polyvinyl chloride. For the sliders of small radius the frictional force increases more rapidly than the area of contact, the effect becoming more marked the smaller the radius of curvature of the slider. At sufficiently light loads the (F, d^2) curves for all the sliders tend to the same straight line. This suggests that the shearing term S is the same for all sliders at any given groove width and that the deviation from the straight line is a measure of the ploughing term. Calculations based on a simple theory developed by Bowden and Tabor (1942) show that with the

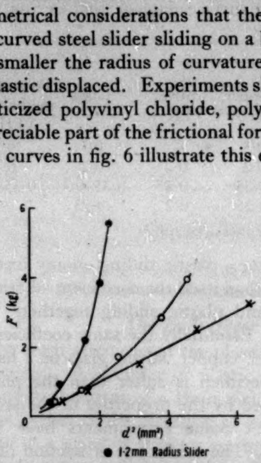

Fig. 6. The relationship between the frictional force and the area of contact for steel sliders of different diameter sliding on plasticized polyvinyl chloride (30 parts of dioctylphthalate per 100 parts of plastic. VPH≃4).

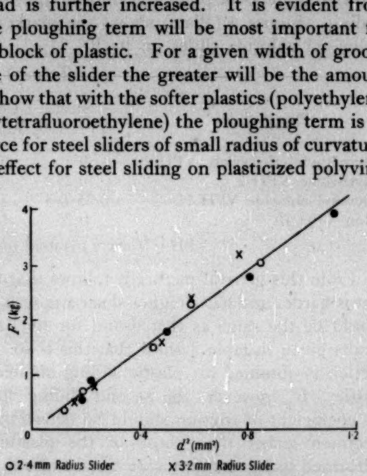

Fig. 7. The relationship between the frictional force and the area of contact for steel sliders of different diameter sliding on polyvinyl chloride. Unplasticized. VPH≃15.

softer plastics the ploughing term accounts for one half or more of the frictional force at the heaviest loads. With the harder plastics (polyvinyl chloride, polymethylmethacrylate, polystyrene) the friction is independent of the radius of curvature of the slider. For example, fig. 7 shows that for polyvinyl chloride the results for three different sliders all lie on one straight line. Calculations confirm that with these plastics the ploughing term is small ($P<\frac{1}{5}F$).

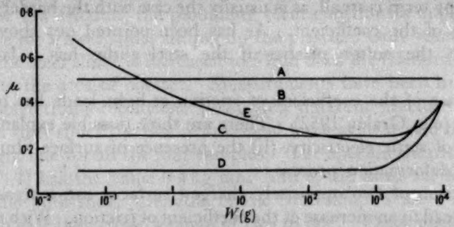

Fig. 8. 1·2 mm radius steel slider sliding on a block of plastic. The variation of the coefficient of friction with load. A: Polymethylmethacrylate. B: Polyvinyl chloride. C: Polyethylene (high molecular weight). D: Polytetrafluoroethylene. E: Polyethylene (low molecular weight).

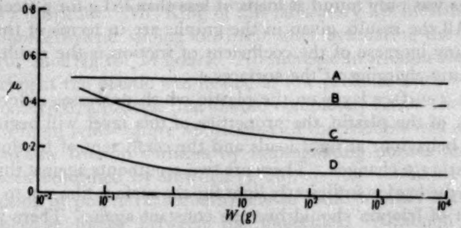

Fig. 9. Plastic slider sliding on a block of plastic. The variation of the coefficient of friction with load. A: Polymethylmethacrylate. B: Polyvinyl chloride. C: Polyethylene (high molecular weight). D: Polytetrafluoroethylene.

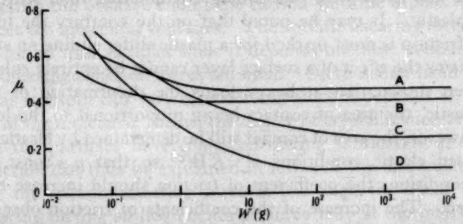

Fig. 10. Plastic slider sliding on a steel plate. The variation of the coefficient of friction with load. A: Polymethylmethacrylate. B: Polyvinyl chloride. C: Polyethylene (high molecular weight). D: Polytetrafluoroethylene.

These results again stress the similarity of the frictional behaviour of metals and plastics.

The Coefficient of Friction and the Applied Load

The way in which the coefficient of friction varies with load is shown in figs. 8, 9, 10. The coefficient of friction is reproducible to ± 0·05 at loads above 100 g, at lighter loads the reproducibility decreases to ± 0·1.

With some of the plastics the coefficient of friction is constant over the whole of the load range investigated. With others increases of the coefficient of friction may occur at heavy or at light loads. The increase of the coefficient of friction at heavy loads is only found for a steel slider sliding on the soft plastics. That no similar increase is found for the other two sliding combinations confirms the view that the increase with the steel slider is due to the large ploughing term. If the ploughing term is small, as is usually the case with the harder plastics, there is no increase of the coefficient. As has been pointed out above, this is also observed with the softer plastics if the steel slider has a large radius of curvature.

The increase of the coefficient of friction at light loads has been found by other workers (e.g. Gralén 1952). There are three possible explanations of this: (i) the effects of static electricity, (ii) the presence of surface films and (iii) the nature of the deformation process.

The attraction of two oppositely charged surfaces can increase the applied load and thus lead to an increase of the coefficient of friction. With the Whitehead apparatus the load can be measured as the slider is removed from the flat surface so that it is possible to measure the true load, i.e. the nominal applied load plus the load due to the electrostatic attraction of the surfaces. Measurable adhesion of the surfaces was only found at loads of less than 0·1 g for a steel slider sliding on plastic. All the results given in the graphs are in terms of the true applied load. Thus any increase of the coefficient of friction is the result of something other than static charging of the surfaces.

If there is a surface layer on the plastic which possesses different properties from the bulk of the plastic, the properties of this layer will begin to dominate the frictional behaviour at light loads and the coefficient of friction may change because the ratio s/p changes. There are two arguments against this explanation. Firstly, when the load is sufficiently light for the surface film not to be penetrated the coefficient of friction should become constant again. There is no evidence that this occurs. Secondly, when a plastic slider slides on a steel plate any surface film on the slider will be rapidly worn away. The effect of a surface film should therefore have less effect with this sliding combination than with a steel slider sliding on a plastic. It may be noted that on the contrary the increase of the coefficient of friction is most marked for a plastic slider sliding on steel. In spite of these criticisms the effect of a surface layer cannot be entirely ruled out.

It has been shown that at heavy loads the deformation of the plastic is apparently plastic, the area of contact being proportional to the load. At very light loads, however, the area of contact will be determined by elastic deformation. Under idealized elastic conditions $A=KW^{2/3}$ so that $\mu=\text{const.}/W^{1/3}$. Thus under these conditions the coefficient of friction should increase rapidly as the load is reduced. The increase of the coefficients of friction observed is much less rapid than that predicted by the above equation. Presumably the change from plastic to elastic deformation is not abrupt, that is, there is a gradual change from $A\propto W$ to $A\propto W^{2/3}$. Calculations (using Hertz's equations) of the load at which the coefficient of friction should begin to increase give results which are much higher than the loads actually observed. This shows very clearly that the surface asperities play an important part in determining the nature of the deformation (Bowden and Tabor 1950, p. 14). Further work is required to put this explanation on a quantitative footing.

The Frictional Properties of Polytetrafluoroethylene

Extremely low coefficients of friction are obtained with this plastic. Apart from this, the frictional properties follow the general pattern described in the previous sections. Thus the coefficient of friction is substantially the same ($\mu = 0{\cdot}05$–$0{\cdot}10$) irrespective of the nature of the second sliding surface, demonstrating that it is the properties of the plastic that determine the friction. Because of the low friction, the ploughing term contributes appreciably to the frictional force for a steel slider sliding on the plastic. Only when the radius of curvature of the steel slider is increased to 5 mm does the frictional force become proportional to the area of contact. Measurements have been made using four samples of polytetrafluoroethylene possessing different mechanical properties. For the 5 mm steel slider the plot of frictional force against area of contact gives a single straight line for all the four samples. The specific shearing force during sliding ($s = F/A$) has the value 0·4 kg/mm^2 and is the same for all the samples. In contrast the bulk shear strengths of the four samples are 1·2, 1·4, 2·0 and 2·4 kg/mm^2 so that they cover a range of two to one. These results suggest that shearing during sliding occurs preferentially at the interface rather than within the bulk of the plastic.

It would seem that the low friction is not due to the presence of a surface film which acts as a lubricant. Mr. King of this laboratory has measured the friction of polytetrafluoroethylene sliding on itself after evacuating the apparatus to a pressure of 10^{-6} mm Hg for 24 hours. No increase in friction was found. In a further experiment the plastic was heated at low pressure until marked thermal degradation occurred, a process that should completely renew the surface layers. On cooling to room temperature no increase in the friction was observed. The preparation of low friction surfaces by impregnating porous metals with this plastic has been described by Bowden (1950).

The adhesion of polytetrafluoroethylene to itself or other materials depends upon the cohesive forces between the molecules. Although the polytetrafluoroethylene molecule possesses large dipoles, as Hanford and Joyce have pointed out (1946), the comparatively large size of the fluorine atoms will effectively screen the positive end of the carbon–fluorine dipole. This screening action reduces the molecular cohesion. The specific shearing force during sliding is the same for all four samples since it depends on these cohesion forces and it will be low since the cohesion forces are small. On the other hand a bulk property such as shear strength can vary considerably since it depends on factors such as the rigidity of the molecular chains, the degree of crystallization and the efficiency with which the particles have coalesced during fabrication (Fergusson 1949). The low friction can thus be explained in terms of the molecular structure.

Because the specific shearing force is less than the shear strength of the plastic, shearing during sliding occurs preferentially at the interface rather than within the bulk of the polytetrafluoroethylene. However, when polytetrafluoroethylene slides on a material that has a shear strength less than 0·4 kg/mm^2 (the normal shearing force per unit area during sliding) marked transfer of the soft material to the plastic occurs. For example, when a freshly cut block of the very soft metal sodium is rubbed on polytetrafluoroethylene easily visible fragments of metallic sodium remain adhering to the plastic. In a further experiment a hemispherical polytetrafluoroethylene slider was pressed on to a freshly cut block of sodium under a load of 1 kg. After the slider had been rotated to break up the hydroxide film on the sodium a load of 1 kg was required to pull the slider away. Fragments of metallic sodium remained sticking to the slider. It is thus possible to obtain a coefficient of adhesion of unity between polytetrafluoroethylene and a metal, provided that the metal is sufficiently soft. These experiments demonstrate the essential similarity of the frictional behaviour of polytetrafluoroethylene and the other plastics.

§ 3. DISCUSSION

The investigation has shown that the frictional behaviour of plastics is similar to that of metals. With metals cold welding occurs at the areas of intimate contact and the frictional resistance is essentially equal to the force required to shear these junctions.

With plastics strong adhesion occurs and the shearing takes place within the bulk of the softer material rather than at the interface. The frictional force is thus equal to the product of the area of contact and the bulk shear strength of the softer material. Consequently, when a plastic slides on a hard material the coefficient of friction is the ratio of the effective yield pressure of the plastic to the shear strength of the plastic. In general, the coefficient of friction is independent of the nature of the hard material whether this be a metal, glass or a harder plastic. Transfer of the plastic to the hard material occurs during sliding. On the other hand, when a plastic slides on a softer material, the friction is primarily determined by the properties of the softer material. In this case marked transfer of the soft material to the plastic is found. At the slow speeds of sliding used in these experiments the frictional heating is insufficient to produce appreciable thermal softening. Thus the transfer of material during sliding is due to a process analogous to the cold welding which occurs between sliding metals.

With a steel slider sliding on a very soft plastic such as polyethylene the coefficient of friction increases in the load range 1 to 10 km. With these very soft plastics the force required to plough out the groove on the plastic is a large fraction of the frictional force and the increase of the coefficient of friction results from this large ploughing term. When the ploughing term is small, as is the case when the steel slider has a large diameter or when a plastic slider slides on steel, the coefficient of friction does not increase at heavy loads. These results support the suggestion of Bowden, Moore and Tabor that, to a first approximation, the frictional force can be considered as the sum of the force required to overcome the adhesion of the surfaces and the force required to groove the surfaces.

It has been found that in general the coefficient of friction increases at light loads. This increase may be due to the presence of a surface layer with different properties from the bulk of the plastic. The most likely explanation, however, is that there is a change from a plastic type of deformation to an elastic deformation as the load is reduced. The change is gradual and there is a corresponding gradual change in the friction from $\mu =$ constant (independent of load) at heavier loads to a slow increase in μ as the load is reduced.

In one important respect the frictional behaviour of polytetrafluoroethylene differs from the other plastics. The adhesion during sliding is not sufficiently great for shearing to occur within the bulk of the plastic. Although the adhesion is small it is finite and with very soft metals marked adhesion and metallic transfer can occur. The low adhesion can be explained in terms of the molecular structure.

One important observation is that when shearing occurs within the bulk of one of the specimens rather than at the interface it is the properties of the softer material that determine the magnitude of the friction and it is the softer material that is transferred to the harder. However, a more detailed investigation of the surface damage using radioactive metal sliders (Rabinowicz and Shooter 1952) shows that some transfer of the hard metal to the plastic takes place during sliding. The amount involved is very small and the force required to tear out these fragments is a negligible part of the total frictional force. While not appreciably affecting the friction the plucking out of these fragments from the harder metal shows that a soft plastic can produce wear of a harder metal.

ACKNOWLEDGMENTS

We wish to express our thanks to Dr. F. P. Bowden for his continued interest in the work, to the Ministry of Supply (Air) for a Research Grant and to Imperial Chemical Industries for supply of the various plastics used, and for a maintenance grant to one of us (K. V. S.).

REFERENCES

Bowden, F. P., 1950, *Research*, **3,** 147.

Bowden, F. P., and Leben, L., 1939, *Proc. Roy. Soc.* A, **169,** 938.

Bowden, F. P., Moore, A. J. W., and Tabor, D., 1943, *J. Appl. Phys.*, **14,** 80.

Bowden, F. P., and Tabor, D., 1939, *Proc. Roy. Soc.* A, **169,** 391; 1942, C.S.I.R. (Aust.) Bull. No. 145; 1950, *The Friction and Lubrication of Solids* (Oxford : University Press).

Fergusson, W. C., 1949, *Chem. & Ind.*, 586.

Gralén, N., 1952, *Proc. Roy. Soc.* A, **212,** 491.

Gralén, N., and Lindberg, J., 1948, *Proc. Swed. Inst. Text. Res.*, No. 6.

Gralén, N., and Olofsson, B., 1947, *Proc. Swed. Inst. Text. Res.*, No. 3.

Hanford, W. E., and Joyce, R. M., 1946, *J. Amer. Chem. Soc.*, **68,** 2082.

Rabinowicz, E., and Shooter, K. V., 1952, *Proc. Phys. Soc.* B, **65,** 671.

Shooter, K. V., 1952, Royal Society Symposium on Friction (in the press).

Shooter, K. V., and Thomas, P. H., 1949, *Research*, **2,** 533.

Tingle, E. D., 1950, *Trans. Faraday Soc.*, **46,** 93.

Whitehead, J. R., 1950, *Proc. Roy. Soc.* A, **201,** 109.

The Transfer of Metal to Plastics during Sliding

By E. RABINOWICZ and K. V. SHOOTER

Research Laboratory for the Physics and Chemistry of Surfaces, Department of Physical Chemistry, Cambridge

Communicated by D. Tabor; *MS. received* 12*th March* 1952

ABSTRACT. Investigations have been carried out on the amount of metal transferred when a radioactive metal is slid over the surface of a plastic. It is found that in every case metal fragments are transferred to the plastic in amounts that are of the same order of magnitude for the various metals and plastics examined. The close similarity of the results with those obtained with sliding metals suggests that, by a process analogous to the welding that occurs between metal surfaces, strong local adhesion occurs when metal and plastic are pressed and slid together.

As part of a programme of work on the frictional properties of plastics a study has been made of the transfer of metal to plastic that occurs when a hemispherical metal specimen (radius of curvature $\frac{1}{8}$ in.) slides on a flat block of plastic. The metal specimens were made radioactive by irradiation in the B.E.P.O. at Harwell. The sliding experiments were performed using the Bowden–Leben (1939) friction apparatus with a sliding speed of 0·01 cm/sec and loads of 2 to 4 kg. After the sliding experiments the blocks of plastic were placed in contact with a photographic plate and exposed for a suitable period. Typical autoradiographs obtained on developing the plates are shown in figs. 1 and 2 (Plate). From the density of blackening the average amount of metal transferred to the plastic per centimetre of sliding was calculated using the method described by Rabinowicz and Tabor (1951). The results are shown in the table.

Amount of Metal transferred per cm of Sliding when Metal Slider traverses Block of Plastic once. Load 4 kg.

Plastic	Amount of metal transferred (10^{-8} g)					Coeff. of friction
	1% Cr steel	Cd	Ag	Zn	Cu	
Polyethylene	1	8	1	1	*	0·2
Nylon	3	15	1	5	6	0·2
Polytetrafluoroethylene	*	3	1	1	1	0·1
Polyvinyl chloride	1	1	3	1	3	0·4–0·5
Polyvinyl chloride (30 parts per 100 plasticizer)	1	5	1	1	1	0·3–0·4
Polyethyleneterephthalate	6	*	1	1	1	0·2

* No experiments with these combinations.

Detailed analysis of the results given in the table cannot be made as the order of reproducibility is not very high, individual values sometimes varying by as much as a factor of two. However, it is clear from these experiments that when a hard metal slides on a softer plastic fragments of metal are left adhering to the surface of the plastic. This phenomenon, the wear of a hard by a soft material, has been previously observed, for instance by Moore (1948) and Rabinowicz and Tabor (1951), who have shown that a soft metal can pluck out fragments from a harder metal.

The amount of radioactive material transferred to the plastic, whilst appreciable, is considerably less than the transfer that occurs in the analogous case of the sliding of dissimilar metals at the same load and speed (e.g. steel on copper, transfer 6×10^{-7} g/cm; steel on plastic, transfer 10^{-8} g/cm). The amount of metal transferred to the plastic is on an average increased five times if the metal is slid 25 times over the same track, but this effect was not investigated in greater detail.

No direct correlation has been found between the coefficient of friction and the amount of metal transferred to the plastic. The average amount of transfer is roughly the same irrespective of the nature of the plastic or of the metal, though nylon generally produces more pick-up than the other plastics. Analogous results have been obtained by Rabinowicz and Tabor in their work on the transfer of metals to one another. The fact that the amount of metal transferred to the plastic polytetrafluoroethylene is of the same magnitude as for the other plastics contrasts remarkably with its extremely good self-lubricating properties (Shooter and Thomas 1949).

Figures 1 and 2 show that the transfer of metal to plastic occurs only at a limited number of discrete points; the behaviour is similar to that observed for a metal sliding on metal as shown in fig. 3. For the metal sliding on plastic two distinct types of transfer have been found. In fig. 1 the fragments of metal are distributed across the whole width of the track whilst in fig. 2 the fragments are concentrated along the edges of the track. Again both types of behaviour are found in the case of sliding metals. Rabinowicz (1951) has explained the concentration of the metal fragments along the edges of a track as the result of the screening of the central portion of the radioactive metal specimen by inactive material picked up from the other surface. Evidence of such transfer of plastic to metal has been given by Shooter and Tabor (1952).

This tearing out of fragments from the metal slider clearly shows that strong adhesion occurs between the plastic and metal during sliding. By contrast if experiments are carried out under conditions of static loading, little normal adhesion is found between a metal and a plastic, and this has been attributed to the release of elastic stresses as the load is removed (McFarlane and Tabor 1950). Radioactive measurements under these conditions show that metal is in fact transferred to the plastic. For example for a silver slider pressed on to polytetrafluoroethylene with a load of 2 kg the amount of metal transferred to the plastic is 10^{-10} g. This shows that adhesion does occur under static loading conditions but the amount of metal transferred is much less than during sliding. A similar behaviour is found with metals (Rabinowicz and Tabor 1951).

These experiments show that appreciable wear of a hard metal slider occurs when it slides on a plastic. Part of the material transferred to the plastic may come from the breaking up of the oxide film under stress. However, the fragments are usually too thick to consist wholly of oxide and must consist, at least in part, of metallic particles plucked from the slider as a result of the adhesion. In some cases the fragments are large enough to be clearly recognized as metallic. This process of metal transfer is closely analogous to the welding and shearing that occur when two metals slide together (Bowden and Tabor 1950).

ACKNOWLEDGMENTS

Our thanks are due to Dr. F. P. Bowden and Dr. D. Tabor who supervised this investigation, to the Department of Scientific and Industrial Research for a maintenance grant to E. R., and to Imperial Chemical Industries, Plastics Division, for a maintenance grant to K. V. S.

REFERENCES

Bowden, F. P., and Leben, L., 1939, *Proc. Roy. Soc.* A, **169**, 371.

Bowden, F. P., and Tabor, D., 1950, *Friction and Lubrication of Solids* (Oxford : Clarendon Press).

McFarlane, J. S., and Tabor, D., 1950, *Proc. Roy. Soc.* A, **202**, 224.

Moore, A. J. W., 1948, *Proc. Roy. Soc.* A, **195**, 231.

Rabinowicz, E., 1951, *Brit. J. Appl. Phys.*, Suppl. No. 1, p. 82.

Rabinowicz, E., and Tabor, D., 1951, *Proc. Roy. Soc.* A, **208**, 455.

Shooter, K. V., and Tabor, D., 1952, *Proc. Phys. Soc.* B, **65**, 661.

Shooter, K. V., and Thomas, P. H., 1949, *Research*, **2**, 533.

On the Dielectric Constant of the Water in Wet Clay

BY L. S. PALMER
University College of Hull

MS. received 28th April 1952

ABSTRACT. Some recent experimental values of the variation of the dielectric constant of wet clay with moisture content cannot be explained on the assumption that the clay particles and water molecules form a simple mixture. The results can, however, be theoretically deduced by considering relatively dry clay to consist of closely packed water-coated clay particles in an air matrix and relatively wet clay to consist of clay particles uniformly distributed in a water matrix, the water associated with the clay having an effective dielectric constant which varies exponentially from that of 'bound' water (about 3) to that of 'free' water (about 80) as the percentage of water is gradually increased. The conclusion follows that water films have a very low dielectric constant compared with that of water in bulk.

§ 1. INTRODUCTION

SOME recent ultra-high-frequency radio measurements by Cownie and Palmer (1952) of the dielectric constant of wet clay showed a variation with increase of moisture content which is not explicable by any simple theory. In particular, the graph obtained by plotting the real part of the complex dielectric constant against the percentage weight of moisture associated with the clay displayed a point of inflection which cannot be reproduced from the theoretical assumption that the clay particles and water molecules merely mix together.

The experimental results can, however, be explained by assuming the water exists in two different 'states' and exhibits progressively different characteristics as it is increased in amount relative to the clay particles. This is not altogether a new suggestion because several authors (Freymann and Freymann 1951, Tausz and Rumm 1934, Thomas 1947) have referred to 'solid' and 'liquid' water, to 'bound' and 'free' water, or to 'non-available' and 'available' water.*

The following section outlines the general physical picture of the changes which are believed to occur as water is gradually added to dry clay. Furthermore, a quantitative study of the consequences of such changes enables Cownie and Palmer's experimental results to be reproduced theoretically. From such a study certain conclusions follow concerning the dielectric constant of the water.

§ 2. THE ROLE OF WATER IN WET CLAY

For simplicity in the first instance it will be assumed that dry clay consists of small spheres of solid material, all of the same size, which, when shaken together, but not artificially compressed, will fill about 75%† of the total volume occupied by the clay; the remaining 25% consisting of an air 'matrix'; that is, dry clay will be considered as a system of closely packed uniform spherical clay particles with air filling the interspaces—Gassmann's 'dry system' (Gassmann 1951).

If a small quantity of water is now added to the clay and evenly distributed throughout the volume, it is assumed that the water will tend to coat each clay particle with a very thin film. It will also be assumed that these water-coated clay spheres will be closely packed, with the air matrix continuing to fill the interspaces; but the total volume will naturally be slightly greater. As more water is added to the mixture, these films on the clay spheres will thicken and tend to become distorted until there is sufficient water present to displace the air and completely fill the interspaces.

---

* As distinct from water of crystallization.

† Theoretically $100\pi/3\sqrt{2}$ or approximately 74% for closest packing of identical spheres.

The physical picture then changes and, as more and more water is added, the system becomes one in which clay spheres are uniformly distributed throughout a water matrix.

This is not the only model that could have been suggested, but it seems to be a reasonable one, and has the additional advantage of being susceptible to relatively simple mathematical treatment.

The abnormal mechanical properties of water films consisting of layers of oriented molecules are well known, and it is realized that such 'bound' molecules also exhibit abnormal dielectric properties. Furthermore, there is no reason to suppose that the water films on the clay particles would cease to exist when more and more water is added to the system. But such additional water molecules, not being in the form of films, would not be restricted in movement. They would be free to orient themselves at random. Thus, if the clay particles continue to be effectively coated with water films, the properties of the water matrix would gradually change from those of 'bound' water to those of 'free' water as the amount of water is progressively increased. Only with infinite dilution would the water exhibit its normal properties. For this reason, in the quantitative study in the following section, it has been assumed that the effective value of the dielectric constant of the water matrix increases exponentially from that of 'bound' water (presumably of the same order as that of ice) to the normal value for 'free' water as more and more water is added to the clay.

There is evidence to suggest that the binding forces operative on the water molecules at a solid–water interface are structure sensitive, that is, the efficacy of the solid in binding and orienting the water molecules varies with the nature of the solid. For example, the work of Schofield (1946) on the theory of the Gouy electric double layer deals with electrostatic binding forces, which are necessarily structure sensitive. He assumes the dielectric constant of the water to be 80.

Again, the properties of the interlayer water in halloysite (Brindley and Goodyear 1948) and montmorillonite (Méring 1946) indicate that the binding forces depend on the nature and configuration of the atoms in the surface layers of the solid constituent of the particular clay mineral.

The physical nature of the binding forces is not under consideration in the present discussion, but it has been known for some time (Webb 1926) that the dielectric constant of water is reduced in the presence of an intense electric field, and Conway, Bockris and Ammar (1951) published curves (based on the work of Webb) which show variations in the dielectric constant of water very similar to those assumed here for the water associated with the clay and depicted in fig. 3. It is not, however, intended to suggest that the basis for the graph in fig. 3 is fundamentally electrical, although such a possibility is not to be excluded.

It is possible to treat the foregoing physical ideas quantitatively, and by suitably choosing certain arbitrary constants an explanation of Cownie and Palmer's results can be obtained. This is done in the following section.

§ 3. QUANTITATIVE CONSIDERATIONS

Various authorities (Böttcher 1945, Bruggeman 1935, Lorentz 1880, Rayleigh 1892, Van Vessem and Bijvoet 1948) have published formulae for calculating the dielectric constant of a mixture from a knowledge of the dielectric constants of its constituents and of their size and spatial distribution. That deduced by Bruggeman for solid spherical particles uniformly distributed throughout a fluid matrix is particularly applicable to the present problem and will therefore be adopted in the following calculations. Bruggeman's formula may be written

$$\epsilon=\epsilon_1-(\epsilon_1-\epsilon_2)V(\epsilon/\epsilon_2)^{1/3}, \qquad \ldots\ldots(1)$$

where ϵ is the effective dielectric constant of the mixture, ϵ_1 and ϵ_2 are the dielectric constants of the spherical particles and of the matrix respectively. V is the ratio of the volume occupied by the matrix to the total volume.

In the particular problem under consideration ϵ_1 is the effective value (ϵ_S, say) of the dielectric constant of the water-coated clay spheres when the total amount of water is insufficient to fill the interspaces and form a uniform matrix of water. For this relatively dry condition ϵ_2 will be 1, the dielectric constant of the air matrix. With relatively wet clay ϵ_1 will be that of the clay particles (ϵ_C, say) and ϵ_2 will, according to the idea suggested above, increase exponentially from the dielectric constant of 'bound' water ϵ_B to that of 'free' water ϵ_F, the resultant value of ϵ_2 for the water matrix being indicated by ϵ_W.

Thus two further formulae are necessary: one for the effective dielectric constant ϵ_S of the water-coated clay spheres and a second formula for the variable dielectric constant ϵ_W of the water matrix.

The first formula can be deduced from fundamental principles, and is as follows:

$$\epsilon_S=\epsilon_W[(y^3+2)+2(y^3-1)\epsilon_W/\epsilon_C]/[(2y^3+1)\epsilon_W/\epsilon_C+(y^3-1)], \qquad \ldots\ldots(2)$$

where ϵ_W is the variable dielectric constant of water given by eqn. (4), ϵ_C is that for the clay spheres (approximately 3 for silica) and y is the ratio of the radius a of the coated sphere to that b of the solid clay core. Values of y can be calculated for different percentages of added water. If the percentage moisture content x is defined, as in Cownie and Palmer's work, by the weight of water associated with 100 grammes of dry clay, then $x/100=\frac{4}{3}\pi(a^3-b^3)/\frac{4}{3}\pi b^3\delta$, where δ is the density of the clay particle and the density of water ('bound' and 'free') is taken to be unity.

Thus

$$y^3=(1+x\delta/100). \qquad \ldots\ldots(2a)$$

Furthermore, the relation between x as defined above and V in eqn. (1) is given by

$$V=x\delta/(100+x\delta). \qquad \ldots\ldots(3)$$

The equation for ϵ_W must fulfil the conditions already stated and is therefore given by

$$\epsilon_W=\epsilon_F-(\epsilon_F-\epsilon_B)e^{-\alpha x}, \qquad \ldots\ldots(4)$$

where α determines the exponential rate of increase of ϵ_W with x. α is an arbitrary constant which will depend on the efficacy of the 'bound' water to lower the dielectric constant of the main bulk of water. It may be expected to decrease with conditions which tend to promote the formation of large areas of water films, that is, with the smallness of the spherical clay particles. This point is being investigated experimentally. For the boulder clays used by Cownie and Palmer the value of α is taken to be 0·044; this value produces the best fit of eqn. (1) to the experimental data.

Given the density δ of the clay particles to be 3, the values for the dielectric constant of clay with various percentages of added water may now be computed.

By putting $V = 0{\cdot}25$ (Gassmann 1951) in eqn. (3), it follows that added water will be just sufficient to fill the interspaces between closely packed spheres when x lies between 11 and 12%. Consequently Bruggeman's formula (1) will apply to water-coated spheres of variable $\epsilon_1 (= \epsilon_S)$ in an air matrix of constant $\epsilon_2 (=1)$ for values of x not greater than, say, 15%, and will apply to clay spheres of constant $\epsilon_1 (= \epsilon_C = 3)$ in a water matrix of variable $\epsilon_2 (= \epsilon_W)$ for values of x not less than, say, 10%. There will be some transition between these values of x where the system with an air matrix passes over to one with a water matrix.

For values of x less than 15% eqn. (1) reduces to

$$\epsilon = \epsilon_S - K_1 \epsilon^{1/3}, \qquad \ldots\ldots (1\,a)$$

where $K_1 = (\epsilon_1 - \epsilon_2) V \epsilon_2^{-1/3} = 0{\cdot}25(\epsilon_S - 1)$; ϵ_S is given by eqn. (2), which is plotted in the graph of fig. 1. The resulting calculations of ϵ from eqn. (1 *a*) are shown by the dotted graph in fig. 4.

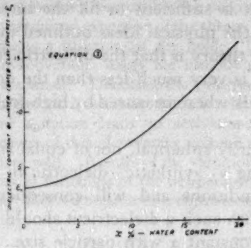

Fig. 1.

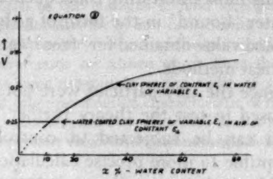

Fig. 2.

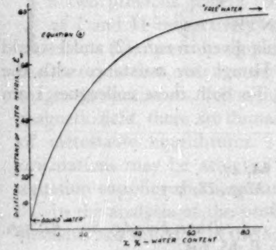

Fig. 3.

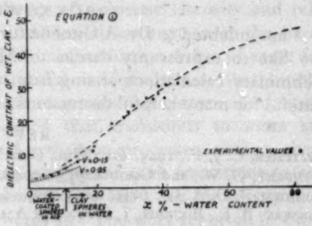

Fig. 4.

For values of x greater than 10% eqn. (1) reduces to

$$\epsilon = \epsilon_C + K_2 \epsilon^{1/3}, \qquad \ldots\ldots (1\,b)$$

where $K_2 = (\epsilon_2 - \epsilon_1) V \epsilon_2^{-1/3} = (\epsilon_W - 3) V \epsilon_W^{-1/3}$; V is given by eqn. (3) and is plotted in the graph of fig. 2. ϵ_W is given by eqn. (4) and is shown in fig. 3 for $\epsilon_B = 3$ and $\epsilon_F = 80$. Values of ϵ from eqn. (1 *b*) are shown by the broken line in fig. 4.

§4. COMPARISON WITH EXPERIMENTS AND CONCLUSIONS

In fig. 4 Cownie and Palmer's results are shown by the dots, which fall as closely as could be expected along the broken line representing eqn. (1 *b*), but seem to lie above the dotted line representing eqn. (1 *a*). This discrepancy for small values of x can be explained by realizing that, when carrying out the actual measurements, the clay was rammed down into a brass tube which formed the terminal section of a concentric transmission line. This was done to ensure a uniform packing and so prevent spurious reflections from discontinuities. As a result of this ramming, the figure of 0·25 assumed for V in the foregoing calculations is probably too high. If V is reduced to 0·15, the chain line curve is obtained from eqn. (1 *a*). From the agreement of this chain line graph with the experimental values, it would seem reasonable to suppose that the process of ramming the clay had distorted the particles and compressed more clay into a given space than would be possible by simply shaking true spheres.

The comparatively close agreement between theory and experiment for values of x greater than 15% is partly due to the value adopted for α in eqn. (4). Nevertheless, the two forms of eqn. (1) and the consequent reproduction of a point of inflection where the water content is sufficient to fill the interspaces between the clay particles tends to support the physical ideas outlined in §2.

The most interesting consequence of the theory is that the dielectric constant of water 'bound' in the form of a thin film is very much less than the normally accepted value obtained for 'free' water in bulk when measured by high-frequency electrical methods.

Since the clay particles were not necessarily spherical, nor of equal size, it is proposed to test the theory further by using a 'synthetic' dielectric in a form which can be subjected to controlled conditions and will consequently be susceptible to more precise calculations. With such a dielectric it should also be possible to determine the variation of the constant α with particle size. In the meantime it is felt that the foregoing discussion may help to throw some further light upon the somewhat obscure phenomenon of 'bound' or 'solid' water.

ACKNOWLEDGMENTS

I am indebted to Dr. A Cunliffe for the formula given in eqn. (2) and I would also like to express my thanks to Mr. J. M. Hough for assistance with the preliminary calculations arising from eqn. (1). To both these colleagues I am grateful for many helpful discussions.

REFERENCES

Böttcher, C. J. F., 1945, *Rec. Trav. Chim. Pays-Bas*, **64**, 47.

Brindley, G. W., and Goodyear, J., 1948, *Mineralog. Mag.*, **28**, 407.

Bruggeman, D. A. G., 1935, *Ann. Phys., Lpz.*, **24**, 636.

Conway, B. E., Bockris, J. O'M., and Ammar, I. A., 1951, *Trans. Faraday Soc.*, **47**, 756.

Cownie, A., and Palmer, L. S., 1952, *Proc. Phys. Soc.* B, **65**, 295.

Freymann, M., and Freymann, R., 1951, *C. R. Acad. Sci., Paris*, **232**, 401.

Gassmann, F., 1951, *Geophysics*, **16**, 673.

Lorentz, H. A., 1880, *Wied. Ann.*, **9**, 641.

Méring, J., 1946, *Trans. Faraday Soc.* B, **42**, 205.

Rayleigh, Lord, 1892, *Phil. Mag.*, **34**, 481.

Schofield, R. K., 1946, *Trans. Faraday Soc.* B, **42**, 219.

Tausz, J., and Rumm, H., 1934, *Kolloid Beihefte*, **39**, 58.

Thomas, M., 1947, *Plant Physiology*, 3rd edn., (London : Churchill), p. 103.

Van Vessem, J. C., and Bijvoet, J. M., 1948, *Rec. Trav. Chim. Pays-Bas*, **67**, 191.

Webb, T. J., 1926, *J. Amer. Chem. Soc.*, **48**, 2589.

Magnetic Viscosity under Discontinuously and Continuously Variable Field Conditions

By R. STREET, J. C. WOOLLEY and P. B. SMITH
The University, Nottingham

Communicated by L. F. Bates ; *MS. received* 21*st April* 1952

ABSTRACT. For a ferromagnetic specimen exhibiting magnetic viscosity, the intensity of magnetization increases continuously with time under steady external field conditions. An account is given here of investigations to determine the influence on magnetic viscosity of changes in the magnetic field applied to the specimen, two cases of discontinuous and continuous changes in field being considered. The latter case is of practical importance when direct measurements of magnetic viscosity are made using specimens with demagnetization coefficient other than zero since the effective field acting in the specimen is then continuously variable in time. It is found that both cases can be adequately described by extending the previously proposed formal theory of magnetic viscosity in which it was supposed that the domain processes responsible for magnetization can be activated by thermal agitation.

The required extension of the theory consists in assuming that the activation energy of the domains is a function of the field. The experimental results show that the changes in domain activation energy are linearly proportional to the changes in field strength, if the latter are small. Denoting the constant of proportionality by q, and considering a possible domain model, it is shown that q is related to the elementary volume of the material in which thermal agitation leads to activation. Measurements on alnico show that the linear dimensions of this elementary volume are of the same magnitude as the width of a domain boundary wall. Results of the variation of q and other parameters characteristic of magnetic viscosity as functions of the temperature of the specimen are also presented and it is shown that the observed behaviour is consistent with the present views on the metallurgical structure of alnico.

§ 1. INTRODUCTION

In two previous papers (Street and Woolley 1949, 1950, to be referred to as I and II respectively) a formal theory of magnetic viscosity and related effects has been developed. The fundamental assumption at the basis of the theory is that over certain ranges of the magnetization curve of some ferromagnetic specimens, following upon an initial sudden increase in the applied magnetic field, there are domains with their magnetization vectors in orientations of metastable equilibrium. It is assumed that transitions to more stable orientations may be achieved by thermal activation processes, that is, thermal agitation supplies the necessary activation energy for such transitions to occur.

In the analysis of the process it is necessary to know the initial numbers of domains as a function of the activation energy E. The work reported in I and II shows that good agreement between the theory and the results of measurements on alnico, a high coercivity permanent magnet material, is obtained if it is assumed that initially the number of domains having activation energies between E and $E+dE$, denoted by $f_0(E)\,dE$, is a constant for all allowed values of E. Hence $f_0(E)\,dE$ may be replaced by $p\,dE$ where p is a constant. The idealized initial distribution is represented diagrammatically in fig. 1 (a). It is of course not implied that this assumption is rigorously exact in practice. However, the experimental results in I and II show that any departures of $f_0(E)$ from a constant value p, over the range available for experiment, are small, i.e. $f_0(E)$ must be a slowly varying function of E. As thermal activation proceeds the value of $f(E)$ for the lower values of E will progressively and significantly diminish with time. Thus the distribution function $f_t(E)$ at a given time t after the initial change in the applied field will have the form indicated in fig. 1 (*b*) in which the hatched area OPab represents those domains which have been activated in time t. In I and II it was assumed that on the average each of the domains so activated contributed the same amount $\bar{\imath}$ to the holomagnetization of the specimen and thus $\bar{\imath}\cdot$(Area OPab) represents the increase in holomagnetization during time t. Further analysis shows that the lower energy limit of the distribution function Pa moves to the right of the diagram at a speed inversely proportional to time which implies that the area swept out by Pa, and also the holomagnetization, increases as the logarithm of time.

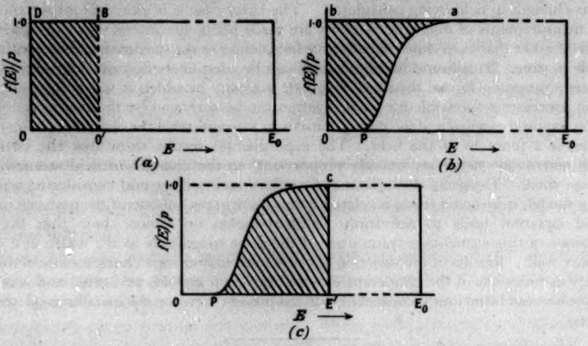

Fig. 1. Distribution functions of domains in terms of activation energy. For explanation of hatched areas, see text.

In the measurements of incremental permeability described in II, an additional magnetic field increment ΔH_e was made at various times after the initial sudden increase in field had taken place. In the analysis of the process it was considered that the application of ΔH_e changed the orientations of all domains of activation energy less than some limiting value E'. Hence, subject to the assumptions detailed above, the observed change of magnetization was taken to be proportional to the hatched area PE′c shown on fig. 1 (*c*), together with an unknown contribution due to magnetic viscosity occurring with E′ as the new zero of activation energy. The analysis and the supporting experimental work were specifically confined to cases where ΔH_e was always sufficiently large for the point c to lie on the effectively horizontal part of the distribution function as indicated in fig. 1 (*c*). Under these conditions the unknown contribution to the observed change in intensity of magnetization due to magnetic viscosity is a constant independent of the magnitude of ΔH_e and hence may be suitably eliminated.

In this paper the above work is extended to include the phenomena of magnetic viscosity occurring, firstly, in cases where ΔH_e is positive and sufficiently small so that E′ falls within the range OP of fig. 1 (*c*), where the distribution function is effectively zero. Secondly, cases where ΔH_e is negative, for which E′ lies to the left of the point O of the figure and thirdly, cases where the internal field is a continuously variable function of time are examined. (This last case is of considerable practical importance since the intensity of magnetization of a specimen exhibiting magnetic viscosity is a continuously variable function of time and hence the internal field is also continuously variable if the specimen has a non-zero demagnetizing factor.) In order to preserve a logical sequence in the description of these extensions typical experimental observations, using alnico specimens, are first described; then, with these results as a guide, the formal theory, appropriate to the cases where discontinuous field changes are applied, is developed (§5.1). It is then possible to design further experimental tests of the theory and the results of these are given in §5.2. The formal analysis of magnetic viscosity occurring when the field acting is continuously varying with time and the experimental verification of the predictions of this analysis are included in §6. §7 is concerned with the development of expressions relating the various parameters characteristic of the magnetic behaviour of the specimens. Finally, the physical significance of the results obtained is discussed in §8.

§2. APPARATUS

In I, measurements of magnetic viscosity were made by observing the time increase of the intensity of magnetization of rod specimens using conventional magnetometric methods and a suspended magnet magnetometer. The relatively long period of oscillation of this type of instrument precludes its use in measurements where the intensity of magnetization is changing rapidly with time, for the magnetometer deflections cannot accurately follow rapid changes in the deflecting field. In the type of experiment described here, the time rate of change of intensity of magnetization is large when the applied field is changed discontinuously and also at the beginning of any magnetic viscosity experiments, since the time rate of change of intensity of magnetization is inversely proportional to the time which has elapsed from the beginning of the experiment. These considerations led to the replacement of the suspended magnet magnetometer by a saturated core magnetometer, or fluxgate, which accurately responded to changes in the magnetic field acting on it with a time lag of less than 10^{-2} second.

It is only necessary to describe the apparatus briefly here as the principles involved have already been adequately described by Hine (1951). Two carefully annealed permalloy wires are mounted in two identical solenoidal coils joined in series opposition and connected to a stable oscillator of frequency f. When zero ambient field acts on the permalloy cores the total flux linking a solenoidal secondary coil, completely surrounding the permalloy cores and their associated exciting coils, is zero. However, if an external field is applied along the length of the permalloy wires a first harmonic signal of frequency $2f$ is induced in the secondary coil. Within limits the amplitude of the induced first harmonic signal is roughly linearly proportional to the applied field intensity and moreover the phase of this signal changes by 180° when the applied field is reversed in direction. It is found in practice that maximum sensitivity, i.e. maximum first harmonic signal amplitude for a constant applied field, is obtained by trial adjustment of the frequency f and the amplitude of the exciting current.

In the fluxgate used here the permalloy cores were of length 40 mm, diameter 0·5 mm and maximum sensitivity was obtained with $f = 5{\cdot}5$ kc/s. In the complete form of the apparatus accurate linearity was achieved by applying a large amount of negative feedback to the system. This was done by rectifying the first harmonic signal derived from the secondary coil in a phase sensitive rectifier and passing the resultant direct current through a solenoidal feedback coil wound directly over the secondary coil of the fluxgate. The arrangement of the apparatus is shown in the block schematic diagram of fig. 2. The current flowing in the feedback coil was found to be a linear function of the field intensity acting along the permalloy cores with an accuracy within about $\frac{1}{4}$%.

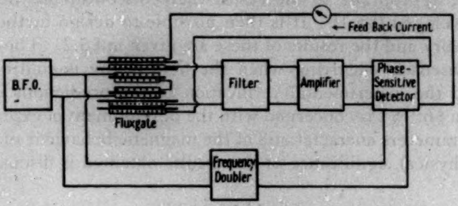

Fig. 2. Block schematic diagram of fluxgate circuit.

The fluxgate was mounted in the Gauss B position with respect to the rod specimen under investigation as indicated in fig. 3. The specimen was supported symmetrically either in an electric oven, the heater of which was wound non-inductively and fed with d.c. when required or, when measurements were made below room temperature, in a Dewar vessel containing refrigerants. The required external magnetic fields were applied by means of a surrounding water-cooled solenoid. The latter was wound in two parts; the main winding was fed from a 280 v battery of accumulators, connected in the circuit 1 of fig. 3, and gave a maximum field of approximately 1 000 oersteds. A subsidiary smaller winding was connected to either of the two circuits 2 and 3 through switch K of fig. 3. The currents flowing in the circuits 1 and 3 were measured by means of a potentiometer and standard series resistances. It was necessary to neutralize the fields acting at the fluxgate due to currents flowing in both the main and subsidiary windings of the solenoid. This was done by means of two suitably adjusted coils C_m and C_s separately connected in series with the windings.

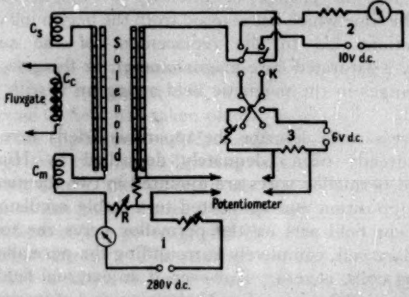

Fig. 3. Circuit diagram of solenoid and associated circuits.

Accurate measurements could only be made if the currents in both the main and subsidiary windings of the solenoid remained constant, to a relatively high degree of accuracy, for several minutes. It was found in practice that the 280 v battery available did not alone supply sufficiently stable currents within the required limits. Consequently a rotary, oil-cooled potentiometer R was connected in parallel with the main winding as shown in fig. 3 and by manual adjustment of R throughout a measurement it was found possible to maintain constant main winding current to an accuracy of within about ±1 in 15 000.

The fluxgate was placed inside and along the axis of a solenoidal coil C_c which was used to calibrate the feedback current of the fluxgate circuit in terms of the ambient field. In addition, when measurements were being made at points on the hysteresis cycle far removed from the coercive force point, a constant current was passed through C_c in order to reduce the mean resultant field acting on the fluxgate (averaged over the time required for an experiment) to zero. Under these conditions it was thus possible to use the fluxgate at maximum sensitivity.

§ 3. SPECIMENS

The specimens used in the measurements described below were of approximate percentage composition, Al, 10; Ni, 18; Co, 12; Cu, 6; Fe, 54 (alnico alloy). The majority of the measurements were made on cylindrical rod specimens of length 30 cm and diameter 0·6 cm approximately. In the experiments where it was necessary to know accurately the demagnetization coefficients, specimens in the form of prolate ellipsoids of revolution were used. These had a common semi-minor axis of 0·30 cm and their lengths varied from 7 cm to 2 cm, giving a range of the demagnetization coefficient from 0·2 to 1·1. The ellipsoidal specimens were heat treated so as to produce a common coercive force of about 230 oersteds, since preliminary experiments on the effects of heat treatment of alnico had shown that this was a suitable value at which to make measurements.

§ 4. EXPERIMENTAL METHODS

Generally, before any measurement was made, a cyclic state of magnetization was established in the specimen in the usual way, using the circuit 1 of fig. 3. At an appropriate point in the magnetization cycle, a current was established in the subsidiary solenoid connected to circuit 2, which produced a field along the specimen of about 20 oersteds. The field due to the current in the main solenoid was then adjusted to the required operating value H, always preserving a cyclic order of magnetization, and in such a direction as to oppose the 20-oersted field set up by the subsidiary solenoid current. The resultant field acting on the specimen was thus $H-20$ oersteds. At zero time, the current in circuit 2 was broken, and hence the applied field increased rapidly to the required operating value H. Measurements were then made of the variation of the feedback current in the fluxgate as a function of time, and hence the required variation of the intensity of magnetization ΔI of the specimen as a function of time was calculated.

In certain measurements it was necessary to apply a further increment ΔH_e in the external field at some time t_1 after the 20-oersted increment had been made. This was done by establishing a suitable current in circuit 3 at time t_1, the direction of the current being so arranged to give positive or negative increments ΔH_e as required. (From the considerations of § 1 a negative field increment ΔH_e

opposes the main solenoid field, whereas a positive ΔH_e aids the main solenoid field.)

In §7 equations will be derived relating the parameters characteristic of the magnetic viscosity to the irreversible susceptibility of the substance concerned, under the same conditions of magnetization. Thus in addition, measurements of susceptibility also had to be made. A difficulty arises in this case since, for any material showing magnetic viscosity, the intensity of magnetization is a function not only of the applied field, but also of time. Thus in any practical case, because a finite time is required for measurements to be made (e.g. time of swing of ballistic galvanometer, etc.), the observed change in intensity ΔI will be due not only to the change in field ΔH_e applied, but also to the magnetic viscosity occurring during the time of measurement (this was shown in II). Thus, for example, if a ballistic method is used, the measured value of $\Delta I/\Delta H_e$ will depend on the time of swing of the galvanometer. Similarly, if a magnetometric method of measurement is used, the value of I will vary continuously even when discontinuous changes of the applied field ΔH_e are made. In cases when the magnetic viscosity is small, then the contribution to ΔI due to the magnetic viscosity may be sufficiently small to be neglected, in which case normal methods of measuring dI/dH can be used. This is generally true in the region of magnetization near the demagnetized condition, and this is the region where measurements have been made by Néel and his collaborators. When measurements are made near the coercive force point of such materials as alnico, etc. the magnetic viscosity contribution is sufficiently large to invalidate completely any measurements of dI/dH made by the usual methods. For this reason, it is necessary here to choose rather arbitrarily some systematic method of measuring dI/dH which will make allowance for the effect of magnetic viscosity. One method, (*a*), would be to measure ΔI at relatively long times after the field increment ΔH_e had been applied. In this way, ΔI would contain effectively the total contribution to the change in intensity of magnetization due to magnetic viscosity effects. This was the method used in paper I, and the slope of the magnetization curve then gave the required value of dI/dH at any point. The disadvantage of this method is that it is difficult to obtain accurately consistent results, because of the drift in the solenoid current, and therefore in H, during the long period when magnetic viscosity is occurring. (Values of up to 40 minutes for each step were necessary in practice.) A second possible method, (*b*), of measuring the magnetization curve is to apply the increments in field at regular intervals of time t_a, and to make observation of the intensity of magnetization at some fixed time t_b after each application of ΔH. Measurements using method (*b*) were made on the same specimen of alnico which was used in the work described in I, with $t_a = 1$ minute and $t_b = 45$ seconds. The resulting magnetization curve was found to be similar, within the limits of experimental errors involved, to that obtained by method (*a*). In subsequent measurements of dI/dH it was found most convenient to use method (*b*), although recognizing that the procedure is rather arbitrary.

§ 5. DISCONTINUOUS FIELD CHANGES

As pointed out in § 1, an increment ΔH in the field acting on a specimen changes the activation energy of the individual domains. The average field acting on the domains is the internal field, and ΔH_i the change in the internal field produced by an increment ΔH_e in the applied field is effective in causing the changes in activation energy. For sufficiently small values of ΔH_i, it is assumed that the resulting changes in activation energy are such that the shape of the profile Pa in fig. 1 (*b*) is unaltered and that effectively there is only a change in the zero of the activation energy scale by an amount E'. With this assumption, as shown in fig. 4, the origin O of the activation energy scale moves to O′ or O″ on the application of a positive or negative ΔH_i respectively. In general, we may write $E' = F(\Delta H_i)$, the form of the function F being such that the sign of E' is the same as that of ΔH_i.

5.1. *Discontinuous Changes in Applied Field*: *Zero Demagnetization Coefficient*

The principles involved in the analysis of the case where discontinuous field changes are made are more obvious if carried out assuming the ideal case where the specimen has zero demagnetization coefficient. This will be done first, and then similar principles will be applied to analyse the practical case where the specimen has a non-zero demagnetization coefficient.

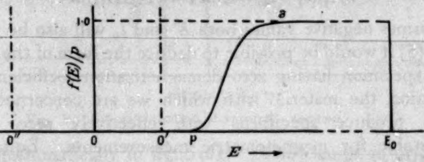

Fig. 4. Diagram showing the change in the origin of the activation energy axis from O to O′ or O″ on the application of a field increment $+\Delta H_i$ or $-\Delta H_i$ respectively.

For the case of a specimen having zero demagnetization coefficient, at a constant absolute temperature T, the time rate of change of $f(E)$ due to thermal activation is

$$\frac{d}{dt}f(E) = -Cf(E)\exp(-E/\boldsymbol{k}T) \qquad \ldots\ldots(1)$$

where C is a constant (cf. I, eqn. (1)) for, in this case, there is no variation of the internal field, and therefore no variation of the activation energy of the domains due to variation in the intensity of magnetization. Hence integrating (1) with respect to t and inserting the initial condition that $f(E) = p$ at zero time

$$f(E) = p\exp\{-Ct\exp(-E/\boldsymbol{k}T)\}. \qquad \ldots\ldots(2)$$

At any time t the position of the profile Pa along the E axis can be conveniently defined by that value of E at which $f(E) = p/2$. With this definition and using eqn. (2) the position of the profile at any time t_1, is given by E_1, where

$$\tfrac{1}{2} = \exp\{-Ct_1\exp(-E_1/\boldsymbol{k}T)\}. \qquad \ldots\ldots(3)$$

If now at time t_1 an increment in the internal field ΔH_i is made, there will be a change $E' = F(\Delta H_i)$ in the activation energy of all the domains. Thus the position of the profile relative to the new zero of activation energy, e.g. O′, will now be E_2, where $E_2 = E_1 - E'$. In a hypothetical case where magnetic viscosity occurs with the origin of activation fixed at O′ the profile reaches the energy E_2 in a time $t_1 - t_0$ where t_0 is defined by

$$\tfrac{1}{2} = \exp\left\{-C(t_1 - t_0)\exp\left(-\frac{F_1 - E'}{\boldsymbol{k}T}\right)\right\}. \qquad \ldots\ldots(4)$$

When the profile has moved to any position beyond E_2 the magnetic viscosity is produced by a movement of the profile represented by the equation

$$\tfrac{1}{2} = \exp[-C(t-t_0)\exp\{-(E-E')/\boldsymbol{k}T\}]$$

and the increase in the intensity of magnetization ΔI due to magnetic viscosity is proportional to $\ln(t-t_0)$.

Since ΔI depends only on the position of the profile with respect to the origin, the expression immediately above will also represent ΔI at times greater than t_1, in the case where a discontinuous increment ΔH_1 has been applied at time t_1. Hence the effect of the increment ΔH_1 on the magnetic viscosity occurring after time t_1 is equivalent to a change in the time origin from 0 to t_0. Thus it is to be expected that, for times from 0 to t_1, the variation of ΔI should be proportional to $\ln t$ whereas, when a discontinuity in the effective field occurs at t_1, ΔI should be proportional to $\ln(t-t_0)$ for values of t greater than t_1. Therefore t_0 may be determined by analysis of the variation of ΔI for times greater than t_1. From eqns. (3) and (4)

$$\ln t_1/(t_1-t_0) = E'/\boldsymbol{k}T = \{F(\Delta H_1)\}/\boldsymbol{k}T. \qquad \ldots\ldots(5)$$

When ΔH_1 assumes negative values both E' and t_0 will also be negative.

From eqn. (5) it would be possible to deduce the form of the function $F(\Delta H_1)$ for any given specimen having zero demagnetization coefficient. However, in the case of alnico, the material with which we are concerned here, it is not practicable to produce specimens with effectively zero demagnetization coefficients suitable for magnetometric measurements. Equation (5) is not necessarily applicable to cases where specimens of non-zero demagnetization coefficients are used and it is now necessary to repeat the above analysis taking into account the effect of the demagnetizing field.

5.2. *Discontinuous Changes in Applied Field: Non-zero Demagnetization Coefficient*

If the intensity of magnetization of a specimen increases by an amount ΔI, due to any cause, then the internal field acting changes by an amount $-D\Delta I$ where D is the demagnetization coefficient. When the intensity of magnetization is increasing with time, e.g. when the specimen exhibits magnetic viscosity, the internal field will similarly decrease as a function of time. (A typical value of the increase in ΔI from 5 seconds to 120 seconds after the beginning of an experiment, using a specimen with $D=0{\cdot}02$, is 45 gauss. Hence during this period of time the internal field decreases by about 0·9 oersted.) It follows that the activation energies of the domains continuously increase with time, or, in terms of the graphical representation proposed above, the origin of the activation energy axis moves continuously to the left of the diagram. At any time t the displacement of the origin from its initial position will be $F\{-D\Delta I(t)\}$ where $\Delta I(t)$ is the increase of intensity of magnetization from zero to time t.

Consider now the type of experiment where a positive increment* $+\Delta H_1$ occurs in the internal field at time t_1. The activation energy diagram immediately after t_1 is shown in fig. 5 (*a*). The activation energy $\mathscr{E}$ of the domains at the mid-point of the profile, measured with respect to the instantaneous origin, is given by

$$\mathscr{E} = E_1 + G(t_1) - F(\Delta H_1) \qquad \ldots\ldots(6)$$

---

* In the interests of clarity, the analysis is specifically confined to the case of positive increments, ΔH_1. The case where ΔH_1 is negative is similar.

where E_1 is defined in fig. 5 (*a*), and

$$-G(t)=F\{-D\Delta I(t)\}. \qquad \ldots\ldots(6a)$$

As in § 5.1, in order to transform the effect of ΔH_1 into a change in the time origin, it is again necessary to consider a hypothetical case where magnetic viscosity is allowed to proceed continuously without any discontinuous changes in H_1 until the profile is once again in exactly the same position relative to the instantaneous origin as in fig. 5 (*a*). Then, as before, for positions of the profile beyond this point, the magnetic viscosity will be the same in both cases. This hypothetical case is shown diagrammatically in fig. 5 (*b*). The change in origin of time t_0 is that value of t for which the activation energy of the domains (measured from the instantaneous origin) at the mid-point of the profile in (*b*) is equal to $\mathscr{E}$, i.e. t_0 is given by

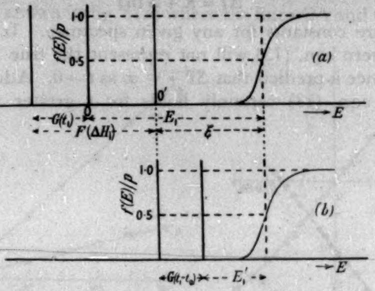

Fig. 5. For explanation of symbols, see text.

$$E_1'+G(t_1-t_0)=E_1+G(t_1)-F(\Delta H_1) \qquad \ldots\ldots(7)$$

as is seen by comparison of figs. 5 (*a*) and 5 (*b*).

In the special case when $D=0$ the last expression reduces to that already derived in § 5.1. The quantities E_1 and E_1' may be determined from a modification of eqn. (1):

$$\frac{d}{dt}f(E)=-Cf(E)\exp\left\{-\frac{E+G(t)}{\boldsymbol{k}T}\right\} \qquad \ldots\ldots(8)$$

introducing the fact that the activation energy increases with time as explained above. Integrating (8) gives

$$\ln\frac{f(E)}{p}=-C\exp\left(-\frac{E}{\boldsymbol{k}T}\right)\int_0^t\exp\left\{-\frac{G(t)}{\boldsymbol{k}T}\right\}dt. \qquad \ldots\ldots(9)$$

Consequently E_1 and E_1' are defined by equations of the same form as (9), obtained by putting $f(E)/p=\frac{1}{2}$ and $t=t_1$ and t_1-t_0 respectively. Subtraction of these two equations leads to

$$\exp\left(-\frac{E_1}{\boldsymbol{k}T}\right)\int_0^{t_1}\exp\left\{-\frac{G(t)}{\boldsymbol{k}T}\right\}dt=\exp\left(-\frac{E_1'}{\boldsymbol{k}T}\right)\int_0^{t_1-t_0}\exp\left\{-\frac{G(t)}{\boldsymbol{k}T}\right\}dt. \quad \ldots.(10)$$

Rearranging eqn. (10) and substituting for $E_1'-E_1$ from eqn. (7)

$$R\Phi(t_1)=\Phi(t_1-t_0) \qquad \ldots\ldots(11)$$

where

$$R=\exp\left\{-\frac{F(\Delta H_1)}{\boldsymbol{k}T}\right\}, \quad \Phi(x)=\exp\left\{\frac{G(x)}{\boldsymbol{k}T}\right\}\int_0^x\exp\left\{-\frac{G(t)}{\boldsymbol{k}T}\right\}dt. \quad \ldots\ldots(12)$$

For further development of the theory it is necessary to have information from which the form of the functions F, and hence G, and the variation of ΔI as a function of time may be evaluated. This information can only be obtained by experiment and consequently the relevant experimental results will now be given.

(i) The results of measurements of the increase of magnetization ΔI due to magnetic viscosity, using ellipsoidal specimens of alnico, are plotted as a function of time, fig. 6; they show that, to a good approximation,

$$\Delta I = K + S \ln t \qquad \ldots\ldots(13)$$

where K and S are constants for any given specimen. It is obvious that for times tending to zero eqn. (13) will not represent the true variation of ΔI as a function of time since it predicts that $\Delta I \to -\infty$ as $t \to 0$. Additional experiments have shown that eqn. (13) certainly holds for t greater than approximately 0·5 second.

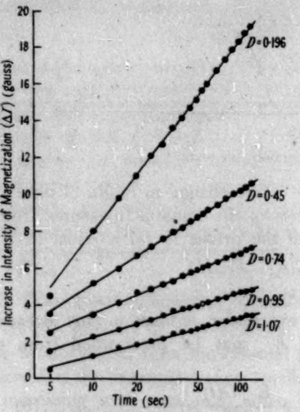

Fig. 6. The variation of intensity of magnetization of ellipsoidal specimens as a function of time. The different demagnetization coefficients D are given on the curves.

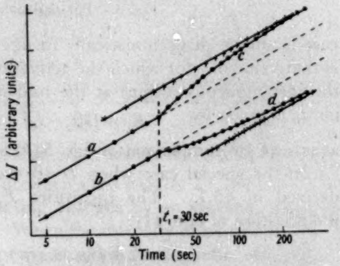

Fig. 7. Influence of increments of field applied to specimen at time $t_1 = 30$ sec. Upper curve ΔH_1 positive, lower curve ΔH_1 negative.

(ii) Measurements were made on the influence of discontinuous field changes on magnetic viscosity occurring in the specimen of length 30 cm described in § 3 which had a demagnetization coefficient of 0·018 and a coercive force of 350 oersteds. Typical results, obtained when both positive and negative field increments were applied at a time $t_1 = 30$ seconds, are shown in fig. 7. The general form of these curves is in qualitative agreement with the predictions already made above, i.e. the time rate of variation of intensity of magnetization is either increased or decreased when respectively either a positive or negative ΔH_1 is applied. Again, by a suitable transformation of the origin of time by an amount t_0, the curved portions c and d of the graphs in fig. 7 can be converted into straight lines of slopes equal to those of the portions a and b respectively.*

* Analytical methods for the derivation of t_0 from the experimental results have been given by Smith (1952).

From these curves it can be seen that for small field increments the majority of the magnetization is time dependent, i.e. the discontinuity obtained by extrapolating the two portions of each curve (for example *a* and *c* to the point t_1) represents only a small instantaneous change in the intensity of magnetization. Thus for practical purposes the change in internal field ΔH_i, obtained by correcting ΔH_e for the demagnetizing field, may be taken as ΔH_e within small limits of error.

(iii) Experiments were carried out to determine the variation of t_0 as a function of t_1, for constant values of the field increment ΔH_i. Typical results of $t_1 - t_0$ plotted against t_1 are shown in fig. 8 (*a*) where the lines OA and OB were obtained with positive and negative incremental fields respectively of magnitude 1·00 oersted. From such curves as these it is concluded that, for a constant value of ΔH_i,

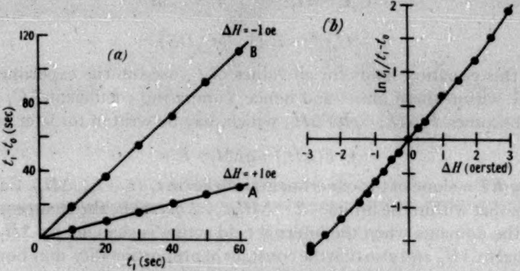

Fig. 8. For explanation of symbols, see text.

$$t_1 - t_0 = At_1 \qquad \ldots\ldots(14)$$

where A is a constant for times t_1 at which experiments were made and which range up to 60 seconds.

Hence substituting the experimental result of eqn. (14) into (11)

$$R\Phi(t_1) = \Phi(At_1) \qquad \ldots\ldots(15)$$

where R and A are constant for constant ΔH_i. By differentiation of (15) with respect to t_1, $R\Phi'(t_1) = A\Phi'(At_1)$ and hence

$$t_1\Phi'(t_1)/\Phi(t_1) = At_1\Phi'(At_1)/\Phi(At_1). \qquad \ldots\ldots(16)$$

Equation (16) is an identity for the values of t_1 used in the experiments. Since $A \neq 1$

$$t_1\Phi'(t_1)/\Phi(t_1) = C_1, \text{ a constant independent of } t_1. \qquad \ldots\ldots(17)$$

Integration of (17) leads to

$$\Phi(t_1) = C_2 t_1^{C_1} \qquad \ldots\ldots(18)$$

where C_2 is an integration constant, independent of t_1. Substituting for $\Phi(t_1)$ from (18) in eqn. (15) gives $R = A^{C_1}$ and hence from the definitions of R and A

$$F(\Delta H_\text{i})/\boldsymbol{k}T = C_1 \ln t_1/(t_1 - t_0). \qquad \ldots\ldots(19)$$

Equation (19) differs from the equation already derived in the case where the specimen has a zero demagnetization factor (eqn. (5)) only in that an additional constant factor C_1 appears on the right-hand side of eqn. (19). Again, guided by experimental observations, it can now be shown as follows that $C_1 = 1$ for the specimens on which the experiments were made.

Further experiments were carried out to determine how the quantity $\ln t_1/(t_1-t_0)$ varied as a function of ΔH_1. From eqn. (19) $\ln t_1/(t_1-t_0)=(1/C_1\boldsymbol{k}T)\{F(\Delta H_1)\}$ and consequently the experimental results serve to determine the form of the function $F(\Delta H_1)$. Measurements were made with values of ΔH_1 varying from $+2$ to -2 oersteds, and the results are shown in fig. 8(*b*); the straight line graph shows that $\ln t_1/(t_1-t_0)=g\Delta H_1$ where g is a constant for $-2<\Delta H_1<+2$ (oersteds). Hence,

$$F(\Delta H_1)=gC_1\boldsymbol{k}T\Delta H_1 \qquad \ldots\ldots(20)$$

and hence from eqn. (6*a*) $G(t)=gC_1\boldsymbol{k}TD\Delta I(t)$ and from eqns. (12*b*), (13), (18) and (20)

$$C_2t_1^{C_1}=t_1^{gC_1DS}\int_0^{t_1}t^{-gC_1DS}\,dt\,*$$

or

$$C_2t_1^{C_1}=t_1/(1-gC_1DS). \qquad \ldots\ldots(21)$$

Since this equation holds for all values of t_1, used in the experiments, (21) is an identity within these limits and hence, comparing coefficients, $C_1=1$. Thus eqn. (20) becomes $F(\Delta H_1)=g\boldsymbol{k}T\Delta H_1$, which may be written for later convenience as

$$F(\Delta H_1)=q\Delta H_1=E' \qquad \ldots\ldots(22)$$

where $g=q/\boldsymbol{k}T=$ slope of the experimental curve ($\ln t_1/(t_1-t_0)$, ΔH_1). Equation (22) thus shows that within the limits $-2<\Delta H_1<+2$ oersteds, the change in activation energy of the domains when the internal field acting is changed by ΔH_1, is linearly proportional to ΔH_1, and also that the constant of proportionality may be determined from experimental results. Presumably if ΔH_1 ranges over a wider range of values the expansion of $F(\Delta H_1)$ will contain terms in ΔH_1 of higher order than the first. Such non-linear expansions are neglected, since the experimental work described here was confined to ranges of the variables where the eqn. (22) is applicable. In summary, the experimental criteria which are necessary to justify this procedure are: (i) The variation of the intensity of magnetization in the absence of a discontinuous change of applied field must be proportional to the logarithm of the time measured from the beginning of the experiment. (ii) The quantity t_1-t_0 must be linearly proportional to t_1. (iii) $\ln t_1/(t_1-t_0)$ must be linearly proportional to ΔH_1 over a range including $\Delta H_1=0$.

§ 6. CONTINUOUSLY VARIABLE DEMAGNETIZING FIELDS

6.1. *Formal Theory*

The obvious feature of fig. 6, in which are plotted the results of magnetic viscosity measurements on specimens of the same type of material but differing in their demagnetization coefficients D, is that the slope of the (ΔI, $\ln t$) graph decreases with increasing D. In this section it will be shown that such a result is to be expected from the formal theory of magnetic viscosity discussed above. As already summarized in eqn. (13), the results presented in fig. 6 show that $\Delta I=K+S\ln t$ where K and S are constants for a specimen of a given material and shape. During a magnetic viscosity experiment the demagnetizing field, acting in opposition to the applied field, will steadily increase in magnitude, being given by $D(K+S\ln t)$ at time t. The activation energies of the domains

* In this equation it has been assumed that (13) gives the variation of intensity of magnetization during magnetic viscosity at all values of time, including $t=0$. As has already been pointed out above, this cannot be true for $t\rightarrow 0$. However, the form of the integral (eqn. (12)) is such that negligible error is incurred in practice by assuming that (13) holds for all values of t from 0 to t_1. An expression for the error involved in such an assumption has been derived by Smith (1952).

will therefore increase with time, a process which may be represented in terms of the graphical representation of fig. 5 (*a*) by the origin O moving continuously to the left of the diagram. The distance the origin has moved during time t will be given by $F\{-D(K+S\ln t)\} = -(m+qDS\ln t)$ in terms of the first-order theory developed in § 5, where $m = qDK$. If at time t, $f(E)\,dE$ is the number of domains having activation energies in the range E to $E+dE$, measured from the point O of fig. 5 (*a*) at time zero, then the rate of activation of these domains at time t will be

$$\frac{d}{dt}f(E) = -Cf(E)\exp\left\{-\frac{E+qDS\ln t+m}{\boldsymbol{k}T}\right\}. \qquad \ldots\ldots(23)$$

Integrating (23) between the limits 0 and t *

$$\ln\frac{f(E)}{p} = -\frac{C}{A}\exp\left\{-\frac{E+m}{\boldsymbol{k}T}\right\}t^{A}$$

where $A = 1 - qDS/\boldsymbol{k}T$; p has already been defined in eqn. (2). Writing

$$\lambda = C\exp\{-(E+m)/\boldsymbol{k}T\} \qquad \ldots\ldots(24)$$

it follows from the previous equation that

$$f(E) = p\exp(-\lambda t^{A}/A) \qquad \ldots\ldots(25)$$

and substituting (25) in (23)

$$(d/dt)f(E) = -p\lambda\exp(-\lambda t^{A}/A)\exp\{(A-1)\ln t\}.$$

As in I, it is now assumed that on the average each activation process contributes $\bar{\imath}$ to the intensity of magnetization of the specimen. Hence the total rate of change of intensity of magnetization of the specimen due to activation of the domains is

$$\frac{d}{dt}(\Delta I) = -\bar{\imath}\int_{E}\frac{d}{dt}f(E)\,dE. \qquad \ldots\ldots(26)$$

The integration extends over all the allowed activation energies, i.e. from zero to E_0 the upper limit (see fig. 1). During the time of an experiment the probability of activation of the domains having large activation energies will be vanishingly small. Consequently the contribution to $(d/dt)(\Delta I)$ by domains having such large activation energy is negligible and therefore the upper limits of the integral of eqn. (26) may be taken as infinity. The integration is best carried out by changing the variable E to λ; from (24) $d\lambda = -(\lambda/\boldsymbol{k}T)\,dE$. Substituting for $(d/dt)f(E)$ from (25), eqn. (26) becomes

$$\frac{d}{dt}(\Delta I) = \bar{\imath}p\boldsymbol{k}Tt^{A-1}\int_{\lambda_0}^{0}\exp\left(-\frac{\lambda}{A}t^{A}\right)d\lambda,$$

where $\lambda_0 = C\exp(-m/\boldsymbol{k}T)$. Hence

$$\frac{d}{dt}(\Delta I) = \frac{\bar{\imath}p\boldsymbol{k}T}{t}A\left[1-\exp\left(-\frac{\lambda_0 t^{A}}{A}\right)\right].$$

In order to recover the experimental result that the change in intensity of magnetization due to magnetic viscosity is proportional to $\ln t$, it is necessary to assume that $\exp(-\lambda_0 t^{A}/A) \ll 1$. Taking typical values of the constants involved, it can be shown that this inequality is valid over the time range from 5 seconds upwards for all the ellipsoidal specimens used, as $\exp(-\lambda_0 t^{A}/A) < 0{\cdot}01$ in all cases. Hence $\Delta I = \bar{\imath}p\boldsymbol{k}TA\ln t + \text{const.}$ or

$$\Delta I = S_0(1 - qDS/\boldsymbol{k}T)\ln t + \text{const.} \qquad \ldots\ldots(27)$$

---

* See previous footnote on the validity of integrating integrals of this type between 0 to *t*.

where $S_0 = \bar{\imath}p\boldsymbol{k}T$. It will be noted that eqn. (27) reduces, in the case where $D=0$, to $\Delta I = S_0 \ln t + \text{const.}$, which has already been derived and discussed in I.

It is important to recognize that eqn. (27) gives that part of the observed change in intensity of magnetization which is due to thermal activation of the domains, a process which is irreversible in nature. A contribution to the intensity of magnetization due to reversible magnetic processes may also be present. In the present case, since the demagnetizing field increases with time, a reversible change of magnetization $= -DI(t)\chi_{\text{rev}}$ will take place, where χ_{rev} is the reversible magnetic susceptibility of the material. The total observed change of magnetization at any time t will then be the algebraic sum of the irreversible and reversible contributions, i.e. $\Delta I = S_0(1 - qDS/\boldsymbol{k}T)\ln t + \text{const} - D\chi_{\text{rev}}(S \ln t + K)$ or

$$\Delta I = [S_0(1 - qDS/\boldsymbol{k}T) - D\chi_{\text{rev}}S]\ln t + \text{const.} \qquad \ldots\ldots(28)$$

Comparing now eqns. (13) and (28), the observed slope S of the $(\Delta I, \ln t)$ curve for a given specimen is

$$S = S_0(1 - qDS/\boldsymbol{k}T) - D\chi_{\text{rev}}S, \qquad \ldots\ldots(29)$$

or rearranging

$$\frac{1}{S} = \frac{1}{S_0} + D\left(\frac{q}{\boldsymbol{k}T} + \frac{\chi_{\text{rev}}}{S_0}\right). \qquad \ldots\ldots(30)$$

Equation (30) thus represents the variation of S for a range of specimens manufactured from the same material but having different demagnetization coefficients D.

In order to check eqn. (30) experimentally, the reciprocals of the observed S values determined from the measurements on the ellipsoidal specimens described in § 3 and given in fig. 6, are shown plotted against D in fig. 9. The resulting straight line confirms the theoretical predictions and from it the values of $S_0 = \bar{\imath}p\boldsymbol{k}T$ (the slope of the $(\Delta I, \ln t)$ curve which would be obtained for an ideal specimen with $D=0$) and $(q/\boldsymbol{k}T + \chi_{\text{rev}}/S_0)$ may be determined. The value of χ_{rev} for the material of the specimen was measured and hence $q/\boldsymbol{k}T$ was found to be 0·83 oersted^{-1}. Measurements were also carried out on the longest of these ellipsoidal specimens using the method of discontinuous field variation described in § 5 and the result obtained was that $q/\boldsymbol{k}T = 0{\cdot}82$ oersted^{-1}. The good agreement between these values determined by independent experimental methods demonstrates the value of the formal theory and justifies the necessary approximations made in its development.

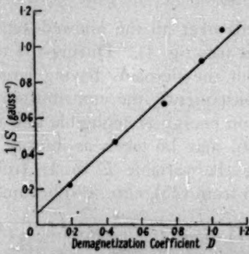

Fig. 9. The reciprocals of the slopes of the lines of fig. 6 plotted as a function of the demagnetization coefficients of the specimens.

§ 7. RELATION BETWEEN MAGNETIC VISCOSITY AND IRREVERSIBLE SUSCEPTIBILITY

7.1. *Formal Theory*

The domain processes responsible for the increment in magnetization at any point on the magnetization curve, consequent upon an increment in the applied field, may be divided into two groups, viz. those which contribute reversibly and those which contribute irreversibly to the magnetization of the material. The view that magnetic viscosity is due to the activation of domain processes which are in metastable equilibrium shows that the net contribution to the magnetic viscosity due to the activation of the reversible processes is zero. For such processes the domains return to their original stable positions once the perturbing action of the thermal fluctuations has been removed. On the other hand, in the case of the irreversible processes if the action of the thermal fluctuations is sufficiently large more stable domain configurations are achieved, hence on the removal of the perturbation a return to the original state is not possible. Hence as a good approximation it is possible to identify magnetic viscosity with the irreversible contribution to the magnetization of a material on the application of a field increment, considering the same domain processes to be responsible for the magnetic viscosity and for the irreversible component of the magnetic susceptibility. An approximate relation may then be derived between the quantities q and S characteristic of magnetic viscosity and the irreversible susceptibility.

A measure of the irreversible susceptibility may be derived by considering that an increment $+\Delta H_i$ in the internal field acting is applied at time $t=0$, i.e. at a time when the initial activation energy distribution function, shown in fig. 1 (*a*), has not been disturbed by thermal activation processes. Following the arguments already proposed above, the effect of ΔH_i is to move the origin of the activation energy axis to the right of the diagram, to O′, by an amount $\mathrm{OO}'=q\Delta H_i$. The number of domains which are activated by ΔH_i is represented by the area OO′BD of fig. 1 (*a*), $=pq\Delta H_i$. Thus the irreversible change of intensity of magnetization due to the activation of this number of domains is $\bar{i}pq\Delta H_i$, i.e. $\Delta I_{\mathrm{irr}}=\bar{i}pq\Delta H_i$ and $\chi_{\mathrm{irr}}=\bar{i}pq$. Since $\bar{i}p\boldsymbol{k}T=S_0$ (see eqn. (27))

$$\chi_{\mathrm{irr}}=qS_0/\boldsymbol{k}T. \qquad \ldots\ldots(31)$$

7.2. *Experimental*

In order to have a sufficiently wide range over which the predictions of eqn. (31) could be checked experimentally the quantities $q/\boldsymbol{k}T$, S and χ_{rev} were measured at a number of different points on the hysteresis cycle of the rod specimen of length 30 cm described in § 3. The values obtained, together with S_0, calculated from eqn. (30), are plotted as a function of the applied field in fig. 10. The practical determination of the ideal irreversible susceptibility χ_{irr} as defined in § 7.1 is strictly impossible owing to the disturbing effects of magnetic viscosity already discussed in II. However, it is believed that the method of measurement described in § 3 gives values of susceptibility approximating fairly well to the ideal. The difference between the measured (total) susceptibility and the reversible susceptibility, which is approximately equal to the irreversible susceptibility as defined above, is plotted against the field applied to the specimen in fig. 11. Also in this figure are plotted the values of $qS_0/\boldsymbol{k}T$ and it will be seen that there is reasonable agreement between the measured irreversible susceptibility and $qS_0/\boldsymbol{k}T$, as predicted by eqn. (31). The observed errors can probably be accounted for by the difficulties associated with the exact experimental measurements of χ_{irr}.

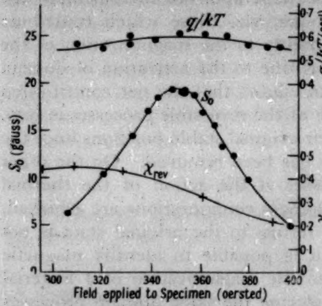

Fig. 10. Variation of $q/\boldsymbol{k}T$, S_0 and χ_{rev} as functions of the steady field applied during measurement.

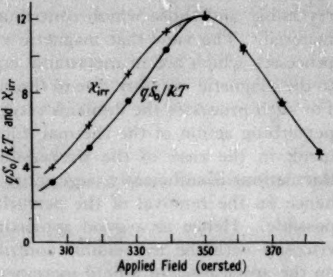

Fig. 11. Variation of χ_{irr} and $qS_0/\boldsymbol{k}T$ as functions of the steady field applied during measurement.

§ 8. DISCUSSION

Néel has recently developed a formal theory of the type of magnetic viscosity phenomena (traînage irréversible) described above, which is strictly applicable only to the Rayleigh region of magnetization of a ferromagnetic material (see for example the review article by Néel (1951)). In this theory the magnetic viscosity is represented formally by a time dependent fictitious field acting on the domains which varies, in terms of the symbols defined above, according to the relation $(S_0/\chi_{\mathrm{irr}})\ln t$. As already pointed out in § 7, the precise measurement of χ_{irr} in the specimens used in the present work is difficult, if not impossible. Consequently, comparison between Néel's theory and the present results is made more certain if the fictitious field envisaged by Néel is written as $(\boldsymbol{k}T/q)\ln t$ (see eqn. (31)). Néel has suggested that, at a fixed temperature, the value of $\boldsymbol{k}T/q$ is dependent only on the material of the specimen and is a constant throughout the whole of the magnetization cycle. The results plotted in fig. 10 show that in fact $\boldsymbol{k}T/q$ is reasonably constant over wide ranges of the magnetization curve; the values of the intensity of magnetization over which measurements were made extend from -300 to $+500$ gauss. From fig. 10 $\boldsymbol{k}T/q = 1{\cdot}76 \pm 0{\cdot}1$ oersteds at every point on the magnetization curve at which measurements were made. Barbier (1950) has made measurements of $\boldsymbol{k}T/q$ at points lying within the Rayleigh region using a similar specimen of alnico with a coercive force of 350 oersteds. The present measurements of $\boldsymbol{k}T/q$ at points on the magnetization curve, about the coercive force point, are in good agreement with Barbier's value of 1·7.

In his discussion of the mechanism responsible for 'traînage irréversible', Néel considers that the changes in intensity of magnetization due to magnetic viscosity are due to the thermal activation of domain boundary walls. On activation the domain boundary wall sweeps through a volume v which corresponds to a Barkhausen discontinuity. As a first approximation Néel has considered that v is independent of the temperature of the specimen and it then follows, from his analysis, that $\boldsymbol{k}T/q$ should be directly proportional to $T^{1/2}$. Results obtained by Barbier using an unspecified alnico specimen, and quoted by Néel (1951), indicate that in the Rayleigh region $\boldsymbol{k}T/q$ varies as $T^{3/4}$ approximately

Experiments have been carried out to determine the variation of $\boldsymbol{k}T/q$ at the coercive force point, as a function of the absolute temperature, for the specimen of alnico used in the measurements described in §§5 and 7. The results are shown in fig. 12 and it is seen that under these conditions $\boldsymbol{k}T/q$ is a linear function of T, at least over the temperature range from 90° K to 500° K, i.e. q is constant over this temperature range. The measured values of S_0 ($=\bar{i}p\boldsymbol{k}T$) as a function of absolute temperature are also plotted in fig. 12 and the resulting straight line shows that the product $\bar{i}p$ is also independent of the temperature of the specimen.

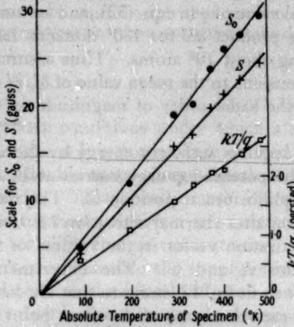

Fig. 12. Variation of S_0, S and $\boldsymbol{k}T/q$ as functions of absolute temperature.

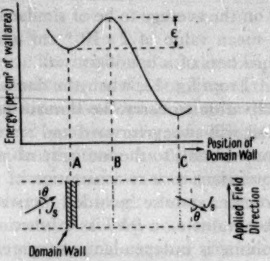

Fig. 13. Energy of domain system as a function of the position of the boundary wall.

An alternative physical interpretation of the quantity q may be derived from its definition given by eqn. (22), from which it may be seen that to a first order q is the ratio of the change in activation energy of the domains to the change in internal magnetic field. Consider now the variation in energy of a system of two domains as a function of the position of the boundary wall separating the domains, for constant internal field H_1. The situation envisaged is indicated diagrammatically in fig. 13; the directions of the two spontaneous magnetization vectors J_s are drawn in the usual way to ensure that the normal components of the vectors are continuous in passing through the boundary. As a result of the magnetization process let the boundary wall occupy the mean position A. Due to thermal processes, the nature of which does not enter into the discussion, the boundary wall will oscillate at random with A as a mean position. The activation energy ϵ per cm² of wall area is indicated on the diagram and is a measure of the difference in energy with the boundary wall at positions B and A. Now suppose the internal field changes by an amount ΔH_1. The resultant change in the difference between the energies of the system (per cm² of wall area) with the wall at points B and A is, to the first order in ΔH_1, $2\cos\theta J_s \Delta H_1 \delta l$ where δl is the distance from A to B. Thus if the area of the boundary wall is a the change in activation energy of the system is $E' = 2\cos\theta J_s \Delta H_1 a \delta l$. Hence from eqn. (22)

$$q = 2\cos\theta J_s a \delta l. \qquad \ldots\ldots (32)$$

.B
5
2

If magnetization proceeds by boundary movements between 180° domains, then $q=2J_s a\delta l$. The experimental observations given above show that q is independent of temperature and of the point of measurement on the magnetization curve. On the above interpretation, these experimental results show that, during the magnetization of the specimen of alnico investigated, the mean value of the product $a\delta l$ is a constant independent both of temperature and of the point of measurement on the magnetization curve. This conclusion seems to be a reasonable one from experiments on an alnico specimen which has been heat-treated to have a fairly high coercive force, since it is likely that the precipitated phase will provide centres for trapping the domain boundaries. It would appear very unlikely that the position and number of the precipitate 'impurities' embedded in the matrix would change appreciably over the range of temperature investigated. Substituting the experimental value of q in eqn. (32), and assuming an approximate value of $J_s=10^3$ gauss, the product $a\delta l$ for 180° domains has a value of 10^{-17} cm^3, i.e. a volume containing about 10^6 atoms. Thus assuming a on the average to be of similar linear dimensions to the mean value of δl, δl has a mean value of 2×10^{-6} cm which is of the same order of magnitude as the thickness of a boundary wall.

From fig. 13, when the domain system acquires sufficient energy by thermal activation to carry the domain wall over the potential energy barrier at B, the wall will sweep forward and reach stable equilibrium at position C. The mean contribution to the intensity of magnetization after thermal activation $\bar{\imath}$ is hence equivalent to a re-orientation of the magnetization vector in the volume of the domain system included between positions A and C. The experimental observations on $\bar{\imath}p\boldsymbol{k}T$ as a function of T, given in fig. 12, indicate that the latter volume is independent of temperature for measurements at the same point on the magnetization curve. In this interpretation, it is seen that the volume of material contributing to $\bar{\imath}$ is not necessarily related to the volume $a\delta l$. This distinction is not made in Néel's work.

It is possible to control the number and size of the precipitate islands in a material such as alnico by suitable heat treatment processes. By investigating these alloys by the methods described above, it would seem possible to obtain information concerning the processes of magnetization which may not be available from more conventional measurements. Such investigations are proceeding, and it is hoped to publish further details at a later date.

ACKNOWLEDGMENTS

The authors wish to thank Professor L. F. Bates for the facilities of his laboratory and for his encouragement throughout the work. Their thanks are also due to Imperial Chemical Industries Ltd. for the loan of electronic equipment, to Dr. Alun Edwards and Dr. K. Hoselitz who kindly supplied the specimens of alnico, to Mr. A. Hine for his helpful advice on the use of fluxgates and to Mr. J. H. Phillips who gave valuable assistance during the later stages of the experimental work.

REFERENCES

Barbier, J. C., 1950, *C. R. Acad. Sci., Paris*, **230**, 1040.
Hine, A., 1951, *Proc. Instn. Elect. Engrs.*, Pt. II, **64**, 485.
Néel, L., 1951, *J. Phys. Radium*, **12**, 339.
Smith, P. B., 1952, *Thesis*, University of Nottingham.
Street, R., and Woolley, J. C., 1949, *Proc. Phys. Soc.* A, **62**, 562 ; 1950, *Ibid.*, B, **63**, 509

The Threshold Gas Pressure Required to Sustain a Stable Arc in a Magnetic Field

By N. L. ALLEN
Electron Physics Department, University of Birmingham*

Communicated by J. Sayers; MS. received 28th April 1952

ABSTRACT. Measurements of the minimum pressure required for the operation of stable, pulsed, high-current arcs in hydrogen and air, in strong longitudinal magnetic fields, have been compared with earlier results obtained with helium. The values obtained are shown to be approximately those predicted by theoretical reasoning from the earlier work. Some relevant processes occurring in the discharge are discussed.

§ 1. INTRODUCTION

The conditions under which a stable electric arc may be maintained in a gas at low pressure are derived from the conditions for the stability of the double space-charge sheath of electrons and positive ions existing at the cathode. This sheath must contain a layer of positive ions of sufficient concentration to draw a large electron current density from the cathode spot. For stability, the gas concentration must allow adequate ionization per primary electron to maintain the supply of ions to the sheath. A longitudinal magnetic field reduces the lateral diffusion of ions to the walls of the tube, so enhancing their drift to the cathode. It also produces, at low pressures, a greater efficiency of ionization in the positive column on account of the helical paths of the electrons. Thus the threshold pressure required for stable operation is reduced by the action of the field. This paper contains the results of an investigation made by the author into the threshold pressure for pulsed high-current arcs between tungsten rod electrodes, and comparison is made with earlier work by Burhop, Massey and Page (1949), who used lower current arcs.

Theoretically, Burhop *et al.* adapted the conclusions of Bohm (1949) to show that the minimum pressure p, at which a stable arc of current J_c can exist, is given by:

$$\frac{J_c}{p}=\frac{f_k}{\alpha}\left(\frac{m_+}{m_e}\right)^{1/2}\psi(J_c,J_v), \qquad \ldots\ldots(1)$$

where f_k is the fraction of the ions formed which reaches the cathode sheath, α is a parameter of the order of unity, m_+ and m_e are the ion and electron masses respectively, and $\psi(J_c,J_v)$ is a function relating the rate of production of ions in the discharge column to the flux of neutral molecules through the column. J_v is the arc voltage drop.

Burhop *et al.* (1949) showed how this expression could be used for comparison of threshold pressures for discharges in different gases. J_c cannot be calculated absolutely for different values of p, since f_k cannot easily be estimated theoretically, but it is reasonable that f_k will be greater for light rather than for heavy ions in a longitudinal magnetic field, because the former are the more readily directed to the cathode by the field. The parameter α expresses the efficiency of the cathode in supplying the electron current density expected from a given positive ion current density to the sheath. It depends upon the nature of the cathode and may be calculated from the ratio of the positive ion to the electron current density (Langmuir 1929). As an approximation, this ratio will be assumed the same for each gas, and the cathodes will be assumed to be emitting thermionically in each case.

---

* Now N.R.L. Postdoctorate Fellow, Division of Physics, National Research Council of Canada, Ottawa.

Comparing discharges in hydrogen and helium

$$\frac{p^{\mathrm{H}}}{p^{\mathrm{He}}}=\frac{J_c^{\mathrm{H}}}{J_c^{\mathrm{He}}}\,\frac{f_k^{\mathrm{He}}}{f_k^{\mathrm{H}}}\,\frac{\alpha^{\mathrm{H}}}{\alpha^{\mathrm{He}}}\left(\frac{m_+^{\mathrm{He}}}{m_+^{\mathrm{H}}}\right)^{1/2}\frac{\psi^{\mathrm{He}}(J_c,J_v)}{\psi^{\mathrm{H}}(J_c,J_v)}, \qquad \ldots\ldots(2)$$

where the superscripts H, He signify the respective gases to which the quantities apply. The ratio of f_k's was deduced by Burhop *et al.* for different gases from measurements of J_c and p.

§ 2. EXPERIMENTAL TECHNIQUE

Burhop *et al.* tested the theory by using heated cathode discharges of a few amperes in various gases in longitudinal magnetic fields up to 11 700 gauss. In the present case, a pulsed magnetic field was set up in a specially designed solenoid (Champion 1950, Champion and Allen 1952). The field varied sinusoidally over one complete cycle, lasting 10 msec, and fields up to a peak of 23 000 gauss were available.

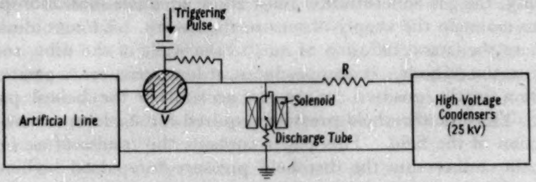

Circuit connections to the discharge tube.

In synchronism with the first half-cycle of the magnetic field pulse, a 'cold-cathode' discharge of current 96 amp was initiated, in hydrogen or air, between the ends of tungsten rod electrodes, 5·1 cm apart, in a glass-walled discharge tube of diameter 3·2 cm. The energy for the discharge was stored in the condensers of an artificial line, charged to 5 000 volts. This pulse was approximately rectangular and lasted 2 milliseconds. Breakdown of the gap was achieved by the application of a steady 25 000 volt initiating potential applied through a high resistance R to the anode, as shown in the figure. The two circuits were isolated from each other at all stages of operation by the resistance R and switching valve V. At low pressure, breakdown occurred only when the magnetic field was applied. A low-current discharge (about 1 amp) then passed. The sharp negative impulse given to the cathode of V when breakdown occurred caused the valve to conduct and, as the potential fall across the low-current discharge was less than 5 000 volts, the heavy current of the arc was able to pass. The form and stability of the arc current, and its phase relative to the magnetic field, were observed on an oscilloscope by observing the voltage drop across a small resistance in series with the discharge tube.

The tube was outgassed by baking and prolonged passage of arcs. It may be observed here that at the pressures employed in these experiments, as in those of Burhop *et al.*, the electronic and molecular free paths were greater than the dimensions of the discharge tube.

The technique used by Burhop *et al.* consisted of increasing the filament heating current gradually until the maximum current for arc stability was attained under steady conditions of gas pressure, magnetic field and anode voltage. Instability was marked by the onset of gross irregular fluctuation ('hash') in the steady discharge current, as observed with an oscilloscope. This criterion was applied in the present case. Their arrangement differed from the present one in that the cathode was situated outside the confines of the main discharge chamber, thereby allowing a free circulation of gas around it.

§ 3. EXPERIMENTAL RESULTS

The lowest pressure of hydrogen at which an arc of 96 amp was passed was $3{\cdot}2\times10^{-3}$ mm Hg, in magnetic fields of 1 475 gauss upwards. In all cases when breakdown was achieved, stable arcs of all currents up to this value were able to pass. The experiment was repeated with air in the tube. In this case, the gap was broken down and arcs passed at a minimum pressure of $2{\cdot}05\times10^{-4}$ mm Hg in magnetic fields of 2 000 gauss or more. The results of Burhop *et al.* for discharges of currents up to 6 amp in helium in magnetic fields greater than 1 900 gauss gave values of p^{He} between $2{\cdot}1\times10^{-3}$ mm Hg and $3{\cdot}1\times10^{-3}$ mm Hg with an arc potential drop of 200 volts. In the present case, the arc potential drop was 190 volts.

Substitution of appropriate values in eqn. (2) shows that $p^{\mathrm{H}_2}:p^{\mathrm{He}}=1{\cdot}5$ approximately for currents of 96 amp and 6 amp in hydrogen and helium respectively, at constant magnetic field. Similarly, $p^{\mathrm{H}}:p^{\mathrm{He}}=2{\cdot}5$ for the same current ratio in completely dissociated hydrogen at equal gas density. This predicts a threshold pressure of at least $3{\cdot}0\times10^{-3}$ mm Hg in hydrogen.

In the case of air, the ratio $p^{\mathrm{air}}:p^{\mathrm{He}}$ for a current of 96 amp in undissociated air would equal 2·0 approximately, and in completely dissociated air, 0·7. Thus, the threshold pressure would be predicted as at least $1{\cdot}5\times10^{-3}$ mm Hg.

§ 4. DISCUSSION

These results may be compared with the threshold pressures expected for a current of 6 amp in hydrogen and air. In these cases, approximate values are respectively: $p^{\mathrm{H}_2}:p^{\mathrm{He}}=1{\cdot}4$, $p^{\mathrm{H}}:p^{\mathrm{He}}=1{\cdot}8$, $p^{\mathrm{air}}:p^{\mathrm{He}}=0{\cdot}3$ (undissociated), $p^{\mathrm{air}}:p^{\mathrm{He}}=0{\cdot}2$ (dissociated). Thus, theory indicates that the threshold pressure for hydrogen is greater than, and that for air less than, the value for helium with the same current. Further, it shows that the threshold pressure increases slowly with a large increase in arc current. In the case of hydrogen, the experimental agreement is good. With air, the agreement is poor, but here the complex nature of the gas has been ignored in the theory, making it difficult to assess the true significance of the result.

The theory takes no account of ionization by secondary plasma electrons, liberated by collisions of the primary electrons from the cathode, or of the fact that f_k, the fraction of ions reaching the cathode, may vary with the arc current J_c. The former process is of importance at high current. This would effectively increase $\psi(J_c, J_v)$ in the expression and hence reduce the threshold pressure required. The variation of f_k is unknown. The evidence from the work of Burhop *et al.* is inconclusive, but suggests that in general f_k may increase with J_c. The present result for hydrogen does not throw much further light on the importance of either of these factors.

It is of interest to consider the general state of the arc at high current and low pressure. The arc current, supplied by the artificial line, increased at a finite rate, and the current reached 6 amp after 20 μsec. In this time, most neutral molecules in the tube had been able to pass through the column in the course of their thermal motion (assumed at room temperature) with a finite chance of ionization. Bohm (1949) points out that the total rate of ionization of neutral particles entering a surface area A of the column is:

$$R = \frac{Anv_n}{4}\left\{1-\exp\left(-\frac{J_e\sigma_i l}{v_n}\right)\right\}, \qquad \ldots\ldots(3)$$

where n is the concentration of neutral particles per cm^3, v_n is the average velocity of the neutral particles, σ_i is the ionization cross section for appropriate electron energy, l is the average distance traversed by the molecules in the column and J_e is the electron current (almost the same as J_c above).

Substitution shows that at a pressure of $3{\cdot}2\times10^{-3}$ mm Hg, a value of about 5×10^{17} ions/sec is obtained for the rate of ionization of neutral particles from a section of the arc column of radius 1 cm and length 1 cm*, for a current of 6 amp. It is clear that since the electron and ion free paths are greater than the inter-electrode spacing, recombination in the arc column is improbable. Thus, although the magnetic field reduces lateral diffusion of charged particles, the arc column brings about little increase in gas density within itself. The ions are removed to the cathode rapidly, mainly without collision, and the above figure gives, therefore, the approximate rate at which the ions reach the cathode. From the volume considered, the thermal flux of neutral hydrogen molecules is $2{\cdot}6\times10^{19}$ per sec (at room temperature). Thus, at this pressure, the arrival of positive ions from a discharge current of 6 amp constitutes an additional 2% to the flux of particles arriving at the cathode region. An analogous result occurs with air. At 96 amp (achieved after 0·3 msec), the positive ions form an additional 30% to the neutral flux. This estimate will be reduced if the gas temperature rises appreciably in this time. Thus, if recombination is extensive at the surfaces near the cathode, an appreciable localized increase of pressure may occur there, setting up a pressure gradient in the tube. Part of the arc column may therefore exist in a pressure of gas lower than that which is nominally the threshold pressure, ionization in this region being greatly assisted by the plasma electrons produced in the regions of increased gas density. Such a process may result in a change of state of the arc with a greater rate of ion production near the cathode, but it is difficult to reconcile it with the unexpectedly high pressures required for the higher currents in the experimental curves 5·11 to 5·13 of Burhop *et al.*, where the transport of particles is still comparatively small.

It is relevant to record here also the experimental fact that due to 'clean-up' of gas, the pressure of hydrogen was reduced from $3{\cdot}2\times10^{-3}$ mm Hg to less than

---

* Although the mean free path of the electrons may be appreciably greater than 1 cm with these conditions, the mean free path of the neutral atoms will likewise be greater. Consequently, the calculated quantities will not be the absolute values of the respective fluxes, but their ratio should give the approximate value of the ratio of the actual fluxes.

$2{\cdot}7 \times 10^{-3}$ mm Hg in the course of each 2 msec pulse. Thus, the arc was sustained by an average pressure lower than the threshold in the latter part of the pulse. It is probable that electrode vapour was produced in sufficient quantities to sustain the arc under these conditions. Extensive sputtering evident near the electrodes tended to support this view. The work of Tanberg (1930), using a copper cathode, suggested that even with tungsten electrodes production of electrode vapour may be appreciable for arc currents larger than a few amperes. Precise data on the proportion present are not available, but an accumulation of vapour near the electrodes would increase the rate of ion production there.

ACKNOWLEDGMENTS

The author wishes to acknowledge many helpful discussions with Professor J. Sayers and Dr. K. S. W. Champion. The work was made possible by the award to the author of a grant by the Department of Scientific and Industrial Research.

REFERENCES

BOHM, D., 1949, *The Characteristics of Electrical Discharges in Magnetic Fields* (New York : McGraw-Hill), Chap. 4.

BURHOP, E. H. S., MASSEY, H. S. W., and PAGE, G., 1949, *The Characteristics of Electrical Discharges in Magnetic Fields* (New York : McGraw-Hill), Chap. 5.

CHAMPION, K. S. W., 1950, *Proc. Phys. Soc.* B, **63**, 795.

CHAMPION, K. S. W., and ALLEN, N. L., 1952, *Elect. Engng.*, in the press.

LANGMUIR, I., 1929, *Phys. Rev.*, **33**, 954.

TANBERG, R., 1930, *Phys. Rev.*, **35**, 1080.

The Thermal Conductivity of Rare Gases

BY W. G. KANNULUIK AND E. H. CARMAN
Physics Department, University of Melbourne

Communicated by L. H. Martin; *MS. received* 10*th April* 1952

ABSTRACT. The thermal conductivity of the rare gases is determined in absolute measure by a 'hot wire' method at selected temperatures in the range −183° C to 306° C. The experimental values of the thermal conductivity are shown to be in good agreement with the values calculated according to the recent theory of Hirschfelder, Bird and Spotz in the above range of temperature. The quantity $\epsilon = K/\eta c_v$ is shown to be independent of the temperature, but the value of ϵ increases slowly with the molecular weight from a value 2·43 for helium to a value 2·58 for xenon.

§1. INTRODUCTION

THE present paper is an account of an experimental investigation of the conductivity of the rare gases between −183° C and +306° C. The work was undertaken primarily to test the recent extension of Chapman's theory (1912, 1916, 1918) due to Hirschfelder, Bird and Spotz (1948, 1949). The latter evaluated the collision integrals in the theory assumed valid for spherically symmetrical molecules. Their work is based upon the following interaction law :

the molecules attract each other according to the inverse sixth power and repel each other according to the inverse twelfth power of their separation. It may reasonably be assumed that the above theory would apply to the rare gases.

Previous work on the temperature variation of the conductivity of the rare gases is rather restricted in amount and in its temperature range. The principal investigations are those of Eucken (1911, 1913) on helium and argon between −252° c and 100° c, Weber (1918) on neon between −183° c and 100° c, and Johnston and Grilly (1946) on helium between −193° c and 100° c. In each case a 'hot wire' method was used but only in the case of Johnston and Grilly were absolute measurements of the conductivity made. In the present work determinations of the thermal conductivity of the five rare gases are made in absolute measure at selected temperatures in the range −183° c to 306° c. A hot wire method is used.

§ 2. DESCRIPTION OF THE CONDUCTIVITY CELL

The conductivity cell was specially designed for use over a considerable range of temperature. A platinum wire 11·6 cm long and 1·5 mm in diameter is mounted along the axis of a thin-walled metal tube approximately 7 mm in internal diameter. The tube was made from an alloy of 90% platinum and 10% iridium for greater mechanical strength. This choice of materials also ensures negligible differential expansion. The method of electrically insulating the wire from the tube is shown in the figure.

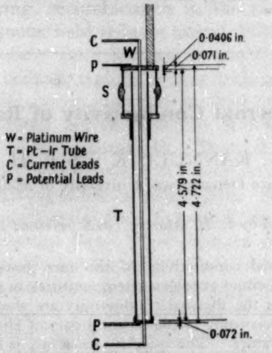

The conductivity cell has the following dimensions : diameter of the wire 0·1465 ± 0·0001 cm, length of the wire 11·631 ± 0·0005 cm, mean internal diameter of the tube 0·7169 ± 0·0005 cm.

§ 3. THEORY

A complete account of the theory of the 'hot wire' method used in the present work has been given in an earlier paper by Kannuluik and Martin (1934). The theory used is based upon the actual distribution of the temperature in the steadily heated wire and in the ambient gas, subject to the boundary condition that both ends of the wire and the wall of the tube are held at a constant temperature, taken for convenience as an arbitrary zero.

The differential equation for the steady flow of heat along the wire and in the ambient gas is

$$\lambda\pi b^2 \frac{\partial^2\theta}{\partial z^2} + 2\pi bK\left(\frac{\partial\theta}{\partial r}\right)_{r=b} + \frac{I^2\rho(1+\alpha\theta)}{J} = 0 \qquad \ldots\ldots(1)$$

where λ and K are respectively the thermal conductivities of the wire and the gas, I is the steady current in the wire, $\rho_\theta = \rho(1+\alpha\theta)$ is the resistance per unit length of wire at temperature θ, J is the mechanical equivalent of heat, and $2b$ is the diameter of the wire.

The exact solution of (1) subject to the above boundary condition is given by Kannuluik and Martin (1934).

For practical purposes it is more convenient to assume a strictly radial flow of heat from the wire surface and to make a correction for the end effect. On this basis eqn. (1) assumes the simpler form

$$\lambda\pi b^2 \frac{\partial^2\theta}{\partial z^2} + 2\pi bh\theta + \frac{I^2\rho(1+\alpha\theta)}{J} = 0, \qquad \ldots\ldots(2)$$

where

$$h = K/b\ln(a/b) \qquad \ldots\ldots(3)$$

and $2a$ is the internal diameter of the tube. The quantity h (the external conductivity) is directly measured in all 'hot wire' experiments.

The solution of (2) is :

$$f(\beta l) = \left(\frac{1}{\beta l}\right)^2\left(1 - \frac{\tanh\beta l}{\beta l}\right) = \frac{2\pi b^2\lambda J(\bar{R}-R)}{R^2I^2\alpha l}, \qquad \ldots\ldots(4)$$

with

$$\beta^2 = \frac{2h}{b\lambda} - \frac{I^2R\alpha}{2\pi b^2J\lambda l},$$

where $\bar{R}$ is the resistance of the wire when a current I amperes is flowing; and R is the resistance at the bath temperature, i.e. for $I=0$.

Relation (4) is a good approximation to the exact solution of eqn. (1). A comparison of this with (4) discloses that, over a wide range of gas conductivities, the values of K obtained from (4) and (2) are too high by a little less than 1%. In the present work we have used the approximate theory and have applied this correction to the values of K given by (4) and (3).

By expanding $\tanh\beta l$ in (4) as a power series the following convenient formula giving λ explicitly can be obtained:

$$\lambda = \frac{1}{6}\,\frac{\bar{R}RI^2\alpha l}{\pi b^2J(\bar{R}-R)}\left(1 + \frac{1}{30}\,\frac{RI^2\alpha l}{\pi b^2J\lambda}\right)\left(1 - \frac{4}{5}\,\frac{h_Rl^2}{b\lambda}\right). \qquad \ldots\ldots(5)$$

This formula is a valid approximation except at temperatures above 100° c. Here the general formula (4) should be used for determining λ.

§ 4. ABSENCE OF CONVECTION

The effect of convection on the conductivity of a gas confined between coaxial cylindrical surfaces has been studied experimentally by Weber (1917) and theoretically by Ulsamer (1936). Ulsamer's analysis leads to the following conclusions. The effect of convection increases according to (*a*) the cube of the annular gap between the cylindrical surfaces, (*b*) the temperature drop across the annular gap, and (*c*) the square of the density of the gas. In accordance with (*c*) the test of the absence of convection over a range of gas pressure is that the observed conductivity is independent of the pressure. This test disclosed that convection was entirely absent in the conductivity cell used in the present work even at pressures somewhat above atmospheric pressure. This was achieved by making the annular gap sufficiently small and by adopting working conditions for the cell giving a small temperature drop across the annular gap of about 3° only.

§5. THE TEMPERATURE 'JUMP' EFFECT

Even in the absence of convection effects the apparent conductivity of a gas may still decrease as the pressure of the gas is reduced on account of the existence of the temperature 'jump' which occurs at the surface of the wire and the inner surface of the tube. To take this effect into account it is necessary to replace relation (3) by the more general relation

$$h = K \Big/ b\left\{\ln\frac{a}{b} + \gamma\left(\frac{1}{a} + \frac{1}{b}\right)\right\},$$

where γ is the temperature 'jump' distance and is inversely proportional to the gas pressure.

In the working range of gas pressures (35 to 76 cm Hg) used in the present work, the temperature jump term $\gamma(a^{-1} + b^{-1})$ was negligible in comparison with $\ln a/b$. This is one of the advantages of employing a thick heating wire instead of the fine wires used in the traditional forms of the 'hot wire' method. The fact that the gas conductivities determined in the present investigation by applying (4) and (3) are independent of the pressure over the working range of pressures implies (*a*) the complete absence of convection, (*b*) that the temperature jump effect is negligible.

§6. TEMPERATURE CONTROL

The authors have determined the gas conductivities in the present work at selected fixed points on the International Temperature Scale.

The following standard or sub-standard temperatures were reproduced:

(i) The temperature of equilibrium between liquid oxygen and its vapour (−182·97° c).
(ii) The temperature of equilibrium between solid carbon dioxide and its vapour (−78·5° c).
(iii) The melting point of ice (0° c).
(iv) The boiling point of water (100° c).
(v) The temperature of equilibrium between liquid naphthalene and its vapour (218·0° c).
(vi) The temperature of equilibrium between liquid benzophenon and its vapour (305·9° c).

For reproducing points (iv), (v) and (vi) in the above list a simple metal hypsometer heated by a bunsen flame was used in each case. A U-tube water manometer to record the gas pressure was found useful for regulating the gas flame to give a steady temperature. The CO_2 point (ii) proved to be the most difficult to reproduce. It was found necessary to use a stirred bath of CO_2 slush (solid CO_2 with alcohol or petroleum ether) since an unstirred bath could not take up the heat dissipated in the conductivity cell rapidly enough to prevent an appreciable overall rise of temperature in the wall of the cell.

The following is a brief description of the stirred bath. A cylindrical Pyrex glass container 14 inches long and 3 inches in diameter is insulated on the outside with a layer of cotton wool. A wire gauze cylinder 11 inches long and 1½ inches in diameter is open at the top and closed at the bottom. This is mounted axially in the glass container with the lower end of the cylinder 1½ inches above the bottom of the container. The annular space between the cylinder and the container is filled with fragmented solid CO_2. The container is filled with the liquid and the conductivity cell immersed in the liquid within the gauze cylinder. The liquid contents of the cylinder are stirred with a mechanically operated plunger-type stirrer. The plunger consists of a thin vertical brass rod with attached metal vanes and in the up and down movement of the stirrer the vanes are always close to the cell wall. This type of stirred bath maintains the equilibrium temperature with complete steadiness. It may be operated indefinitely provided solid CO_2 is added from time to time. The equilibrium temperature is recovered within a few minutes after adding the solid CO_2.

The temperature of the liquid oxygen used for the oxygen point was checked by means of an oxygen vapour pressure thermometer provided with a vacuum-jacketed stem. The bulb of the thermometer touched the wall of the cell at its middle point. An unstirred liquid oxygen bath is subject to irregular fluctuations of temperature; these, however, disappear when the liquid oxygen is stirred in the same way as the CO_2 bath. With the oxygen and the CO_2 bath the authors found that thermocouple readings were more reliable than barometer readings for following the changes in the bath temperature on account of changes in the atmospheric pressure.

§7. CALIBRATION OF THE CONDUCTIVITY CELL

This involves an accurate determination of the following quantities: (*a*) the resistance R of the wire, (*b*) the temperature coefficient of resistance α, (*c*) the wire conductivity λ. All three quantities have to be known at each of the standard and sub-standard temperatures given in the preceding paragraph.

A five-dial low-resistance Wolff potentiometer is used to measure corresponding values of $\overline{R}$ and I in terms of a standard 0·01 ohm Tinsley resistance and a Weston standard cell. The resistance measurements are made to six significant figures for four or five values of the heating current I. A linear relation connects $1/\overline{R}$ and I^2, and by plotting corresponding values on a large sheet of squared paper R is obtained by extrapolation to zero current.

The corresponding values of α are obtained from the above resistance measurements by applying the formulae used in platinum thermometry connecting the resistance and the temperature. For the temperature range 0° to 306° c the following formula is used: $R=R_0(1+At+Bt^2)$, while for the range $-183°$ c to 0° c the appropriate formula is $R=R_0\{1+At+Bt^2+C(t-100)t^3\}$ where R_0 is the value of R at 0° c, t is the temperature in degrees centigrade and A, B and C are constants.

After evaluating A, B and C the required values of the temperature coefficient α are deduced by differentiating the two resistance formulae and applying the defining relation $\alpha=R^{-1}\,dR/dt$. It is convenient to carry out the calibration with the cell highly evacuated. (A two-stage oil diffusion pump with cold trap was used to reduce the pressure below 10^{-5} mm Hg.) The wire conductivity can then be calculated for each of the temperatures by means of formula (5) using the set of observations of $\overline{R}$ and I made at each temperature.

In this way the complete calibration of the conductivity cell can be made to depend on a single set of observations made at each temperature. The calibration data are given in table 1.

Table 1. Calibration of the Constants of the Conductivity Cell

$A=0{\cdot}0039573$; $B=-5{\cdot}695\times10^{7}$; $C=-4{\cdot}175\times10^{-12}$

t (° c)	R (ohm)	α	(cal cm^{-1} sec^{-1} ° c^{-1})
−182·97	0·00171601	0·01727	0·1657
−75·5	0·00471235	0·005929	0·1645
0	0·00687701	0·003957	0·1679
100	0·00955924	0·002765	0·1721
218·0	0·0126236	0·002021	0·1753
305·9	0·0148190	0·001675	0·1776

The effect of an error in the determination of λ on the gas conductivity is dealt with below.

§ 8. EXPERIMENTAL RESULTS

In preparing for measurements of the rare gases the conductivity cell was connected to the high vacuum pumping system and to a mercury lift to which was attached an open tube mercury manometer. After evacuating the system as completely as possible the pumping system was sealed off and the gas (quoted as spectroscopically pure) was introduced from the source of supply—a one-litre glass flask. This flask was then sealed off thus leaving a compact closed system consisting of the cell, the mercury lift and the attached manometer. By this arrangement all the conductivity measurements on a particular gas were made on a single sample of the gas. The apparatus was filled with gas at atmospheric pressure, but by means of the mercury lift measurements could be made at any intermediate pressure down to a limiting pressure of 7 cm Hg.

The procedure followed for determining a gas conductivity is similar to that for the wire conductivity. A few observations of $\overline{R}$ and I for different values of I are made in order to check the value of R at the particular temperature. Then a series of observations of $\overline{R}$ and I for a single heating current are made for a series of gas pressures.

An example of the procedure followed in determining a gas conductivity is given in table 2. The figures refer to observations on neon at 100° c.

Table 2. Conductivity of neon at 100° c; mean temperature of gas 101·4° c

Pressure (cm Hg)	I (ampere)	$(\overline{R}-R)$ (ohm)	$f(\beta l)$	β^2	$K'\times10^5$	$K\times10^5$
75·07	3·6197	0·00007589	0·095876	0·18726	13·93	13·58
66·43	3·6201	0·00007587	0·095831	0·18739	13·94	13·59
57·42	3·6201	0·00007585	0·095805	0·18747	13·95	13·59
50·14	3·6200	0·00007592	0·095894	0·18721	13·93	13·57
41·89	3·6201	0·00007602	0·096024	0·18684	13·83	13·47
33·82	3·6201	0·00007598	0·095969	0·18700	13·92	13·56
25·56	3·6201	0·00007590	0·095868	0·18729	13·94	13·58
17·40	3·6201	0·00007581	0·095755	0·18760	13·96	13·60

To obtain the correct value of the conductivity at 100° c the following corrections are applied: a radiation correction amounting to $0{\cdot}16\times10^{-5}$, reduction of the conductivity to 100° c using a temperature coefficient of K equal to 0·003, a 'radial flow' correction of amount $0{\cdot}14 \times 10^{-5}$. Each of these corrections is subtractive.

Values of the conductivity of the five rare gases over the temperature range are listed in table 3.

Table 3. The Conductivities of the Rare Gases ($K \times 10^5$)

t (° c)	He	Ne	A	Kr	Xe
−182·97	16·55	4·89	1·41	—	—
− 78·5	27·06	8·76	2·93	1·52	0·915
0	34·06	11·10	3·94	2·08	1·23
100	41·65	13·57	5·06	2·72	1·68
218·0	49·47	15·95	6·14	3·40	2·08
305·9	55·04	17·89	6·85	3·88	2·37

§ 9. REMARKS ON THE 'HOT WIRE' METHOD USED IN THE PRESENT WORK

(i) *The Radiation Correction*

Both the wire conductivity λ and the gas conductivity K are subject to a correction on account of the heat transfer by radiation. At temperatures below 0° c the correction is very small; above 0° c it increases rapidly with the temperature. The computed amounts of the correction to λ at temperatures 0, 100, 218, 306° c are 1, 3, 8, 20% respectively. Since the computation of the radiation correction is an approximation only, the absolute values of λ at the two highest temperatures may be subject to an error on this account. It is important to examine the effect of this on the gas conductivity.

If we assume the value of h_R at 306° c computed from $4e\sigma T^3$ is correct, then for the measurements at 306° c it can be shown that an error of $\pm 50\%$ in h_R leads to an error of only $\pm 3\%$ in K for krypton ($K = 3{\cdot}88 \times 10^{-5}$ at 306° c) and to an error of $\pm 0{\cdot}5\%$ in helium ($K = 55{\cdot}04 \times 10^{-5}$ at 306° c). It follows that the present method is to a considerable extent self-compensating for errors made in estimating the value of h_R. Only in the case of the two gases of very low conductivity, krypton and xenon, is a small error in K at 306° c possible on account of radiation.

(ii) *The Effect of an Error in the Wire Conductivity*

It is essential in the present method that the values of the wire conductivity λ uncorrected for radiation should be determined accurately.

If Q_E/Q is the ratio of the heat conducted out of the ends of the wire per second to the total heat generated in the wire per second, then it is evident that the smaller the gas conductivity K the greater will be the value of Q_E/Q. The results of a simple calculation are given in table 4 where the figures in the first and third columns are corresponding values of K and Q_E/Q. The latter quantity

Table 4. The Heat Flowing through the Ends of the Hot Wire and the Effect of a 1% Error in λ on K

$K \times 10^5$	1	2	5	10	20	30	40	50	60
$\Delta K/K\%$	5·4	2·7	1·1	0·54	0·27	0·18	0·14	0·11	0·09
Q_E/Q	0·86	0·76	0·56	0·39	0·24	0·17	0·14	0·11	0·095

is independent of the heating current in the wire and nearly independent of the gas. The figures in the second column represent the percentage error in the gas conductivity K due to an assumed error of 1% in the wire conductivity.

Clearly the limitations imposed by the wire conductivity on the present method become serious only in gases of very low conductivity (xenon and krypton). The wire conductivities λ at each of the six temperatures are determined to an absolute accuracy much greater than 1%. The data given below in table 5 would indicate that the limit of the method is being approached in the case of the gas xenon.

§ 10. DISCUSSION OF THE RESULTS

The most interesting deduction from the kinetic theory of gases relevant to the present work is the relation $K=\epsilon\eta c_v$ connecting the gas conductivity K with the viscosity η and the isometric specific heat c_v.

For molecules assumed to be spherically symmetrical point centres of force repelling each other according to an inverse fifth power law of interaction Maxwell obtained for the constant ϵ the value of 5/2. The theory of Maxwell was generalized by Chapman to include inverse repulsion between the molecules to the sth power of the interaction distance where s may assume any value up to ∞. The different values of s produce values of ϵ only slightly greater than Maxwell's value of 5/2. Thus it would appear that the value $\epsilon=2{\cdot}5$ is fundamental in classical mechanics and independent of the interaction forces between the molecules. It is also implied in the above theories that ϵ is *nearly* independent of the temperature.

The present work probably represents the most comprehensive attempt at a verification of the above conclusions. The experimental values of ϵ for the five rare gases are given in table 5. These values are computed from the values of K obtained in the present investigation, smoothed values of η obtained from the available viscosity data, observed values of c_v for helium, neon and argon, and calculated values of c_v for krypton and xenon.

That ϵ is independent of the temperature is confirmed by the present investigation, but the values of ϵ for the different gases increase slowly with the molecular weight; in fact, if the values of ϵ are plotted against the molecular weight of the gas, a smooth curve is obtained. The value of $\epsilon=2{\cdot}43$ for helium is appreciably less than the theoretical value of 2·5. The authors are of the opinion that the difference between the observed and the theoretical value of ϵ for helium is real and not fortuitous. In the other rare gases, too, the differences are also significant.

Values of the gas conductivity calculated from the recent theory of Hirschfelder, Bird and Spotz (1948, 1949) are also included in table 5. On this theory the values of K at different temperatures and for the different gases are calculated from the formula

$$K=2{\cdot}6693\times10^{-5}\frac{(MT)^{1/2}H}{r_0^2W_{(2)}^{(2)}}\,\frac{5}{2}c_v$$

where M is the molecular weight, T the absolute temperature. The quantities r_0, H and $W_{(2)}^{(2)}$ are tabulated functions given by Hirschfelder, Bird and Spotz (1948, 1949).

Table 5. The Calculated and Observed Values of K and the Experimental Values of $\epsilon = K/\eta c_v$

	Helium (c_v=0·746)				Neon (c_v=0·150)			
t (° c)	$K_{\mathrm{calc}}\times 10^5$	$K_{\mathrm{obs}}\times 10^5$	$\eta\times 10^7$	$\epsilon=K/\eta c_v$	$K_{\mathrm{calc}}\times 10^5$	$K_{\mathrm{obs}}\times 10^5$	$\eta\times 10^7$	$\epsilon=K/\eta c_v$
−182·97	16·8	16·55	914	2·43	5·00	4·89	1308	2·49
− 78·5	27·7	27·06	1500	2·42	8·85	8·76	2359	2·48
0	34·5	34·06	1873	2·44	11·13	11·10	2965	2·48
100	42·4	41·65	2292	2·44	13·60	13·57	3643	2·48
218·0	50·7	49·47	2732	2·43	16·22	15·95	4353	2·44
305·9	56·3	55·04	3065	2·42	18·02	17·89	4833	2·47
mean				2·43 ± 0·01				2·47 ± 0·01

	Argon (c_v=0·0745)				Krypton (c_v=0·0355)			
t (° c)	$K_{\mathrm{calc}}\times 10^5$	$K_{\mathrm{obs}}\times 10^5$	$\eta\times 10^7$	$\epsilon=K/\eta c_v$	$K_{\mathrm{calc}}\times 10^5$	$K_{\mathrm{obs}}\times 10^5$	$\eta\times 10^7$	$\epsilon=K/\eta c_v$
−182·97	1·38	1·41	755	2·50	—	—	—	—
− 78·5	2·90	2·93	1558	2·52	1·47	1·52	—	—
0	3·92	3·94	2105	2·51	2·06	2·08	—	—
100	5·04	5·06	2700	2·51	2·73	2·72	—	—
218·0	6·18	6·14	3305	2·50	3·43	3·40	—	—
305·9	6·96	6·85	3705	2·48	3·90	3·88	—	—
mean				2·50 ± 0·01				

	Xenon (c_v=0·0227)			
t (° c)	$K_{\mathrm{calc}}\times 10^5$	$K_{\mathrm{obs}}\times 10^5$	$\eta\times 10^7$	$\epsilon=K/\eta c_v$
−78·5	0·85	0·91	—	—
0	1·21	1·23	2105	2·58
100	1·61	1·68	2836	2·61
218·0	2·04	2·08	3552	2·58
305·9	2·34	2·37	4118	2·54
mean				2·58 ± 0·01

ACKNOWLEDGMENT

The authors take pleasure in recording their indebtedness to Professor L. H. Martin for the research facilities provided and in thanking him for his interest in the work.

REFERENCES

Chapman, S., 1912, *Phil. Trans. Roy. Soc.* A, **211,** 433; 1916, *Ibid.*, **216,** 279; 1918, *Ibid.*, **217,** 115.

Eucken, A., 1911, *Phys. Z.*, **12,** 1101; 1913, *Ibid.*, **14,** 324.

Hirschfelder, J. O., Bird, R. B., and Spotz, E. L., 1948, *J. Chem. Phys.*, **16,** 968; 1949, *Chem. Rev.*, **44,** 205.

Johnston, H. L., and Grilly, E. R., 1946, *J. Chem. Phys.*, **14,** 233.

Kannuluik, W. G., and Martin, L. H., 1934, *Proc. Roy. Soc.* A, **144,** 496.

Ulsamer, J., 1936, *Z. Ver. dtsch. Ing.*, **80,** 537.

Weber, S., 1917, *Ann. Phys., Lpz.*, **54,** 325; 1918, *Commun. Phys. Lab. Univ. Leiden, Suppl.*, **42b,** 14.

On the Variations of Lattice Parameters of some Semiconducting Oxides

By L. D. BROWNLEE and E. W. J. MITCHELL*
Research Department, Metropolitan-Vickers, Trafford Park, Manchester

Communicated by B. G. Churcher; *MS. received 28th April* 1952

ABSTRACT. Measurements have been made of the lattice parameters of the substitutional semiconductors Ni(Li)O, $Fe_2(Ti)O_3$ and also of reduced Mg_2TiO_4. The contraction of the nickel oxide lattice, which was briefly reported by Verwey *et al.* (1950), has been observed for a series of compositions. We have also observed the expansion of the Fe_2O_3 lattice associated with the production of Fe^2 ions. Similarly, the expansion which accompanies the reduction of the spinel Mg_2TiO_4 is attributed to the formation of Ti^3 ions. The lattice parameter of stoichiometric nickel oxide is believed to be 4·1726 ± 0·0002 kx (4·1811 Å) while that of unreduced magnesium titanate is found to be 8·425 ± 0·0005 kx (8·442 Å).

---

§ 1. INTRODUCTION

VERWEY and co-workers (1950) have reported lattice parameter measurements of two compositions of the Ni(Li)O system which indicated that a lattice contraction accompanied the incorporation of lithium ions in the nickel oxide lattice. In the atomic model of electronic conductivity in oxides which has been developed by de Boer and Verwey (1937) and Verwey *et al.* (1948, 1950) the conductivity of nickel oxide containing lithium is associated with the production of trivalent nickel ions. It was suggested that the observed lattice contraction was due to these ions which have Goldschmidt radii of 0·35 Å compared with the 0·78 Å of Li^1 and Ni^2 ions.

On the basis of this model the conductivity of an n-type substitutional oxide, for example $Fe_2(Ti)O_3$, results from the presence of a concentration of the larger Fe^2 ions equal to the concentration of substituted Ti^4. It was clearly desirable to extend the lattice parameter measurements to such a system. In this paper we present the results of a series of measurements on the $Fe_2(Ti)O_3$ system which confirm the expected expansion.

In non-stoichiometric compounds the conductivity is, with some exceptions, associated with the presence of higher or lower charged ions, but in these cases there also exist cation or anion vacancies. For example, in reduced magnesium titanate the defect which produces conductivity is an oxygen ion vacancy two of whose neighbouring titanium cations—normally Ti^4—are Ti^3. In § 3 we show, from a series of measurements on magnesium titanate specimens of different conductivity, that the net result of the readjustment of the lattice is an expansion.

On the other hand in an oxide in which electronic conduction is produced by oxidation, as for instance in nickel oxide, the defect consists of an Ni^2 ion vacancy accompanied by two Ni^3 ions. Lattice parameter determinations of nickel oxide specimens which have undergone various heat treatments show that in this case the net effect is a contraction. These results when considered with our measurements on the Ni(Li)O series provide the interesting conclusion that for none of these thermal treatments is stoichiometric nickel oxide obtained.

* Now at University of Reading.

§ 2. EXPERIMENTAL PROCEDURE

(i) *Preparation of Specimens*

The specimens were prepared by the usual sintering techniques. For the nickel oxide–lithium solutions the two carbonates were prefired at 900° c either in powder form or as large discs. Having been pressed into smaller discs the decomposed carbonates were sintered in air at 1 200° c. The amounts of lithium in the sintered samples were determined chemically* and the analysis showed that some of the lithium originally added had been lost during the sintering process. A range of compositions of up to 1 atomic % was prepared for each firing, the colours ranging from green to black while the resistivity fell from $10^7\,\Omega$ cm to $10\,\Omega$ cm as has been found by Verwey *et al.* (1948).

Samples of ferric oxide containing substituted titanium were prepared in a similar manner, by sintering pressed discs of mixtures of ferric and titanium oxides in air at 1 200° c. Chemical analysis showed that only a small fraction of the original titanium content was lost during the firing of these specimens.

Insulating magnesium titanate, Mg_2TiO_4, was prepared by sintering a mixture of the oxides at 1 400° c in air; this material was afterwards rendered black and conducting by controlled reduction in hydrogen at 1 200 to 1 250° c. Jones (1950, unpublished) has found that there is a measurable loss in weight during this reduction—measurable when the final resistivities are less than about $10^6\,\Omega$ cm—and this has been used to calculate the concentration of anion vacancies and Ti^3 ions which are produced.

(ii) *X-Ray Measurements*

Powder photographs of the specimens were taken with a 9 cm camera. In the case of ferric oxide a strong diffraction line was obtained in the region of $\theta = 80°$, using iron filtered cobalt radiation, and there was a measurable variation in the position of this line as the titanium content of the samples was altered. The spacing of the crystal planes giving rise to this reflection was calculated and the change in spacing was taken as a measure of the change in parameter. The displacement of lines for angles less than 80° was too small to measure accurately so that we were not able to use an extrapolation method to determine directly the variations in parameter.

Nickel filtered copper radiation was used for the examination of the spinel magnesium titanate. After indexing the lines on the powder photograph the lattice parameters of specimens were measured using the extrapolation method of Bradley and Jay (1932). For insulating magnesium titanate we find a parameter of $8{\cdot}425 \pm 0{\cdot}0005$ kx ($8{\cdot}442 \pm 0{\cdot}0005$ Å), which is higher than the value of Holgerrsin and Herrlin (1931), $8{\cdot}439 \pm 0{\cdot}003$ Å. The latter, however, was obtained using a 4·99 cm camera and the parameters determined for lines between $\theta = 22°$ and 72° varied in a random manner from 8·422 to 8·454 using copper radiation and from 8·425 to 8·462 using iron.

Until recently nickel oxide has been considered to have a face centred cubic structure but the work of Rooksby (1943, 1948) has shown that at room temperature the lattice is slightly distorted to give a rhombohedral cell of 60° 6′. At temperatures which correspond to its antiferromagnetic Curie temperature the lattice becomes truly face centred cubic with a rhombohedral cell of angle 60°.

---

* This analysis was kindly performed by the Johnson, Matthey Company's Research Laboratories.

This distortion at room temperature was not apparent in our photographs taken with the 9 cm camera. With a 19 cm camera, however, and using nickel radiation we found that, for both the α_1 and α_2 emissions, the 422 line was split into two components, neither of which was perfectly resolved. The addition of progressively larger amounts of lithium to the nickel oxide tended to reduce the separation of the two components and consequently the angle of the rhombohedral cell. We could not obtain detailed measurements of this change because of the broadening of the lines which was also present using the large camera, and which was probably due to slight local variations of the lithium concentration accompanied, as will be described below, by variations in lattice parameter. For the present work, however, we are not concerned with these effects since the displacement of the 422 line due to the change of lattice parameter following the addition of lithium was much greater than the separation of the various components of this line. The lattice parameter measurements of nickel oxide which are reported in this paper were taken using a 9 cm camera in which the variation of parameter with lithium concentration was easily observed but in which the effects of the slight rhombohedral distortion were not apparent. Both copper and cobalt radiations were used for each sample and the lattice spacing calculated from both photographs by means of the Bradley–Jay extrapolation. In all cases good agreement was obtained and each measurement given on fig. 1 or in the table is accurate to ± 0·0002 kx.

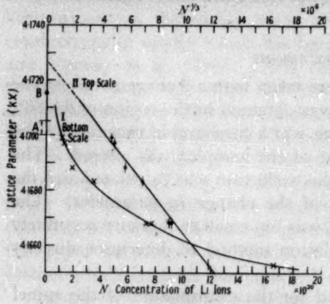

Fig. 1.

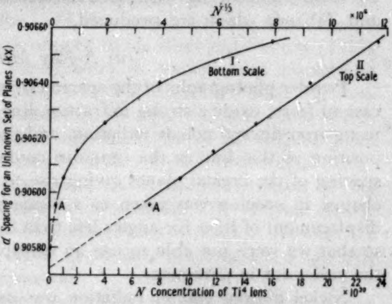

Fig. 2.

§ 3. DISCUSSION OF RESULTS

The results plotted in figs. 1, 2 and 3 show smooth changes of lattice parameter as the concentration of defects is increased. The contraction in $Ni^2_{1-2x}(Li^1_xNi^3_x)O$, predicted by the simple atomic model and previously reported by Verwey (1950), is seen in fig. 1; figs. 2 and 3 show the expansion which is expected on this model, as a result of the production of Fe^2 ions in $Fe^3_{2-2x}(Ti^4_xFe^2_x)O_3$ and Ti^3 ions in reduced Mg_2TiO_4 respectively. The curves II in each case indicate that over the measured range the following relation is valid: $d = d_0 \pm kN^{1/3}$ or $\Delta d^3 = (d-d_0)^3 = \pm k^3N$ where d is the lattice parameter, d_0 and k are constants and N is the concentration of defects. On extrapolating the $(d, N^{1/3})$ curve for magnesium titanate to zero, we see that, within the limits of error, the extrapolated value of spacing corresponds with that measured on a nominally pure specimen. In this condition magnesium titanate is colourless and a good insulator so that we are quite justified in saying that the value 8·425 ± 0·0005 kx refers to stoichiometric magnesium titanate. That the extrapolated value is the same suggests that the constant d_0 above is the lattice parameter of the defect-free crystal. The nominally pure specimens of nickel oxide which we prepared, however, were far from being insulating and had in fact resistivities of the order of 10^7 to $10^8\,\Omega$ cm at room temperature, while the measured lattice spacings never exceed 4·1715 kx as against the extrapolated value of 4·1726. This suggests that in contrast to the magnesium titanate results the $N=0$ nickel oxide specimens were not of stoichiometric composition

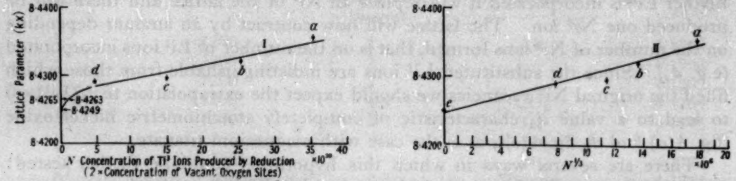

Fig. 3. Curve I shows a conducting sample for which the weight loss was too small to detect, i.e. having $N <$ the value for specimen d, and which had a lattice parameter of 8·4265 kx. A slightly higher resistance specimen gave 8·4263 kx.

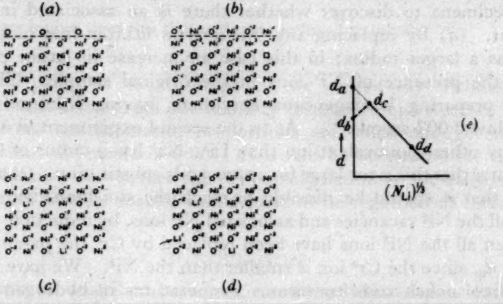

Fig. 4. Formation of defects in nickel oxide and associated change in lattice parameters.

(*a*) Stoichiometric nickel oxide with adsorbed oxygen atoms (d_a). (*b*) Illustrating formation of Ni^2 vacancies (d_b). (*c*) Ni^3 vacancies filled by Li^1 ions (d_c). (*d*) After (*c*) Li^1 ions substituted for Ni^2 (e.g. d_d).

and that there were sufficient Schottky defects produced (fig. 4) under the sintering conditions to affect the lattice parameter. In the case of ferric oxide we know that none of our measurements refers to titanium free material, for subsequent chemical analysis showed that titanium was present in our purest samples. The measured d spacing for such a specimen falls on the (d, $N^{1/3}$) line as is shown in fig. 2, point A.

To account for the nickel oxide results we put forward the hypothesis which is illustrated in fig. 4. As a result of the sintering treatment in air at 1 200° c, we assume that there is a small excess of oxygen brought about by the migration of Ni^2 ions together with two electrons to the surface. With each vacant Ni^2 site there will be associated two Ni^3 ions—or two positive holes—and since the radius of an Ni^3 ion is less than that of Ni^2 the lattice will contract, provided that the effect of an Ni^2 vacancy on the parameter is either negligible or a contraction. In fig. 4(*e*) we have represented the lattice parameter of such a sample by d_b. As the lithium content of the discs is increased these vacancies will be filled by Li^1 ions with the corresponding transition of one Ni^3 to the larger Ni^2 (fig. 4(*c*)). This will result in a lattice expansion until some value d_0 is reached when all the vacancies are filled and for which the Li^1 concentration is equal to the concentration of defects originally present. Subsequently, as each further Li^1 is incorporated it will replace an Ni^2 of the lattice and there will be produced one Ni^3 ion. The lattice will now contract by an amount depending on the number of Ni^3 ions formed, that is on the number of Li^1 ions incorporated (e.g. d_d). Since the substituted Li^1 ions are indistinguishable from those which filled the original Ni^2 vacancies we should expect the extrapolation to $N(Li^1)=0$ to lead to a value d_a characteristic of completely stoichiometric nickel oxide (fig. 4(*a*) and d_a fig. 4(*e*)), as is the case with magnesium titanate.

There are several ways in which this hypothesis could be further tested: (*a*) By following the experimental curve $(d, N^{1/3})$ through the maximum. (*b*) By substituting, instead of lithium, some other monovalent ion of different size from Ni^2 and Li^1; this should give a $(d, N^{1/3})$ plot of different slope but the same intercept. (*c*) By removing the excess oxygen from lithium-free nickel oxide specimens to discover whether there is an associated increase in lattice parameter. (*d*) By replacing any Ni^3 ions in lithium-free nickel oxide by Cr^3 which has a larger radius; in this case an increase in lattice parameter would indicate the presence of Ni^3 ions in the original sample. The first of these involves preparing homogeneous specimens having lithium contents in the range below 0·002 atomic %. As to the second experiment, it seems impossible to use any other monovalent ion than Li^1; Na^1 has a radius of 0·98 Å and it will be seen later that this is too large for appreciable substitution. (*c*) has the advantage over (*d*) that it should be possible to reach the stoichiometric value, that is to remove all the Ni^2 vacancies and associated Ni^3 ions, by reduction, whereas with (*d*) even when all the Ni^3 ions have been replaced by Cr^3 the parameter will still be less than d_0, since the Cr^3 ion is smaller than the Ni^2. We have therefore heated lithium-free nickel oxide to various temperatures in hydrogen and in vacuum and have found that the lattice parameter can be increased by these treatments, although not to the extrapolated value 4·1726 kx (4·1811 Å). These results are summarized in the table from which it will be seen that the highest parameter we have obtained is 4·1715 kx (4·1800 Å).

When the nickel oxide specimens were analysed to determine the lithium content it was found that they contained varying amounts of sodium—up to 1% by weight of oxide—and there remained the possibility that this had some effect on the lattice parameter. The following evidence is against this: the lattice parameter of high purity Johnson Matthey nickel oxide was found to be 4·1703 kx, that is in the range of values we found for samples heated in air to 1200° c; in a lithium free sample there was 0·49% sodium present and had this been in the lattice substitutionally a resistivity of the order of $10^2\,\Omega$ cm would be expected (cf. measured 10^7 to $10^8\,\Omega$ cm); the sample was found to be spectroscopically free from sodium after powdering, soaking in distilled water for two days and washing. The amounts of sodium present substitutionally therefore could not have been greater than a few parts per million so that the variation from sample to sample must have been less than 1 to 2 parts per million. A rough estimate shows that such variations could only, in the worst case, produce a discrepancy of 0·003 kx.

Summary of Lattice Parameter Measurements of Specially Heat-treated Nickel Oxide

Specimen Number	Temperature (°c)	Time at Temperature (hours)	Atmosphere	Parameter (kx)
1	1200	2	Air	4·1710
2	1200	2	,,	4·1704
3	1200	2	,,	4·1702
3*a*	1200	4·5	CO$_2$	4·1704
3*b*	1300	2	O$_2$ (cooled in CO$_2$)	4·1695
3*c*	250*	1	H$_2$	4·1712
3*d*	860	0·5	Vacuum	4·1714
3*e*	1000†	0·75	,,	4·1715

* At temperatures higher than this the oxide was reduced to metal ($d=3{\cdot}5170$ kx). Partial reoxidation of this metal gave oxide parameter 4·1700 kx : thus no nickel rich oxide formed.

† At temperatures higher than this the oxide was reduced to metal.

As to the real origin of the discrepancy, we cannot say without further experiment whether it arises from our inability to prepare nickel oxide in which the departures from stoichiometric proportions are small enough not to be detected (the present difference of 0·0011 kx would be accounted for by as few as 0·001% of vacancies) or whether the $N^{1/3}$ extrapolation is not valid, in which case the magnesium titanate results would have to be regarded as fortuitous.

§4. CONCLUSION

The measurements described have confirmed the lattice expansion which is expected to accompany the production of n-type conductivity (Fe_2O_3, Mg_2TiO_4), and the contraction in the case of p-type (NiO), in the metallic oxides. The lattice parameter of stoichiometric magnesium titanate has been found to be 8·425 kx (8·441 Å). For the nickel oxide the results have emphasized the difficulty of producing specimens having stoichiometric composition, as is indicated by the failure to obtain a parameter greater than 4·1715 kx (4·1800 Å) while the value to be expected on the basis of our nickel oxide–lithium results is 4·1726 kx (4·1811 Å). That this is higher than values which have been found by previous workers—e.g. 4·1684 kx (4·1780 Å) Cairns and Ott (1933)—could be accounted for by the existence in their specimens of a small concentration of nickel ion vacancies. Verwey's values for nickel oxide containing lithium—e.g. 0·1% 4·1827 Å—were higher than any of these and it would be expected that his lithium free material would have an even larger parameter. This difference remains unexplained.

ACKNOWLEDGMENTS

The authors gratefully acknowledge the assistance of their colleagues Miss K. Whitehead, Miss J. Prescott, Mr. T. H. Barton and Mr. D. P. Jones and wish to thank Dr. R. W. Sillars for his interest and encouragement. The authors also wish to thank Dr. C. Dannatt, Director of Research and Education, and Mr. B. G. Churcher, Manager of the Research Department, Metropolitan-Vickers Electrical Co. Ltd., for permission to publish this paper.

REFERENCES

DE BOER, J. H., and VERWEY, E. J. W., 1937, *Proc. Phys. Soc.*, **49**, 59.
BRADLEY, A. J., and JAY, A. H., 1932, *Proc. Phys. Soc.*, **44**, 563.
CAIRNS, R. W., and OTT, E., 1933, *J. Amer. Chem. Soc.*, **55**, 527.
HOLGERRSIN, S., and HERRLIN, A., 1931, *Z. Anorg. Chem.*, **198**, 69.
ROOKSBY, H. P., 1943, *Nature, Lond.*, **152**, 304; 1948, *Acta Crystallogr.*, **1**, 226.
VERWEY, E. J. W., *et al.*, 1948, *Chem. Weekblad*, **44**, 705; 1950, *Philips Res. Rep.*, **5**, 173.

The Formation of Order in the Alloy $AuCu_3$

BY I. G. EDMUNDS AND R. M. HINDE*
Physics Department, College of Technology, Manchester

Communicated by W. L. Bragg; MS. received 31*st January* 1952

ABSTRACT. The approach to order in $AuCu_3$ has been studied by x-ray examination of single crystals. The distribution of intensity in the diffuse super-lattice reflections was measured from a series of photographs of a stationary crystal, and again from a moving-film photograph, the effect of instrumental broadening being eliminated by Stokes' method.

The intensity in the *hkl* reflection with $(k+l)$ even is given as the Fourier summation

$$I(uvw)=\sum_x \sum_y \sum_z K \exp\{-(\beta x^2+\alpha y^2+\alpha z^2)\} \exp 2\pi i(xu+yv+zw);$$

the constants α and β tend to zero as complete order is approached. The experimental results of Strijk and MacGillavry conform to this expression, and a measure of agreement is obtained with Cowley's observations at a very early stage of ordering.

The discrepancy between the present observations and crystal models proposed by A. J. C. Wilson is discussed, and expressions are derived for order parameters at successive short ranges. It is suggested that the ordering process is similar at all stages, and depends on a tendency for gold atoms to avoid each other; ordered antiphase domains are formed as a consequence of this process.

§ 1. INTRODUCTION

SINCE the early work of Borelius, Johanssen and Linde (1928) the formation of order in the alloy $AuCu_3$ has attracted the attention of many workers. Sykes and Jones (1936, 1938), as the result of an extensive investigation, suggested that, on heating a disordered alloy below the critical temperature, ordering starts by the formation of a large number of small nuclei or domains in each of which the gold atoms all segregate to the corners of the face-centred-cubic cells, or to the centres of one particular set of cube faces. These anti-phase domains are considered as growing until they touch, after which further growth of some domains at the expense of others is more difficult. Sykes and Jones attempted to determine the size of the domains from measurement of super-lattice line-breadths in x-ray powder photographs; they found, however, that the values they obtained varied with the indices of the reflections used, and they concluded that as the domains all fit on to one underlying lattice they do not diffract as independent small particles.

---

* Now at British Insulated Callender's Cables Ltd., Research Laboratories, Wood Lane, London.

Wilson (1943) has calculated the diffraction effects to be expected from such a partially ordered alloy, and finds that the breadths of the various super-lattice lines depend on the way in which neighbouring domains adjoin each other. He considered a number of models, and found that one, in which the domains tended to touch each other across (100) planes in such a way that gold atoms did not come in contact, gave fair agreement with the experimental results of Sykes and Jones. For this model he found that the x-ray intensity distribution could be expressed as a function of two parameters—α, which gave the probability of a change of domain subject to the above condition, and γ, which gave the probability of a change in a random manner as one progressed through the crystal.

These unusual diffraction effects will be more evident in super-lattice reflections from a single crystal, and Wilson (1947, 1949) has predicted the distribution of intensity in the different super-lattice reflections as based on each of his models. The present investigation was undertaken primarily to test Wilson's theory; the exact determination of the intensity distribution should show whether the atomic arrangement can be described in terms of a small number of parameters—such as the α and γ of Wilson's treatment; and if this proved to be so, measurement of the variation of these parameters with time and temperature of annealing should throw light on the kinetics of the formation of order. Preliminary results (Edmunds, Hinde and Lipson 1947) show qualitative agreement with theory; such agreement is also shown in the experiments of Strijk and MacGillavry (1946) who, however, have approached the problem from a different theoretical standpoint. The present paper describes a detailed determination of the intensity distribution in reciprocal space from two single crystals of AuCu$_3$, each in a different partially ordered state; other states are examined qualitatively.

Since this work was begun Cowley (1950) has obtained a distribution of intensity qualitatively very similar to ours, using a single crystal of AuCu$_3$ held at 405°c, that is, above the critical temperature, where only short-range order exists. This result, together with the optical diffraction effects observed by Taylor, Hinde and Lipson (1951) with masks simulating the alloy AuCu$_3$, suggests that the development of order is essentially an increase in short-range order throughout the crystal as opposed to a growth in size of small ordered nuclei in a disordered matrix. These different possibilities will be considered in the light of our experimental results.

§ 2. EXPERIMENTAL RESULTS

2.1. *Preparation of Single Crystals*

The crystals were prepared from copper–gold wire supplied by Messrs. Johnson, Matthey, the wire being made to an approximate composition of 75 atomic per cent copper from spectroscopically pure metals. A chemical analysis of a specimen of the wire adjacent to that used for single crystal growth gave its composition as $73{\cdot}7_4$ atomic per cent copper.

The first attempts to prepare single crystals by straining the wire and afterwards annealing proved unsuccessful. A number of crystals were eventually obtained by heating short lengths of wire in narrow evacuated silica tubes to a temperature above the solidus of the alloy, and then cooling slowly. Most of the small pellets thus formed gave the sharp reflections to be expected from good single crystals.

2.2. *X-Ray Technique*

Each crystal was mounted on the x-ray goniometer with the [100] direction set accurately along the axis of rotation and examined with filtered copper K radiation. For the preliminary qualitative survey the crystal was usually oscillated through an angular range of 15° chosen to cover completely the required super-lattice reflections. If the intensity of x-ray diffraction in any super-lattice spot be considered as spread out in reciprocal space around a lattice point, then the record on the film will correspond to an oblique projection of this intensity distribution.

The measurements on the first crystal were made using the same x-ray goniometer. The crystal was kept stationary, so that the x-ray reflection corresponded to a section of the super-lattice spot by the sphere of reflection; series of photographs were taken with the crystal displaced through successive angles of 30 or 60 minutes, the greatest angular range required to cover one reflection being 7°. To correlate the positions of the reflections on each film of a series, reference marks were made on the film by irradiating it with x-rays through two small holes in the cylindrical film holder. A correlation of intensities from film to film was obtained by recording a transverse section through the centre of the same super-lattice spot; this was done by turning the crystal to the alternative position, in which it gave the same super-lattice reflection.

This correlation of a series of photographs involves much labour, and great care must be taken to avoid errors, the difficulties being increased by the fact that the photographs correspond to oblique sections in reciprocal space. For this reason a moving-film technique was developed, and used to examine the second crystal. The screens on a Weissenberg goniometer were replaced by a single screen with an accurately uniform aperture, about 0·1 mm wide. The photograph from an oscillating crystal gives the intensity distribution in a thin section of reciprocal space perpendicular to the axis of rotation; thus a principal section of the super-lattice spot may be recorded on a single photograph.

The x-ray intensities were measured on a deflection microphotometer in which a spot of light about 0·1 mm in diameter fell on the x-ray film and then diverged on to a photocell. The film was traversed at intervals of 0·1 mm, the intensity being observed every 0·1 mm of traverse. The range of measurement extended well to each side of the diffuse spot, so that the level of the background intensity at the position of the spot could be found by interpolation and subtracted from the observed intensity. In this way any effect due to the thermal and Compton scattering should be eliminated. The effects of temperature factor, absorption and polarization could be assumed constant over the small angular range covered by a single reflection.

2.3. *Instrumental Broadening*

Owing to a number of factors, such as the size of the specimen and the $K\alpha_1\alpha_2$ doubling, a further broadening of the reflections, termed instrumental broadening, will be superimposed on the broadening due to imperfect order. The intensity distribution in a diffuse reflection may be corrected for this effect by a method due to Stokes (1948) if the same reflection is also observed when sharp, that is from a perfectly ordered crystal. If the experimental distribution of intensities in the broad and in the sharp reflections are expressed as Fourier summations, then the Fourier summation whose coefficients are the quotients of the corresponding coefficients in these two summations gives the true intensity distribution. In practice the correction is applied in a principal section of the super-lattice spot in reciprocal space; as the reflection is very nearly symmetrical about such a plane, any correction due to a spread perpendicular to this plane becomes negligible.

§ 3. EXAMINATION OF ORDERING

3.1. *Experimental Measurements*

Crystals were examined at various stages in the growth of order as produced by the heat treatments given in table 1, the crystal being annealed at 500° c for 8 hours or longer and quenched before each heat treatment to remove any long-range order present; the change in the x-ray pattern due to ordering is illustrated in the Plate. The super-lattice reflections are broadened, their shapes depending on the indices of the reflection; thus the 124 reflection is elongated along the layer line $h=1$, while the broadening of the 114 reflection is greatest parallel to the constant ξ curve on a Bernal chart. Both these elongations correspond to a spread of intensity perpendicular to one or other of the reciprocal axes, and it is found in general that the shapes of the spots indicate a disc-like distribution of intensity in reciprocal space, the plane of the disc (which is of finite thickness) being that of the two indices of like parity. This agrees qualitatively with Wilson's theory (1949), but we shall see later that the theory is not adequate to account for the detailed intensity distribution. The nature of the broadening is the same at all stages of ordering, from the very diffuse reflections obtained after annealing for 2 hours at 175° c to the relatively sharp spots after 15 minutes at 344° c. The splitting of the super-lattice reflections reported by Guinier and Griffoul (1947, 1948) for crystals annealed at 175° c, and again for those annealed at 250° c, was not observed.

Table 1. Heat Treatments of AuCu$_3$ Crystals

(*a*)	2 hours at 175° c	Quenched
(*b*)	2 hours at 250° c	Quenched
(*c*)	15 minutes at 300° c	Quenched
(*d*)	2 hours at 300° c	Quenched
(*e*)	45 minutes heating from 160° c to 344° c, followed by 15 minutes at 344° c	Quenched
(*f*)	32 hours cooling from 380° c to 250° c, followed by 16 hours cooling from 250° c to room temperature	

Each alloy was annealed at 500° c for 8 hours and quenched before its final heat treatment.

A 124 reflection of a suitable diffuseness for measurement was obtained from the first crystal after heating it from 160° c to 344° c in 45 minutes, annealing at this final temperature for 15 minutes, and quenching. The measured intensity at some chosen value of ζ was plotted against the azimuth on the cylindrical film, thus giving the variation of intensity along the section of the super-lattice spot by the circle of reflection at this ζ-level—a section parallel to the (100) plane; this was repeated for the other films of the series, the graphs being placed on a common scale of intensity by measurements on the correlating film. From these curves a number of constant-intensity contours were plotted in this constant-ζ section of reciprocal space. The analysis was repeated for different ζ-levels, with measurements taken on the same photographs, thus giving a complete record of the reflection.

The sharp super-lattice reflection required to correct for instrumental broadening was obtained from the same crystal after annealing it for 32 hours between 380° C and 250° C and then cooling to room temperature in 16 hours; the super-lattice reflection was then as sharp as the fundamental reflections. The reflection was analysed as before, but this time the film-to-film correlation was obtained by simultaneously exposing a fixed crystal to the radiation from a second window of the x-ray tube.

The intensity distribution in the central section of the reciprocal-lattice spots, both for the broad and sharp reflections, was next expressed as a two-dimensional Fourier summation, the real and imaginary components of the coefficients G_{yz} and H_{yz} being calculated from the intensities read off at regular intervals round the reciprocal-lattice point. The true intensity distribution in the diffuse reflection is then given by the summation whose coefficients K_{yz} are the quotients H_{yz}/G_{yz}. Then

$$I(vw) = \Sigma\,\Sigma\,K_{yz} \exp 2\pi i(vy + wz), \qquad \ldots\ldots(1)$$

where v and w are coordinates in reciprocal space. The constant-intensity contours for the corrected 124 reflection are shown in fig. 1 (*a*). The 114 reflection was also examined with this crystal, but the measurements were not corrected for instrumental broadening; constant-intensity contours for a section of the uncorrected diffuse reflection are shown in fig. 1 (*b*).

The second crystal to be examined quantitatively, this time by means of the moving-film method, was annealed for 2 hours at 300° C and quenched. With a slot width of 0·11 mm, the position of the screen was adjusted to give the strongest diffuse reflection, and this was taken to correspond to the central section of the reciprocal-lattice spot; the constant-intensity contours for this section were then plotted from measurements on the one film. The broad and sharp 104 reflections, and also the 114 reflections, were plotted in this way, and the corrected intensity distribution for the central section of each spot was derived by Fourier analysis; these are shown in figs. 1 (*c*) and (*d*).

We would expect each intensity distribution to be symmetrical about the super-lattice point, but there is no reason why the origin of v and w in our analysis should fall exactly at this point, and in fact the figures show that it does not do so. A displacement of the origin through a small distance (Δv, Δw) alters the Fourier summation to one with coefficients $K_{yz}(\text{new}) = K_{yz}(\text{old}) \exp 2\pi i(y\Delta v + z\Delta w)$. Table 2 shows some of the Fourier coefficients for the 114 reflection after such a change in origin; the imaginary coefficients, which should vanish if the origin is a centre of symmetry, are seen to be very small. Alternatively, we may take each Fourier coefficient referred to the true origin as real and equal to the modulus of the observed coefficient $\{K_{yz}^2(\text{real}) + K_{yz}^2(\text{imag})\}^{1/2}$, since $|K_{yz}|$ is independent of a change in origin. We adopted this procedure for the 104 and 124 reflections.

3.2. *Analysis of Experimental Data*

It will be seen in fig. 1 that the contours at higher intensities for the 124 reflection (first crystal) and for the 104 reflection (second crystal) are circular within the limits of experimental error. The lower contours tend to be drawn out along the reciprocal axes, but we believe this to be a spurious effect, introduced by the artificial termination of the Fourier series, where the coefficients become unreliable. The contours from the 114 reflection from the second crystal are approximately elliptical, as are also the uncorrected contours for this reflection from the first crystal.

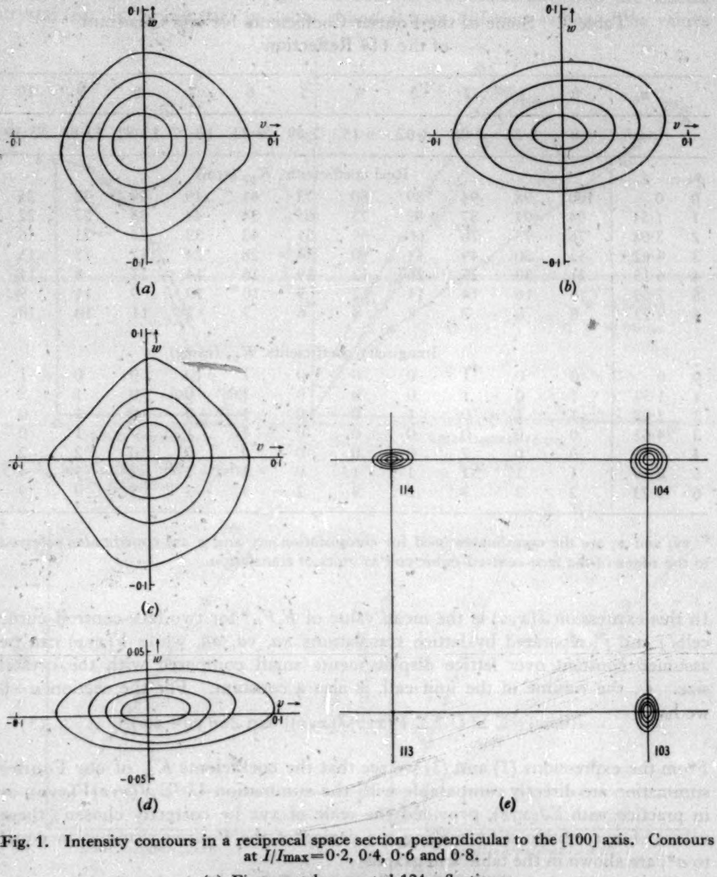

Fig. 1. Intensity contours in a reciprocal space section perpendicular to the [100] axis. Contours at $I/I_{\max}=0{\cdot}2$, $0{\cdot}4$, $0{\cdot}6$ and $0{\cdot}8$.

(*a*) First crystal, corrected 124 reflection.
(*b*) First crystal, uncorrected 114 reflection.
(*c*) Second crystal, corrected 104 reflection.
(*d*) Second crystal, corrected 114 reflection.
(*e*) Second crystal, uncorrected.

A more profitable approach is to consider the variation of the Fourier coefficients K_{yz} with the real-space coordinates (y, z). Wilson (1949) has shown that the intensity distribution at a point in reciprocal space is proportional to an integral, or a summation,

$$I(uvw) = U^{-1} \sum_{x=-\infty}^{\infty} \sum_{y=-\infty}^{\infty} \sum_{z=-\infty}^{\infty} V(xyz)J(xyz) \exp 2\pi i(xu+yv+zw). \qquad \ldots\ldots(2)$$

Table 2. Some of the Fourier Coefficients for one Quadrant of the 114 Reflection

	z_1	0	1	2	3	4	5	6	7	8	9	10
	z	0	1·54	3·08	4·62	6·15	7·69	9·23	10·77	12·31	13·85	15·39
y_1	y	Real coefficients, K_{yz} (real)										
0	0	100	98	94	89	80	72	61	49	39	32	25
1	1·54	94	91	87	82	73	65	54	44	34	27	22
2	3·08	76	73	70	66	59	51	42	33	25	21	16
3	4·62	53	50	49	44	40	34	28	24	17	13	11
4	6·15	31	30	27	26	22	19	16	14	11	8	11
5	7·69	16	16	14	14	12	9	10	10	9	11	9
6	9·23	8	8	7	8	8	6	7	7	11	10	10
		Imaginary coefficients, K_{yz} (imag)										
0	0	0	0	$\bar{1}$	0	0	0	$\bar{1}$	0	0	0	$\bar{1}$
1	1·54	1	0	1	0	0	0	1	0	0	1	$\bar{2}$
2	3·08	1	1	0	1	0	0	1	0	0	1	0
3	4·62	0	0	0	0	0	0	1	1	1	1	0
4	6·15	0	0	2	0	0	0	0	0	0	2	2
5	7·69	1	1	1	1	1	0	1	1	2	3	4
6	9·23	2	3	3	2	4	3	4	5	5	9	9

y_1 and z_1 are the coordinates used for computation. y and z are coordinates referred to the edges of the face-centred-cubic cell as units of translation.

In this expression $J(xyz)$ is the mean value of $F_j F_{j'}^*$ for two face-centred-cubic cells j and j', separated by lattice translations xa, ya, za, while $V(xyz)$ can be assumed constant over lattice displacements small compared with the crystal size. U, the volume of the unit cell, is also a constant. For the section $u=0$ we have

$$I(0vw) = \sum_y \sum_z [U^{-1} \sum_x V(xyz)J(xyz)] \exp 2\pi i(yv+zw). \qquad \ldots\ldots(3)$$

From the expressions (1) and (3) we see that the coefficients K_{yz} of our Fourier summation are directly comparable with the summation $U^{-1}\Sigma_x J(xyz)V(xyz)$, or in practice with $\Sigma J(xyz)$, provided the scale of xyz be correctly chosen; these values of xyz, obtained by making the period of the Fourier summation equal to a^*, are shown in the table and graphs.

The logarithmic variation of the Fourier coefficients along the y and the z axes has been plotted in fig. 2 for the 124 reflection. The curves are parabolic within the errors of experiment; this is confirmed in fig. 3 (*a*), where the graphs of $(\log K_{00} - \log K_{y0})^{1/2}$ and of $(\log K_{00} - \log K_{0z})^{1/2}$ are seen to be straight lines through the origin. Furthermore, and again within the limits of experimental error, the slopes of the lines show that the variation is the same along each of the axes y and z. If this slope be denoted by m, it follows that we may write

$$K_{y0}=K_{00}\exp\{-Ay^2\};\quad K_{0z}=K_{00}\exp\{-Bz^2\},\qquad \ldots\ldots(4)$$

where, for this reflection, A and B are equal and each equal to m^2.

Similar straight line graphs are obtained for the variation of $(\log K_{00}-\log K_{yz})^{1/2}$ along the two axes for both the 104 and the 114 reflection from the second crystal (fig. 3 (*b*)), but the constants A and B have different values. The values

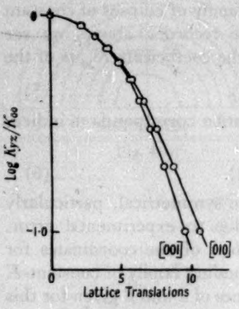

Fig. 2. $\log K_{yz}/K_{00}$. First crystal, 124 reflection.

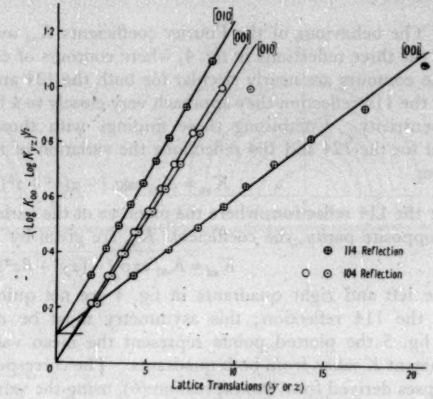

Fig. 3 (*b*)

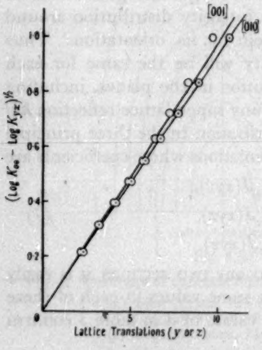

Fig. 3 (*a*)

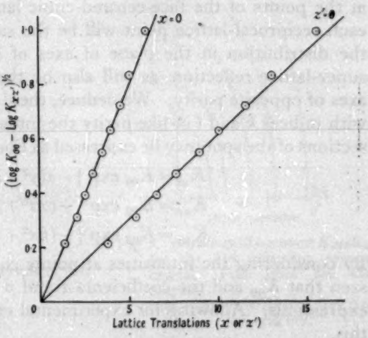

Fig. 3 (*c*)

Fig. 3. $(\log K_{00}-\log K_{yz})^{1/2}$.
(*a*) First crystal, 124 reflection.
(*b*) Second crystal, 104 and 114 reflections.
(*c*) From Strijk and MacGillavry's diagram (1946).

of A and B for the reflections analysed are given in table 3. For the 104 reflection the variation is again seen to be sensibly the same along the two axes of like parity; while for the same crystal the variation along the y axis for both 104 and 114 reflections are roughly comparable. We denote the coefficient A for this latter reflection by α and the coefficient B by β.

Table 3. Values of the Coefficients A and B

First crystal	124 reflection	$A=0{\cdot}020_3$	$B=0{\cdot}022_3$
Second crystal	104 reflection	$A=0{\cdot}025_2$	$B=0{\cdot}027_9$
Second crystal	114 reflection	$A=0{\cdot}030_8=\alpha$	$B=0{\cdot}005_9=\beta$

The behaviour of the Fourier coefficients K_{yz} away from the axes is shown for the three reflections in fig. 4, where contours of constant K have been drawn. The contours are nearly circular for both the 124 and the 104 reflections, while for the 114 reflection they approach very closely to a family of ellipses of constant eccentricity. Combining these findings with those recorded above, we see that for the 124 and 104 reflections the variation of the coefficients K_{yz} is of the form

$$K_{yz}=K_{00}\exp\{-\alpha(y^2+z^2)\}. \qquad \ldots\ldots(5)$$

For the 114 reflection, where the plane yz of the variation corresponds to indices of opposite parity, the coefficients K_{yz} are given by

$$K_{yz}=K_{00}\exp\{-(\alpha y^2+\beta z^2)\}. \qquad \ldots\ldots(6)$$

The left and right quadrants in fig. 4 are not quite symmetrical, particularly for the 114 reflection; this asymmetry must be due to experimental error. In fig. 5 the plotted points represent the mean values of the coordinates for constant K taken from both quadrants. The corresponding family of constant-K ellipses derived from the expression (6), using the values of α and β given for this reflection in table 3, are drawn in full line, and the experimental points are seen to fit the curves satisfactorily.

It can be shown theoretically that, so long as the copper and gold atoms lie at the points of the face-centred-cubic lattice, the intensity distribution around each reciprocal-lattice point will be the same, except for its orientation. Thus the distribution in the plane of axes of like parity will be the same for each super-lattice reflection, as will also be the distribution in the planes, including axes of opposite parity. We deduce, then, that for any super-lattice reflection hkl with indices k and l of like parity the intensity distribution in the three principal sections of the spot may be expressed as Fourier summations whose coefficients are

$$\left.\begin{aligned} K_{yz}&=K_{00}\exp\{-\alpha(y^2+z^2)\}, && \Sigma_x J(xyz),\\ K_{zx}&=K_{00}\exp\{-(\alpha z^2+\beta x^2)\}, && \Sigma_y J(xyz),\\ K_{xy}&=K_{00}\exp\{-(\beta x^2+\alpha y^2)\}, && \Sigma_z J(xyz).\end{aligned}\right\} \qquad \ldots\ldots(7)$$

By considering the intensities at points common to any two sections it is easily seen that K_{00} and the coefficients α and β have the same values in each of these expressions. Allowing for experimental error, the values of α in table 3 confirm this.

One obvious solution for the function $J(xyz)$ is

$$J(xyz)=K\exp\{-(\beta x^2+\alpha y^2+\alpha z^2)\}=K_A, \qquad \ldots\ldots(8)$$

giving $$I(uvw)=\sum_x\sum_y\sum K\exp\{-(\beta x^2+\alpha y^2+\alpha z^2)\}\exp 2\pi i(xu+yv+zw) \ldots(9)$$

again omitting the slowly varying factor $V(xyz)$. For reflections with h and l, and with h and k of like parity, the expressions analogous to (8) are, respectively,

$$\left.\begin{aligned} J(xyz) &= K \exp\{-(\alpha x^2+\beta y^2+\alpha z^2)\} = K_B \\ J(xyz) &= K \exp\{-(\alpha x^2+\alpha y^2+\beta z^2)\} = K_C \end{aligned}\right\}. \qquad \ldots\ldots(8a)$$

It is possible to obtain other functions to satisfy eqns. (7), but these are not simple, so it appears exceedingly probable that the expressions (8) do in fact represent the variation of the quantity $J(xyz)$ with the separation (xa, ya, za) of two cubic cells in the crystal lattice.

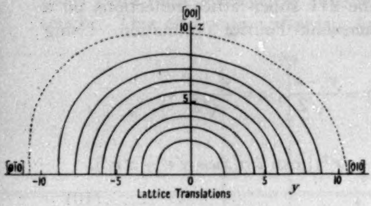

Fig. 4 (*a*)

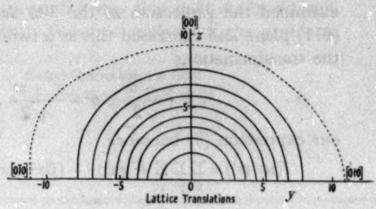

Fig. 4 (*b*)

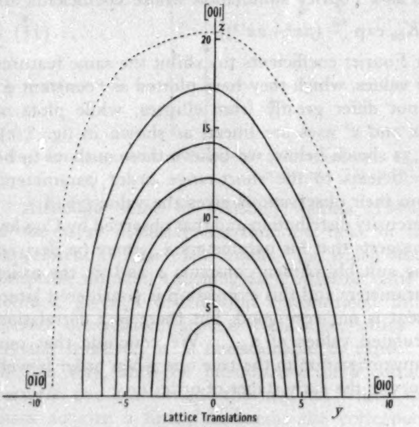

Fig. 4 (*c*)

Fig. 4. Contours of constant K_{yz}/K_{00} at intervals of 0·1.

(*a*) First crystal, 124 reflection.
(*b*) Second crystal, 104 reflection.
(*c*) Second crystal, 114 reflection.

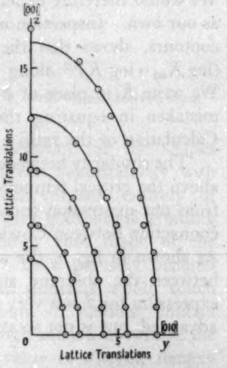

Fig. 5. Contours of constant K_{yz}/K_{00} for the 114 reflection, second crystal. Full lines are the ellipses. $\exp\{-(\alpha y^2+\beta z^2)\} = 0{\cdot}2, 0{\cdot}4, 0{\cdot}6, 0{\cdot}8$ and $0{\cdot}9$.

A reliable value of the ratio $\alpha:\beta$ has been obtained for one state of the crystal only, namely after annealing for 2 hours at 300° c, when the ratio is 5·2 : 1. A rough estimate, from measurements of the uncorrected reflections, gives $\alpha:\beta$ about 4 : 1 for the same crystal when annealed for 15 minutes at 300° c.

3.3. *Comparison with Experimental Data from other Sources*

Before considering the significance of the above results it is of interest to compare them with other published experimental data. As stated above, our intensity distribution in the super-lattice reflections does not agree with that found by Guinier and Griffoul (1947, 1948); these authors have not measured the exact distribution, so that further comparison is difficult, but it is conceivable that a difference in the previous thermal history of the specimens may account for the discrepancy between their results and ours.

Strijk and MacGillavry (1946) have studied a single crystal of $AuCu_3$ annealed for 1 hour at 400° c followed by 12 minutes at 368° c and quenched; they examined the projection of the 300 and the $21\bar{1}$ super-lattice reflections on a (011) plane and expressed this as a two-dimensional Fourier summation. Using the transformations

$$v=\frac{v'-w'}{\sqrt{2}},\quad w=\frac{v'+w'}{\sqrt{2}};\quad y=\frac{y'-z'}{\sqrt{2}},\quad z=\frac{y'+z'}{\sqrt{2}}$$

our expression (9) becomes

$$I(uv'w')=\sum_{x}\sum_{y'}\sum_{z'} K\exp\{-(\beta x^2+\alpha y'^2+\alpha z'^2)\}\exp 2\pi i(xu+y'v'+z'w'). \qquad \ldots\ldots(10)$$

It follows that Strijk and MacGillavry's projection, which is equivalent to $\int_{v'} I(uv'w')\,dv'$, may be expanded as a Fourier summation whose coefficients are

$$K_{xz'}=K_{00}\exp\{-(\beta x^2+\alpha z'^2)\}. \qquad \ldots\ldots(11)$$

We would therefore expect their Fourier coefficients to exhibit the same features as our own. Inspection of their values, which they have plotted as 'constant ϕ' contours, shows that they do not differ greatly from ellipses, while plots of $(\log K_{00}-\log K)^{1/2}$ along both x and z' axes are linear, as shown in fig. 3 (*c*). We write K in place of ϕ since, as shown below, we believe these authors to be mistaken in equating these coefficients to the short-range order parameters. Calculation of the ratio $\alpha:\beta$ from their observations gives the value 6·6 : 1.

The similarity between out intensity distribution and that observed by Cowley above the critical temperature suggests that his parameters α_{xyz} may be derived from our expression for J, using suitably chosen constants α and β; the exact connection between Cowley's parameters and this expression is considered later. As shown in fig. 6, the agreement is not very good, but there is a correlation between the observed and calculated values of α_{xyz}. We conclude that our expression for J is a very close approximation to the true one when order is well advanced, but is not so satisfactory in the early stages of ordering.

§4. THE NATURE OF THE ORDERING PROCESS

4.1

The resemblance between our results and Cowley's makes it highly probable that the ordering process is essentially the same at all stages, and, this being so, the process must be one of increasing short-range order, that is, of local rearrangement of atoms to reduce the number of gold atoms in contact, as suggested by Hume-Rothery and Powell (1935). Additional evidence in support of this contention is supplied by the experiment of Taylor, Hinde and Lipson (1951), who have studied the optical diffraction patterns from masks in which the copper and gold atoms of an $AuCu_3$ alloy were represented by holes of different sizes; the problem was reduced to two dimensions by considering the projection of two adjacent (100) planes on to a single plane. These authors started with a random arrangement of copper and gold atoms, and increased the order in stages merely by interchanging pairs of atoms so as to reduce the number of gold atoms in contact. They obtained a series of diffraction patterns which resembled Cowley's intensity distribution very closely in the initial stages, and which simulated our distribution as order became more advanced.

An examination of the 'atomic' arrangement in these masks (fig. 7) shows that, as order increases, antiphase domains of perfect order are formed, and that in many cases these meet across cube faces in such a way that gold atoms do not touch. This observation affords a link with Wilson's analysis of the problem.

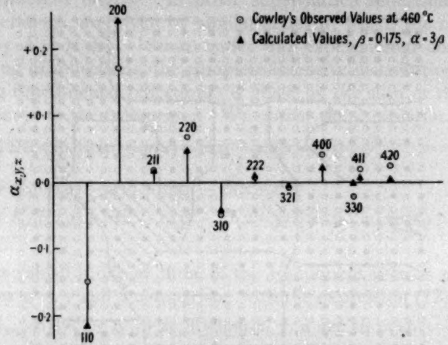

Fig. 6. Comparison of Cowley's (1950) coefficients α_{xyz} at 460°c, with values derived from expressions (13) and (15).

Although some of Wilson's models (1949) will account for the shapes of the X-ray intensity distributions, none of them agrees quantitatively with experiment. His fifth model, in which the crystal consists entirely of antiphase domains touching each other on cube faces with gold atoms avoiding contact, gives a distribution concentrated into infinitely thin discs, of the correct orientation, around each super-lattice point. In a partially ordered crystal, however, it is unreasonable to expect that all domains would touch in this way, and the introduction of a certain amount of random contact between one domain and the next led Wilson to his sixth model, in which the discs acquire a finite thickness; the corresponding value of $J(xyz)$, namely $J = (f_{\mathrm{Au}} - f_{\mathrm{Cu}})^2 \exp\{-2\alpha(|x| + |y|) - 4\gamma(x^2 + y^2 + z^2)^{1/2}/3\}$, is still not in exact agreement with experiment. This model, however, is still over-simplified, since the alloy is regarded as built up of four types of face-centred-cubic cells only, each containing one gold and three copper atoms, thus implying an exceedingly homogeneous alloy on an atomic scale. In practice there will certainly be at least a small proportion of cells without any gold atoms and some with more than one; moreover, the masks used for the optical diffraction experiments suggest that there will also be some regions of the crystal which cannot rightly be regarded as domains at all.

It seems clear, then, that considerations such as these will account for the difference between Wilson's final model and the observed intensity distribution; we may say that, as ordering proceeds, antiphase domains are formed, and that when these touch they *tend* to do so across cube faces without the gold atoms coming in contact. Wilson did not attempt to explain how the formation of these domains came about; our observations suggest that they arise naturally—almost accidentally—as a consequence of increasing short-range order.

4.2. *Short-range Order Parameters*

A number of workers have introduced parameters to express the state of order at varying short ranges in a crystal. Thus, MacGillavry and Strijk (1946) have defined order parameters ϕ_r in terms of the probability of two atomic sites separated by the vector **r**, of components $r_1 r_2 r_3$, being occupied correctly or otherwise with respect to each other. If the first site be occupied by a gold atom, and the probability of the second site being correctly occupied be p, then it is possible to write $\phi_r = (4p-1)/3$ if all the components of r are even, and $\phi_r = 4p-3$ if one component only of r is even. Each parameter varies between zero for complete disorder and unity for complete order; the value of ϕ for nearest neighbour sites is identical with the short-range order parameter defined by Peierls (1936).

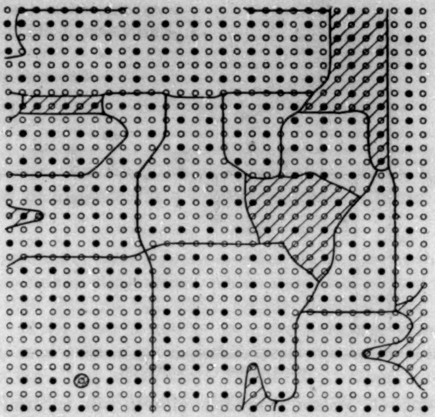

Fig. 7. Part of a mask used by Taylor, Hinde and Lipson (1951) showing the formation of domains due to increased short-range order. ● = gold atoms. ○ = copper atoms. Shaded portions cannot be considered as domains.

The above authors, Strijk and MacGillavry (1946), show that, omitting the fundamental reflections, and in the absence of long-range order as defined by Bragg and Williams (1934), the distribution of x-ray intensity in reciprocal space is periodic, and may be expressed as a Fourier summation:

$$I(uvw) \propto \sum_{r_1} \sum_{r_2} \sum_{r_3 \text{ all even}} 3\phi_r \exp 2\pi i(r_1 u + r_2 v + r_3 w) - \sum_{r_1} \sum_{r_2} \sum_{r_3 \text{ two odd, one even}} \phi_r \exp 2\pi i(r_1 u + r_2 v + r_3 w). \quad \ldots\ldots(12)$$

A comparison with Cowley's analysis, in which the vectors are replaced by $\frac{1}{2}xa$, $\frac{1}{2}ya$, $\frac{1}{2}za$, shows that the coefficients of his Fourier summation are given by

$$\left.\begin{aligned} &\alpha_{xyz}=\phi_{xyz} \text{ if } x,\ y,\ z \text{ are all even,} \\ &\alpha_{xyz}=-\tfrac{1}{3}\phi_{xyz} \text{ if one component only is even.} \end{aligned}\right\} \quad \ldots\ldots(13)$$

[The effect of polarization and the fall-off in scattering factor with angle is omitted.]

Our summation (9) with coefficients K_A has been derived to represent the intensity distribution in one super-lattice reflection, *hkl*, only, where k and l are the indices of equal parity; if, however, the period of the series be taken as $2a^*$, the summation is valid throughout reciprocal space and represents the group of reflections $h+2n_1$, $k+2n_2$, $l+2n_3$, where n_1, n_2 and n_3 are integers. An identical series represents the reflections $h+2n_1+1$, $k+2n_2+1$, $l+2n_3+1$, but referred to a different origin. All other super-lattice reflections, in the two remaining orientations, are given by similar series in which the coefficients K_A are replaced by K_B or K_C. Since under our experimental conditions there is no overlapping of reflections, the complete intensity distribution in reciprocal space (omitting fundamental reflections) is given by the sum of these six series, each being referred to the true origin. We obtain the summation

$$\begin{aligned} I(uvw)=\sum_x\sum_y\sum_z \{&K_A[\exp\{-\pi ix\}+\exp\{-\pi i(y+z)\}] \\ &+K_B[\exp\{-\pi iy\}+\exp\{-\pi i(x+z)\}] \\ &+K_C[\exp\{-\pi iz\}+\exp\{-\pi i(x+y)\}]\}\exp 2\pi i\{xu+yv+zw\}. \end{aligned} \quad \ldots\ldots(14)$$

The coefficients vanish if one or three of the component vectors x, y, z are odd. For other values of x, y and z comparison with the expression (12) shows that

$$\begin{aligned} &\phi_{xyz}\propto\tfrac{2}{3}[K_A+K_B+K_C] \text{ when } x,\ y,\ z \text{ are all even,} \\ &\phi_{xyz}\propto 2[K_B+K_C-K_A] \text{ when } x \text{ is even, } y \text{ and } z \text{ odd.} \end{aligned}$$

With a high degree of order α and β tend to zero while ϕ must tend to unity; we have, therefore,

$$\begin{aligned} \phi_{xyz}=\tfrac{1}{3}[&\exp\{-(\beta x^2+\alpha y^2+\alpha z^2)\}+\exp\{-(\alpha x^2+\beta y^2+\alpha z^2)\} \\ &+\exp\{-(\alpha x^2+\alpha y^2+\beta z^2)\}] \quad \text{when } x,\ y \text{ and } z \text{ are all even,} \\ \phi_{xyz}=[&\exp\{-(\alpha x^2+\beta y^2+\alpha z^2)\}+\exp\{-(\alpha x^2+\alpha y^2+\beta z^2)\} \\ &-\exp\{-(\beta x^2+\alpha y^2+\alpha z^2)\}] \quad \text{when } x \text{ is even, } y \text{ and } z \text{ odd,} \end{aligned} \quad \ldots(15)$$

with similar expressions when y is even or z is even. Cowley's parameters α_{xyz} may be obtained by substituting these expressions in eqns. (13).

Strijk and MacGillavry attempted to derive these short-range order parameters from their experimental observations, but appear to have made the error of assuming cubic symmetry for the intensity distribution of each individual super-lattice reflection. This is equivalent to equating our coefficients K_A, K_B and K_C, and leads to a uniform fall-off in ϕ irrespective of whether x, y or z are even or odd; owing to the difference between the exponents α and β we do not agree with this.

It is evident, of course, that the parameters ϕ are not independent of each other for different values of x, y and z. It will be shown in a later paper that equations may be set up relating these parameters; here it will suffice to say that the expressions (15) satisfy these equations to a very close approximation under our conditions of experiment.

Table 4 shows that the short-range order in our second crystal (annealed for 2 hours at 300° c) is high.

Table 4. Short-range Order Parameters for a Crystal annealed at 300° c for 2 hours

xyz	110	200	211	220	310	222	321	400
ϕ_{xyz}	0·997	0·980	0·948	0·959	0·985	0·940	0·937	0·921

The values are calculated from expression (15) with $\alpha=0{\cdot}0070$, $\beta=0{\cdot}0014_8$; the mean values of α and β in table 3 are divided by 4 owing to the change of period of the Fourier summation.

§5. CONCLUSIONS

A fairly clear picture of the state of a crystal during ordering emerges from a study of all the available data. We believe that an increase in the nearest neighbour order will account for the entire growth of order. When ordering has proceeded some way antiphase domains may be discerned, and further, when these touch they tend to do so with gold atoms avoiding contact with each other; the formation of such domains should not, however, be regarded as fundamental but rather as a natural consequence of increased short-range order.

The short-range order, as described by the parameters ϕ_{xyz} for atoms $\frac{1}{2}xa$, $\frac{1}{2}ya$, $\frac{1}{2}za$ apart, may be expressed in terms of two variables α and β, thus emphasizing the fact that these parameters are not independent; in particular they may be regarded as determined by the values of the parameters for the nearest and next nearest neighbours.

The ratio $\alpha:\beta$ does not appear to remain constant, but it is not possible from the data available to say how the ratio is affected by different experimental factors. It is hoped that a study of the variation of α and β with the time and temperature of annealing will help to explain the physical significance of these quantities, and so throw more light on the kinetics underlying the formation of order.

ACKNOWLEDGMENTS

We wish to thank Dr. H. Lipson for his interest in the work and for many helpful discussions. We are also indebted to the British Iron and Steel Research Association for a maintenance grant to one of us (R. M. H.).

REFERENCES

Borelius, G., Johanssen, C. H., and Linde, J. O., 1928, *Ann. Phys., Lpz.*, **86,** 291.
Bragg, W. L., and Williams, E. J., 1934, *Proc. Roy. Soc.* A, **145,** 699.
Cowley, J. M., 1950, *J. Appl. Phys.*, **21,** 24.
Edmunds, I. G., Hinde, R. M., and Lipson, H., 1947, *Nature, Lond.*, **160,** 304.
Guinier, A., and Griffoul, R., 1947, *C.R. Acad. Sci., Paris*, **224,** 1168; 1948, *Rev. Métall.*, **45,** 387.
Hume-Rothery, W., and Powell, H. M., 1935, *Z. Kristallogr.*, **91,** 23.
MacGillavry, C. H., and Strijk, B., 1946, *Physica*, **11,** 369.
Peierls, R., 1936, *Proc. Roy. Soc.* A, **154,** 207.
Stokes, A. R., 1948, *Proc. Phys. Soc.*, **61,** 382.
Strijk, B., and MacGillavry, C. H., 1946, *Physica*, **12,** 129.
Sykes, C., and Jones, F. W., 1936, *Proc. Roy. Soc.* A, **157,** 213; 1938, *Ibid.*, **166,** 376.
Taylor, C. A., Hinde, R. M., and Lipson, H., 1951, *Acta Crystallogr.*, **4,** 261.
Wilson, A. J. C., 1943, *Proc. Roy. Soc.* A, **181,** 360; 1947, *Nature, Lond.*, **160,** 304; 1949, *X-ray Optics* (London : Methuen).

Iterative Ray-tracing

By W. WEINSTEIN
Technical Optics Section, Imperial College, London

MS. received 20*th March* 1952

ABSTRACT. An iterative ray-tracing method described by T. Smith is shown to give a divergent sequence of approximations in certain cases; when it converges it has only first order convergence according to Hartree's classification of iterative processes. An iterative method which always gives second order convergence is described and the significance of the successive approximations in terms of higher order aberrations is discussed.

§ 1. INTRODUCTION

In 1945 T. Smith described a method of tracing meridian or skew rays through an axially symmetrical optical system with non-spherical refracting or reflecting surfaces; it was an iterative method, intended particularly for use with automatic digital computing machines, and it was suggested that the results of successive applications of the iterative equations gave groups of higher order aberrations of the system. It will be shown in this note that with certain configurations of the rays and the normal to the refracting surface the iteration diverges and that even when it does converge groups of aberrations are not in general obtained. An iterative method which always converges and which gives the distribution of the total aberration among groups of different order will be given.

In Smith's notation x_p, y_p, z_p are the coordinates of the point of incidence of a ray on the pth surface, the origin being at the pole of the surface and the z-axis lying along the axis of the optical system, and ξ_p, η_p, ζ_p are the modified direction cosines, i.e. direction cosines multiplied by refractive index, of the ray in the space between the pth and $(p+1)$th surfaces. The pth surface, in general a non-spherical surface of revolution, is specified by the equation

$$s_p = s_p(z_p), \qquad \text{......(1)}$$

s being the subnormal. In the following subscripts will be omitted when no risk of confusion arises. The usual cartesian sign convention is used.

The ray-tracing equations were given by Smith in matrix form; they can be expanded as follows:

$$\left.\begin{aligned} \xi_p &= \xi_{p-1} - x_p A_p \\ \eta_p &= \eta_{p-1} - y_p A_p \end{aligned}\right\} \quad \text{refraction equations} \qquad \text{......(2)}$$

$$\left.\begin{aligned} x_{p+1} &= x_p - \xi_p D_p \\ y_{p+1} &= y_p - \eta_p D_p \end{aligned}\right\} \quad \text{transfer equations} \qquad \text{......(3)}$$

In these equations $-D_p$ is the reduced distance, i.e. the distance divided by the refractive index, along the ray from the pth to the $(p+1)$th surface and A_p is the generalized power of the pth surface at the point of incidence; thus

$$-D_p = (t_p - z_p + z_{p+1})/\zeta_p, \qquad \text{......(4)}$$

$$A_p = (\zeta_p - \zeta_{p-1})/s_p, \qquad \text{......(5)}$$

where t_p is the axial distance from the pth to the $(p+1)$th surface. Thus $A = (1/r_s)\Delta(N\cos I)$ where r_s is the sagittal radius of curvature of the surface and I is the angle of incidence.

The process of iteration consists in tracing a ray through the system by means of eqns. (2) to (5), using approximate values of z_p and ζ_p; if aberrations are to be determined these approximations are taken to be 0 and N_p respectively for the first iterative cycle, N_p being the refractive index of the medium following the pth surface; on completing the cycle, improved values $\underline{z}$ and $\underline{\zeta}$ are computed from the equations

$$\underline{z} = \frac{1}{2s}\left\{x^2+y^2+2\int_{s(0)}^{s(z)} z\,ds\right\}, \qquad \ldots\ldots(6)$$

$$\underline{\zeta} = \tfrac{1}{2}\{\zeta+(N^2-\xi^2-\eta^2)/\zeta\}, \qquad \ldots\ldots(7)$$

and the ray is again traced by means of eqns. (2) to (5), using new values of D and A computed from these improved values of z and ζ; this cycle is repeated until the successive values of the ray coordinates and direction cosines repeat to the required number of significant figures.

§ 2. THE CONDITION FOR CONVERGENCE

The convergence of the iterative process described in § 1 can be studied by subdividing it in the following manner. Suppose that the coordinates of a ray approaching a certain surface are known exactly; then an iterative process for determining the incidence point of the ray at this surface is provided by eqns. (3), (4) and (6); this will be called the transfer iteration. Similarly, given the incidence point exactly, eqns. (2), (5) and (7) provide an iterative process for the direction of the refracted ray; this will be called the refraction iteration. The process in which each iterative cycle is taken through the whole system will be called the complete iteration. Obviously convergence of the refraction and transfer iterations at every surface of the system is a necessary condition for convergence of the complete iteration; this condition is also sufficient, since a large enough number of complete iterative cycles will ensure convergence of the first transfer, then a further number ensure convergence of the first refraction and similarly for each surface in turn, so that eventually the whole process must converge. It is therefore sufficient to investigate the convergence of the individual refraction and transfer iterations only. This can be done by expressing the error in z or ζ at any given stage as a power series in the error at the preceding stage (Hartree 1948); the iteration is then said to be of the nth order if the coefficients of all terms of degree lower than n vanish; the iteration converges if it is of order 2 or higher, while if it is of order 1 it converges only if the coefficient of the linear term is less than unity in absolute value.

Considering first the transfer iteration, x, y, z are the required coordinates of the ray intersection and ξ, η, ζ are the modified direction cosines of the incident ray, supposed known exactly; let $z_{(n)}$ be the approximation to z obtained after n cycles of the transfer iteration and let $\delta_{(n)} = z - z_{(n)}$. Then from eqns. (3), (4) and (6) it follows that

$$\delta_{(n+1)} = \frac{\xi x+\eta y}{\zeta s}\,\delta_{(n)} + O(\delta_{(n)}^2). \qquad \ldots\ldots(8)$$

The coefficient of $\delta_{(n)}$ does not vanish unless either the projection of the ray on the meridian plane through the point of incidence or the surface normal is parallel to the axis, so that in general the transfer iteration is of order 1. Furthermore, if this coefficient is greater than unity the iteration will diverge.

For the refraction iteration, let ξ', η', ζ' be the required direction cosines of the refracted ray and let x, y, z be the coordinates of the point of incidence, supposed known exactly. Let $\zeta'_{(n)}$ be the nth approximation to ζ' and let $\epsilon_{(n)}=\zeta'-\zeta'_{(n)}$. Then from eqns. (2), (5) and (7) it follows that

$$\epsilon_{(n+1)}=\frac{\xi'x+\eta'y}{\zeta's}\,\epsilon_{(n)}+\mathrm{O}(\epsilon_{(n)}{}^2). \qquad \ldots\ldots(9)$$

Thus the refraction iteration is again in general of order 1, with the same exceptions as for the transfer iteration, and it also diverges if the coefficient of $\epsilon_{(n)}$ in eqn. (9) is greater than unity. It follows that the refraction and transfer iterations at a surface can simultaneously have second order convergence only if the surface normal is parallel to the axis.

The geometrical significance of the divergence conditions can be seen by putting them in the forms

$$\left|\frac{\xi x+\eta y}{\zeta\rho}\right|>\left|\frac{s}{\rho}\right|, \qquad \left|\frac{\xi' x+\eta' y}{\zeta'\rho}\right|>\left|\frac{s}{\rho}\right|, \qquad \ldots\ldots(10)$$

where $\rho^2=x^2+y^2$. Let α be the angle between the z-axis and the tangent plane to the surface at the point of incidence and let β and β' be the angles between the z-axis and the projections of the incident and refracted rays respectively on the meridian plane through the point of incidence; then $\tan\alpha=s/\rho$, $\tan\beta=(\xi x+\eta y)/\zeta\rho$ and $\tan\beta'=(\xi'x+\eta'y)/\zeta'\rho$ and the conditions for divergence become

$$|\beta|>|\alpha|, \quad |\beta'|>|\alpha|. \qquad \ldots\ldots(11)$$

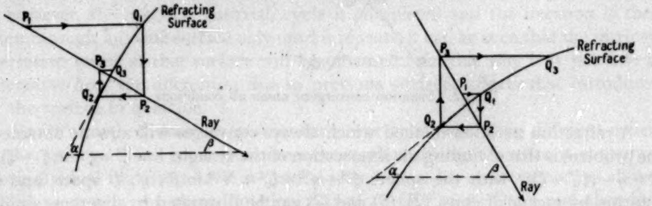

(*a*) (*b*)

Fig. 1. (*a*) Converging iteration.
(*b*) Diverging iteration.

Thus the complete iteration converges when the rays are only moderately inclined to the axis and the refracting surfaces are not very deep, but divergence can occur for systems of large numerical aperture. In fact it was in tracing a ray through a reflecting microscope objective of N.A. 0·7 that the divergence was first noticed.

The process of transfer iteration is illustrated in figs. 1 (*a*) and (*b*), which are projections on to the meridian plane containing the point of incidence; starting with a point P_1 on the incident ray obtained from eqn. (3), by means of eqn. (6) a point Q_1 on the refracting surface having the same x and y coordinates as P_1 is found, then by means of eqns. (4) and (3) a point P_2 on the ray having the same z coordinate as Q_1 is found; the process is then repeated; the angles α and β are indicated and the effect of their relative magnitudes is clear. The diagrams are not, of course, strictly correct since the application of eqn. (6) does not give a point lying exactly on the refracting surface, but the error is of the order of the square of PQ and it rapidly diminishes if the sequence converges.

§3. CONVERGENT TRANSFER AND REFRACTION ITERATIONS

Figure 1 suggests a mode of transfer iteration which would always converge; it is a three-dimensional generalization of the Newton–Raphson method of solving equations. Q_1 would be determined from P_1 as before and then P_2 would be taken as the intersection of the ray with the tangent plane to the surface at Q_1, as in fig. 2; it will be seen from what follows that this process has second order convergence under all conditions.

It follows from eqns. (3), (4) and (6) that to carry out this process eqns. (3) and (4) are used as before but eqn. (6) is replaced by the following for an improved value of z:

$$\underline{z}=\frac{z(\xi x+\eta y)-\tfrac{1}{2}\zeta\left(x^2+y^2+2\int_{s(0)}^{s(z)} z\,ds\right)}{\xi x+\eta y-\zeta s}. \qquad \ldots\ldots(12)$$

If the surface is a quadric of revolution of eccentricity e this becomes

$$\underline{z}=\frac{z(\xi x+\eta y)-\tfrac{1}{2}\zeta(x^2+y^2-(1-e^2)z^2)}{\xi x+\eta y-\zeta s}. \qquad \ldots\ldots(13)$$

When the convergence test of §2 is applied to eqns. (3), (4) and (12) it is found that $\delta_{(n+1)}=O(\delta_{(n)}{}^2)$ i.e. the iteration is of order 2 and therefore convergent under all conditions.

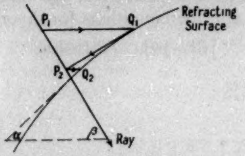

Fig. 2. Iteration convergent under all conditions.

A refraction iteration method which always converges will now be obtained; the problem is that of finding the intersection of the straight line $\xi'=\xi-x(\zeta'-\zeta)/s$, $\eta'=\eta-y(\zeta'-\zeta)/s$ with the sphere $\xi'^2+\eta'^2+\zeta'^2=N'^2$ in ξ', η', ζ' space, and its solution by means of eqns. (2), (5) and (7) can be illustrated by diagrams similar to those in fig. 1. By replacing the sphere by its tangent plane the following equation for an improved value of ζ' is obtained, in place of eqn. (7):

$$\underline{\zeta'}=\frac{\zeta'\{s(N'^2-\xi'^2-\eta'^2)-\zeta'(\xi'x+\eta'y)\}}{\tfrac{1}{2}s(\zeta'^2+N'^2-\xi'^2-\eta'^2)-\zeta'(\xi'x+\eta'y)}. \qquad \ldots\ldots(14)$$

Again it is found that $\epsilon_{(n+1)}=O(\epsilon_{(n)}{}^2)$ so that this refraction iteration is of order 2 and is convergent under all conditions.

The use of eqns. (12) and (14) in place of (6) and (7) respectively ensures that the complete iteration is always convergent.*

§4. THE SIGNIFICANCE OF THE SUCCESSIVE STAGES OF THE COMPLETE ITERATION

It is possible to interpret the successive stages of the complete iteration in terms of the relative magnitudes of the aberrations of different orders of the system. Let x stand for all of the coordinates x, y, ξ, η at all surfaces and let

---

* In all but the simplest iterative processes it is possible for the first approximation to be so poor that the iteration diverges, when according to Hartree's test it should converge, because of the effect of higher order terms in the error expansion, and it is then necessary to start again with a better approximation; in the present case the first approximation is a paraxial ray trace, so that this situation is not likely to occur.

$x_{(n)}$ be the value of x obtained after the nth cycle through eqns. (2) to (5); let z and $z_{(n)}$ be similarly defined for z and ζ and let $z'_{(n)}$ be the value of z corresponding exactly to $x_{(n)}$, i.e. $z'_{(n)}$ would be obtained as the final value if the individual refraction and transfer iterations were carried to completion from ray coordinates $x_{(n)}$.

Since the first cycle is a paraxial trace $x_{(1)}=x+\mathrm{O}(x^3)$, $z_{(1)}=z+\mathrm{O}(x^2)$; but $z'_{(1)}=z+\mathrm{O}(x^4)$ so that $z_{(1)}=z'_{(1)}+\mathrm{O}(x^2)$ and, since eqns. (12) and (14) give second order iteration, $z_{(2)}=z'_{(1)}+\mathrm{O}(x^4)=z+\mathrm{O}(x^4)$; thus from eqns. (2) and (3) $x_{(2)}=x+\mathrm{O}(x^5)$. In the same way it can be shown that $x_{(3)}=x+\mathrm{O}(x^7)$ and generally $x_{(n)}=x+\mathrm{O}(x^{2n+1})$.

Thus at each cycle terms of increasing order are taken into account and the terms $x_{(2)}-x_{(1)}$, $x_{(3)}-x_{(2)}$ etc. may be considered to represent the effects of primary, secondary, etc. aberrations. They will not of course give the power series aberration terms since a term of a given order may include a linear combination of higher order terms in the power series development; also it has still to be determined whether the same linear combination is involved for different rays.

The aberration of any order may be divided into two components, intrinsic and induced; the intrinsic aberration is produced by a surface in an aberration-free incident pencil, while the induced aberration is produced in addition to the intrinsic aberration when the incident pencil already contains aberrations of lower orders; terms corresponding to these are found in analytical aberration expressions. When the complete iterative method described here is used the successive cycles give the total of induced plus intrinsic aberration at each surface; if, however, the first, i.e. paraxial, cycle is completed and the iteration is then taken through any one surface only until it repeats, it can be seen that the intrinsic aberration terms at that surface will be obtained. In this way it is possible to determine how the aberration due to previous surfaces affects that introduced by the surface in question.

Smith's method does not possess the property of separating different orders of aberrations. This is obvious when the method diverges; when it converges the individual iterations have in general only first-order convergence, as shown in §2, so that in the above notation $z_{(2)}=z'_{(1)}+\mathrm{O}(x^2)=z+\mathrm{O}(x^2)$ and therefore $x_{(2)}=x+\mathrm{O}(x^3)$; in the same way it follows that $x_{(n)}=x+\mathrm{O}(x^3)$ so that groups of aberration terms cannot in general be obtained.

Finally it may be pointed out that if it is desired to use the method simply for tracing rays, without regard for the different orders of aberrations, the most rapid convergence will in general be obtained if the individual transfer and refraction iterations are carried to completion at each surface in turn, instead of making complete iterative cycles; in this case, as noted by Smith, it may be possible to start with better approximations to z and ζ, obtained, for example, from a graphical ray-trace or a trace through a slightly different system.

ACKNOWLEDGMENT

Thanks are due to Miss J. M. Drewitt, who noticed a case of divergence of Smith's computing scheme in the course of a ray-trace.

REFERENCES

Hartree, D. R., 1948, *Proc. Camb. Phil. Soc.*, **45**, 230.
Smith, T., 1945, *Proc. Phys. Soc.*, **57**, 286.

LETTERS TO THE EDITOR

The Conductivity and Hall Coefficient of Sintered Lead Sulphide

Numerous measurements have been made on semiconductors prepared as sintered blocks. There has been considerable discussion on the extent to which results obtained from these experiments and from experiments on thin films could be analysed using theory which is only strictly applicable to single crystals. Some workers have maintained that the resistances at the grain boundaries would dominate the characteristics of the specimens (Chasmar 1948, Miller 1951) and that it was doubtful whether Hall effect measurements could be interpreted reliably (Verwey 1951). Others have attempted to apply the single crystal theories to their results, assuming that the effect of the intergranular resistances was not significant (Ehrenberg and Hirsch 1951, Mitchell 1952).

This situation has arisen because very few semiconductors have been prepared as single crystals. We have recently been studying the properties of PbS single crystals and have now made some measurements on sintered specimens of PbS in an attempt to clarify the position. The specimens were prepared by compressing powdered PbS into blocks and sintering at 1100° K for several hours in an atmosphere of H_2S. The blocks had a density of about 80% that of a single crystal. Platinum wires 0·002 in. in diameter were welded to the blocks to make the electrical connections and the conductivity and Hall effect were measured from 77° K up to 800° K.

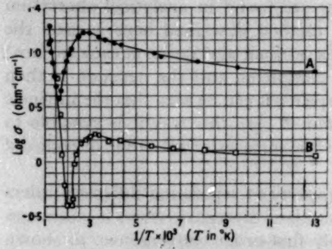

Figure 1. Sintered lead sulphide conductivity.

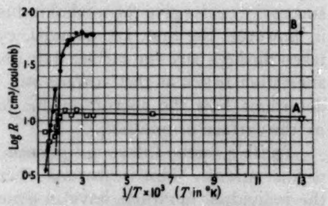

Figure 2. Sintered lead sulphide—Hall coefficient.

The results of the conductivity measurements are shown in fig. 1. On increasing the temperature from 77° K the conductivity starts to increase slowly. It reaches a maximum at a temperature which was near 300° K for the two samples measured; it then decreases as the temperature rises further until it passes through a minimum. At still higher temperatures the conductivity increases rapidly as the temperature is raised. The results of the Hall coefficient measurements are shown in fig. 2. At 77° K the Hall coefficient of both specimens was positive. The change with rise in temperature was very small until near the temperature at which the conductivity passed through its minimum. Near this temperature the Hall coefficient became negative, passed through a maximum and then decreased steadily as the temperature rose further.

On comparing these results with those previously obtained for single crystals it was found that the behaviour of the Hall coefficient is substantially the same as would be found in a single crystal of the same purity over the whole temperature range. This is also true of the conductivity at temperatures above that of its minimum, but at lower temperatures the behaviour of the conductivity is different from that found in single crystals. In single crystals at temperatures below the intrinsic range the concentration of electrons does not vary much with temperature and the conductivity increases as the temperature falls according to the relation $\sigma \propto T^{-5/2}$. In these sintered specimens it was found that this law is obeyed approximately between the temperature of the conductivity minimum and that of the maximum, although the value of σ was two to three times smaller than in a single crystal.

At lower temperatures σ fell as the temperature was reduced. Behaviour of this type has not been observed in single crystals. These results show that in these sintered specimens there is a source of electron scattering at low temperatures which increases in importance as the temperature falls and which does not occur in single crystals of the same purity. This does not appear to be a form of impurity scattering but seems most likely to be scattering at the grain boundaries. These results are not sufficiently detailed to enable the mechanism of the scattering to be deduced. Since it ceases to be very important above room temperature, it could be produced by Schottky barriers because the height of rectifying barriers in PbS is about 0·1–0·2 volt.

The high temperature conductivity data were used to calculate the gap between the full and conduction bands, assuming the $T^{-3/2}$ mobility law. The value obtained was 1·1 ev, which is in reasonable agreement with the value of 1·17 ev previously reported for Sardinian galena and single crystals (Putley 1952).

These results show that in a sintered specimen of PbS the conductivity can be affected by the inter-granular barriers at low temperatures while at higher temperatures the conductivity behaves in a similar way to that found in single crystals. The Hall effect, however, behaves over the whole temperature range in the way that it would in a single crystal of comparable purity. Thus conditions can be chosen in which either of the viewpoints mentioned in the opening paragraph can be valid, and it may therefore be very misleading to attempt to draw conclusions from resistance measurements alone. More reliable conclusions can be obtained by combining the resistance measurements with those of Hall effect. It is clear that when considering a particular material one cannot argue very far by analogy with the results obtained on other substances but that each case must be investigated fully. Unless this is done one cannot place too much reliance on analysis of the type presented by Ehrenberg and Hirsch and by Mitchell since their deductions were based on resistance measurements only. Our results show that in some circumstances the arguments they have presented are justifiable but that this cannot be demonstrated from their experimental results alone.

We wish to thank Mr. W. D. Lawson for preparing the sintered specimens used for these measurements and the Chief Scientist, Ministry of Supply, for permission to publish this letter.

Telecommunications Research Establishment,
Great Malvern, Worcs.
9th June 1952.

E. H. Putley.

Chasmar, R. P., 1948, *Nature, Lond.*, **161**, 281.
Ehrenberg, W., and Hirsch, J., 1951, *Proc. Phys. Soc.* B, **64**, 700.
Miller, P. H., 1951, *Semi-Conducting Materials*, ed. H. K. Henisch (London: Butterworths Scientific Publications), p. 172.
Mitchell, E. W. J., 1952, *Proc. Phys. Soc.* B, **65**, 154.
Putley, E. H., 1952, *Proc. Phys. Soc.* B, **65**, 388.
Verwey, E. J. W., 1951, *Semi-Conducting Materials*, ed. H. K. Henisch (London: Butterworths Scientific Publications), p. 151.

On the Distribution of Transistor Action

Since the first publication on Ge transistors (Bardeen and Brattain 1948) (with a brief reference to the occurrence of the effect in Si), it has been proved that PbS (Gebbie, Banbury and Hogarth 1950) and PbSe (Hogarth 1951) have the same properties. Filamentary transistors are made with Ge (Shockley, Pearson and Haynes 1949).

Work has been carried out in this laboratory on the distribution of the effect among semiconducting materials. On the assumption that diode action is a criterion for the injecting properties in question at metal point contacts, some 500 samples of 300 different solids have been tested for dynamic diode characteristics. A Westcrel Ge diode* and a specimen of high purity Ge† served as comparing standards. About 40 solids were

---

* Kindly lent by Dr. Mataré, French Westinghouse.
† Kindly lent by Dr. Billig, A.E.I., Aldermaston, Berks.

Preliminary Optimum Results for Gain of Transistors made from Ground Semiconductor Filaments with no Additional Surface Treatment. (*A* = cross section, *L* = filament length, *l* = emitter–base distance, min = mineral, tech. p. = technically pure.)

No.	Formula	Origin	Name	Type	Gain (times)	*A* (mm²)	*L* (mm)	*l* (mm)
PST III	$MnO_2.nH_2O$	Min.	Psilomelan	p	6·8	0·002	8·2	0·6
AGT I	Ag_2S	Min.	Argentite	n	5·0	0·010	5	1
SIT III	Si	Tech. p.	Silicon	p	3·4	0·008	4	0·3
SNT XI	SnO_2	Min.	Cassiterite	n	3·3	0·05	5	0·1
BIT III	Bi_2S_3	Min.	Bismuthinite	p	2·2	0·002	2·5	0·4
PTX III	PbS	Min.	Galena	p	1·6	0·018	4·5	0·3
GET II	Ge	Tech. h.p.	Germanium	n	1·5	0·012	5	0·6
CST VII	$CaSi_2$	Tech.		p	1·45	0·012	7	0·8
MST I	MoS_2	Min.	Molybdenite	n	1·4	0·009	2·5	0·2
ZOT V	ZnO	Min.	Zincite	n	1·4	0·012	7	0·2
FST III	FeS_2	Min.	Pyrite	n	1·25	0·012	7	0·2

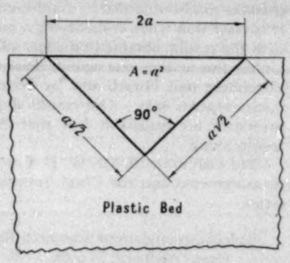

Fig. 1.

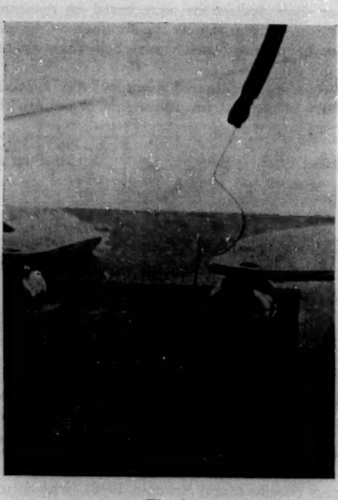

Fig. 2.

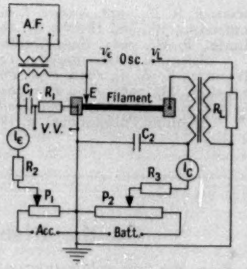

Fig. 3.

Fig. 1. The filamentary cross section is formed triangular-shaped in order to estimate the area with a measuring microscope.

Fig. 2. A mounted specimen.

Fig. 3. Principle of measurement. (A.F. = 3 500 c/s, $R_1 = 200\ \Omega$, $R_2 = 1\ k\Omega$, $R_3 = 10\ k\Omega$, R_L = load, $P_1 = 5\ k\Omega$, $P_2 = 2\ M\Omega$, C_1 and $C_2 = 4\ \mu F$, $V_{acc.} = 21$ v, $V_{batt.} = 120$ v, V.V. = Philips valve voltmeter, Osc. = DuMont Dual Beam Oscillograph Type 279.)

found likely to show transistor action. The table shows the best results of those tested so far for use as filamentary transistors.

The filaments are produced by successive imbedding in a transparent resin setting at room temperature and then grinding on silicon carbide paper in a stream of cold water. After three operations the filament cross section is triangular (fig. 1). No further surface treatment is applied to the specimens mentioned in the table.

After evaporating a thick layer of lead over the ends of the filaments, globules of a tin solder are placed on the lead layer, and the specimen is clamped in a manipulator (fig. 2).

From the measurements (fig. 3) the gain values in the table are calculated as the a.c. signal delivered to the load divided by the a.c. signal input between emitter and base. v_e and v_c are read peak to peak on the screen of a DuMont dual beam oscillograph and corrected according to the valve voltmeter indication. The oscillograph voltage calibrator is re-tested, and the error of measurements is estimated to be less than 5%.

The gain is sensitive to the difference between the two biasing currents I_c, I_e. On the samples showing gain at all, a sharp gain maximum occurred at a certain small value of I_c/I_e. This maximum increases as I_e and I_c are increased together, to an optimum for some samples and to an apparent saturation value for others. The measurements indicate further an optimum emitter–base distance.

The table shows some solids giving rise to transistor effects under similar treatment and measuring conditions. It is however not conclusive that the listed sequence is the correct one if each of the solids mentioned is given its specific proper surface treatment. The difference between GET II (the A.E.I. Ge specimen mentioned) and SIT III is thus rather striking. Bearing in mind the different behaviour of Ge and Si on elementary particle bombardment pointed out by Lark-Horovitz (Henisch 1951) and assuming (Slater 1951) that the mechanical grinding applied produce similar atomic displacements on the filament surfaces, it may seem probable that an n–p hook is created on the Ge surfaces (resulting in a short surface recombination time) and a resistive film on Si (giving the Si filament the appearance of an ' electron guide ').

The author would like to thank the authorities at this Technical University for friendly understanding and financial help, Professor B. Lunn and Dr. N. Engel for valuable suggestions and research facilities, the Geological Museum of Denmark and the Laboratory for Telephony and Telegraphy for mineral collections, the Norwegian Council for Technical and Scientific Research, Otto Møndsteds Fond for helpful advice and financial support and T.H.F. for instrument supplies.

The Technical University of Denmark,
Department of Metallurgy,
Copenhagen.
9th June 1952.

TOR H. TØNNESEN.

BARDEEN, J., and BRATTAIN, W. H., 1948, *Phys. Rev.*, **74**, 230.
GEBBIE, H. A., BANBURY, P. C., and HOGARTH, C. A., 1950, *Proc. Phys. Soc.* B, **63**, 371.
HENISCH, H. K. (ed.), 1951, *Semi-Conducting Materials* (London: Butterworths Scientific Publications).
HOGARTH, C. A., 1951, *Proc. Phys. Soc.* B, **64**, 822.
SHOCKLEY, W., PEARSON, G. L., and HAYNES, J. R., 1949, *Bell Syst. Tech. J.*, **28**, 345.
SLATER, J. C. 1951 *J. Appl. Phys.*, **22**, 237.

The Study of the Changes in Pressure Rise and Current in a Low-Frequency Discharge due to Irradiation

During the last ten years several papers have been published on the effect of irradiation with white light on an ozonizer discharge (Joshi effect). The ozonizer discharge is chiefly used to change the chemical composition of molecules and contains molecules in various metastable states. These metastable states could be dissociated by visible light. Such a dissociation would reasonably be expected to produce changes in the discharge current and the gas pressure. These changes have been studied.

The experimental arrangement used is similar to that used by Joshi and others (Joshi and Narasinhan 1940, Deshmukh 1947). The discharge current is determined by measuring the rectified potential drop across a non-inductive resistance (500 Ω) placed in series with the discharge tube. The ozonizer discharge tube is filled with hydrogen which is prepared by the electrolysis of barium hydroxide solution ($\frac{1}{15}$ N). The gas pressure is measured by a mercury manometer. The changes in gas pressure are measured by a differential oil manometer. A sudden rise *dp* in pressure (which is complete within about one second) on starting a discharge had been observed by Kunz (1922) and by Tyndall and Searle (1918). We have measured a similar sudden rise in pressure, with the tube both exposed and not exposed to the external radiation. We have also noted the corresponding discharge currents.

The light source employed to irradiate the discharge tube consists of three electric bulbs, of 200 watts each, fixed in a wooden box and placed at a distance of about 30 cm from the discharge tube. Such a source also produces changes of pressure due to its heat, but these changes are rather slow and become observable after about 15 seconds. As we have measured the sudden rise in pressure after one second we have neglected the heat effect of the source.

The rise in pressure and the discharge current were noted, in darkness and in light, at ten pressures of hydrogen (viz. 21, 28, 32, 37, 43·5, 50, 56, 63, 68 and 73 cm Hg) and for about ten voltages for every pressure. The results show a decrease in discharge current and an increase in pressure rise. The nature of the variation can be seen from the following values at a pressure of 21 cm Hg.

Applied potential (kv)	Discharge current (mA)		Pressure rise (microbars)	
	Dark	Light	Dark	Light
3·25	3·24	1·87	6	12
3·75	3·57	1·61	12	18
5·00	4·27	3·00	18	27
6·25	4·92	4·38	30	36
7·50	5·40	4·91	36	42
8·75	5·80	5·36	42	50
10·00	6·23	5·80	51	60

In a high pressure electrodeless discharge such as ours the discharge current is mainly due to the electrons, whereas the pressure changes are mainly due to the transfer of heat by 'ionic wind' (Tyndall and Searle 1918). Our observations, therefore, may be explained in terms of a decrease in the number of electrons and an increase in the number of ions. Such changes are probably due to the dissociation of metastable molecules (by external light) to which electrons attach to form negative ions. This suggestion is not incompatible with our knowledge of such processes in a discharge tube (Tüxen 1936, Geballe and Harrison 1951, Loeb 1952).

I am grateful to Professor K. R. Dixit for facilities and helpful discussions throughout the work.

Physics Department,
The Institute of Science, Bombay.
7th July 1952.

V. V. Agashe.

Deshmukh, G. S., 1947, *J. Indian Chem. Soc.*, **24**, 211.
Geballe, R., and Harrison, M. A., 1951, *Phys. Rev.*, **84**, 1072.
Joshi, S. S., and Narasinhan, V., 1940, *Curr. Sci.*, **9**, 536.
Kunz, J., 1922, *Phys. Rev.*, **19**, 165.
Loeb, L. B., 1952, *Phys. Rev.*, **86**, 256.
Tüxen, O., 1936, *Z. Phys.*, **103**, 463.
Tyndall, A. M., and Searle, N. S., 1918, *Phil. Mag.*, **35**, 261.

On the Nature of the Decay of a Meteor Trail

Two papers which have appeared recently on the subject of radio reflections from meteor trails (Kaiser and Closs 1952, Greenhow 1952) put forward the hypothesis that long duration echoes are associated with large cylinders containing electron densities greater than critical; the final decay of the echo is presumed to result from the drop in density occasioned by the normal diffusive expansion of the cylinder. Kaiser and Closs (1952) do not consider the effect of electron–ion recombination, and Greenhow (1952) gives a brief discussion of this effect using the theoretical value for radiative recombination (10^{-12} cm^3/sec) in place of the observed value for the E region (10^{-8} cm^3/sec), thereby disregarding what has been until recently one of the major enigmas in the photochemistry of the ionosphere. The discrepancy between theoretical and observed values appears to be resolved at the present time, however, as the result of an hypothesis by Bates (1950, see also Bates and Massey 1947) which has recently been confirmed by the experiments of Biondi and Holstein (1951). Specifically, Bates suggested the process of dissociative recombination, which could, under fairly general conditions, have easily as large a cross section as is observed. Recent experimental work using microwave cavity discharges has verified the fact that recombination does indeed involve molecular ions when the large cross sections are obtained. Since it is undoubtedly the ionization of molecules which gives rise to the free electrons in meteor trails, there does not appear to be any reason to expect recombination in these trails to be governed by other than the E region process, presumed to be of this type.

Using the figure of 10^{-8} cm^3/sec, and repeating the calculation given in § 3, ii (*d*) of the paper by Greenhow (1952), one finds that for the trail of line density 10^{15}/cm recombination alone would reduce the initial electron density to the critical value in about 8 seconds, as contrasted with the 100 seconds required by diffusion to effect a similar reduction. From this and similar calculations it is apparent that recombination would quickly reduce all high density electron concentrations to virtually the same order of magnitude, if diffusion alone were responsible for the trail expansion. This has been the central problem in accounting for the long duration echoes. It inspired the suggestion by the writer (1951) that a cylindrical shock wave might produce a sufficiently rapid expansion to disperse the high density electron trails before recombination became effective, thus maintaining initial electron content through the decay period. As pointed out, the final decay would then be governed by diffusion and turbulence. To explain the decrease below 2 of the exponent in the wavelength–duration power law one may note that while both diffusion and large scale turbulence give rise to a square law, small scale turbulence yields a signal independent of wavelength (Booker and Gordon 1950). The implications regarding the dispersal of the trail as time progresses are apparent.

The association by the writer (1951) of the observed amplitude fluctuations with the shock wave expansion was clearly meant to apply only to the first few seconds of the life of the trail, during which such a wave could exist. It is only during such a short period that the deep, cusp-like minima are generally observed. Nor would one expect this behaviour with short duration echoes, as Kaiser and Closs (1952) imply when they make the non-existence of these fluctuations a criterion, since it was pointed out that a critical meteor size should exist below which there is insufficient energy to give rise to a shock wave.

On this hypothesis the large-cylinder, metallic behaviour discussed by Kaiser and Closs (1952) and Greenhow (1952) would be expected only during the initial stage of the trail expansion, and this stage must be completed very rapidly if the destructive effects of recombination are to be avoided.

National Bureau of Standards,
Washington 25, D.C.
11th July 1952.

J. Feinstein.

Bates, D. R., 1950, *Phys. Rev.*, **77**, 718; **78**, 492.
Bates, D. R., and Massey, H. S. W., 1947, *Proc. Roy. Soc.* A, **192**, 1.
Biondi, M. A., and Holstein, T., 1951, *Phys. Rev.*, **82**, 962; **83**, 1078.
Booker, H. G., and Gordon, W. E., 1950, *Proc. Inst. Radio Engrs.*, **38**, 401.
Feinstein, J., 1951, *J. Geophys. Res.*, **56**, 37.
Greenhow, J. S., 1952, *Proc. Phys. Soc.* B, **65**, 169.
Kaiser, T. R., and Closs, R. L., 1952, *Phil. Mag.*, **43**, 1.

On the Thermal Properties of the Earth's Interior

Bullard (1950) and Elsasser (1950) have again pointed out the need for more reliable estimates of the thermal property of the Earth's interior. By combining the molecular theory of solids with known seismic data such estimates may be made.

Seismology shows that the mantle is solid and therefore the upper limit to the temperature at any depth is given by the melting point at that depth. Furthermore on the hypothesis of a cooling Earth, the temperature below approximately 700 km is given by the melting point (Jeffreys 1929). Lindemann (1910) has given an expression relating the melting point τ to the 'characteristic frequency'. This characteristic frequency appears in the various theories of the solid state and is thereby related to the velocities of longitudinal and transverse elastic waves.

Expressions may be derived giving the ratio of the melting point at any depth to the melting point at a depth of 100 km in terms of either the density and compressibility, or directly in terms of the velocities of longitudinal and transverse elastic waves. The melting point gradient is found to decrease with depth. Assuming certain reasonable values for the material of the mantle the melting point at a depth of 100 km is computed as $\tau_{100}=1730^\circ$K and at the core boundary $\tau_{2900}=5000^\circ$K. This latter value is one half Jeffrey's (1929) estimate which was obtained by extrapolation of laboratory data.

Verhoogen (1951) has estimated the ratio of the coefficient of volume expansion α to the specific heat at constant pressure c_p and has shown that both α/c_p and the adiabatic gradient decrease with depth. The above method of attack also yields these values and gives results in good agreement with those of Verhoogen. It also shows that Gruneisen's constant γ may be evaluated from Bullen's (1947) seismic data and that it decreases with depth in the mantle.

On the hypothesis of a cooling Earth, Adams (1924) has shown that, if the melting point gradient exceeded the adiabatic gradient, the mantle would have solidified from the inside out. With our data we find that the whole of the region between 1000 km and the core boundary may have solidified at about the same time.

The variation of c_p and the thermal conductivity may also be estimated. Bullard and Elsasser have examined the mechanisms by which convection currents may be maintained in the liquid layer of the core. When we evaluate γ for the core and use our estimate $\tau=5000^\circ$K at the boundary we find the adiabatic gradient in the core to be less than Bullard estimated by a factor of four. A result is that convection currents could be maintained by the heat generated in an inner core with radioactive content equivalent to that of iron meteorites. The conductive heat flow at the base of the mantle is approximately one quarter of that due to convection in the core. Of the models proposed by Bullard and Elsasser, the ' insulated core model ' is to be preferred.

Department of Physics,
University of Western Ontario,
London, Ontario.
26th June 1952.

R. J. Uffen.
A. D. Misener.

Adams, L. H., 1924, *J. Acad. Sci., Wash.*, **14**, No. 20.
Bullard, E. C., 1950, *Mon. Not. R. Astr. Soc., Geophys. Suppl.*, **6**, 36.
Bullen, K. E., 1947, *Theory of Seismology* (Cambridge : University Press).
Elsasser, W. M., 1950, *Trans. Amer. Geophys. Union*, **31**, No. 3.
Jeffreys, H., 1929, *The Earth*, 2nd edn. (Cambridge : University Press).
Lindemann, F. A., 1910, *Phys. Z.*, **11**, 609.
Verhoogen, J., 1951, *Trans. Amer. Geophys. Union*, **32**, No. 1.

CORRIGENDUM

The Influence of Mercury Vapour on Selenium Rectifiers and Selenium Photo-elements, by P. Selényi (*Proc. Phys. Soc.* B, 1952, **65**, 552).

After statement (iii) *insert*: (iii*a*) Neither the capacity nor its variation with the applied reverse voltage will be influenced by the treatment with mercury vapour.

REVIEWS OF BOOKS

The Student's Physics, Vol. III : Properties of Matter, by F. C. CHAMPION and N. DAVY. 2nd edn. Pp. xiv+328. (London and Glasgow: Blackie, 1952.) 27*s*. 6*d*.

The first edition of this well-known textbook was published 16 years ago at the price of 15*s*.; comparing the new edition with the old, one finds that the number of pages in the text has increased from 274 to 305 and the number of examples from 79 to 88.

The structure of the book remains unchanged and it has been brought more nearly up to date by additions such as: the accurate measurement of **g** by Clarke's method, the Boliden and Gulf gravimeters, the reflection method of seismic prospecting, Yarnold and Mason's method of determining the angle of contact, a brief description of the separation of isotopes by gaseous diffusion and a comparison of low-pressure manometers, modern methods of measuring osmotic pressure, Fürth and Zuber's method of measuring the diffusivity of a solute in a liquid, non-Newtonian liquids and more extensive treatment of the methods available for determining Planck's constant, using more accurate values of the fundamental constants.

The general impression is that the revision has not been as thorough as one would expect: for instance, only three or four titles have been added to the lists of references at the ends of the chapters in the new edition. At the same time, the reviewer feels that if a number of University teachers were asked what they would include or omit in a book of this size it is more than likely that each person would give a different answer. And it would be sad if this were not so, because one of the advantages of our system of University teaching is the opportunity it gives to teachers at the Honours stage to introduce their own special interests.

In the review of the first edition in this journal (*Proc. Phys. Soc.*, 1937, **49**, 201), H. R. R. summed up by saying that " the book is well and clearly written and illustrated"; this statement remains true, and the additional matter is given the careful and accurate treatment which was characteristic of the first edition.

R. M. D.

.B
5
2

The Surface Chemistry of Solids, by S. J. GREGG. Pp. ix+297. (London: Chapman and Hall, 1951.) 30*s*.

Dr. Gregg has written a very readable monograph on some of the more general aspects of the surface chemistry of solids. He deals firstly with the general characteristics of solid surface and the adsorption of gases and vapours thereon. A comparison is made between adsorption on solid surfaces and films on the surfaces of liquids, and an adequate treatment is given of the various more important adsorption isotherms which have been advanced. It is a pity that the author did not commence this portion of his treatise by making a clear distinction between chemi-sorption and physical adsorption since the subject matter of chemi-sorption is left until the last chapter, and the different types of adsorption isotherms for the two types of adsorption require definition.

This section of the book is followed by a discussion on the external surface of a solid and its effect on porosity, permeability and sedimentation volume. In the section on the adsorption of liquids by solids the author has given a very clear account of the conditions of spreading of liquids and of the mechanism of lubrication. A chapter is devoted to the determination of the specific surface and surface energy of a solid and, finally, one devoted to catalysis and chemi-sorption.

The book is very readable and contains a great deal of valuable information as well as some excellent photographs. It is well printed on excellent paper and singularly free from misprints.

ERIC K. RIDEAL.

Introduction to Theoretical and Experimental Optics, by J. VALASEK. Pp. 454. (New York: Wiley; London: Chapman and Hall, 1949.) 52*s*.

This book, which is the fruit of the author's thirty years' experience in teaching Optics in the University of Minnesota, is excellent and is to be strongly recommended to Honours students of Physics. In reading the Preface it should be remembered that the graduate student in an American University is occupied with material usually tackled by an English student in his final undergraduate year.

The book is very condensed, the theoretical section covering the whole of Optics with few omissions, and to a remarkable depth, within the compass of but 337 pages. The author is to be congratulated on the skilful way in which he has presented the essentials of most topics without too much sacrificing of detail or glossing over difficulties. The book adequately describes Geometrical optics, Gaussian theory and Lens aberrations. The convention of signs used would be classified under Group II of the Physical Society's *Report on the Teaching of Geometrical Optics*. This may be considered unfortunate since there seems to be in this country a tendency (good in the opinion of the reviewer) towards uniformity in adoption of the Cartesian convention classified in the Report as Group I, case (i).

Dispersive power ω is used in discussing chromatic aberration, instead of its more convenient reciprocal V, usually available from glass-makers' lists.

There is a good treatment of the theory of stops and an excellent discussion on the brightness of images. Interference, Diffraction and Polarization are well treated without being cumbered with detail. No doubt the author's avowed intention to avoid where possible conventional mathematical treatment has precluded him from developing the Kirchhoff diffraction equation, which, with a reference to Drude's *Theory of Optics*, is only quoted. The chapters on Dispersion and the Optics of metals are particularly well done, even within the narrow limits of space which the author has prescribed for himself. Surprisingly, there is, however, no mention of Tolansky's application of multiple beam interferometry to the examination of surface topography. In this connection it may be remarked that what in this country is usually referred to as a pair of Edser–Butler plates for producing channelled spectra appears under the heading of a Fabry–Perot etalon, a term which here is more usually restricted to the etalon with larger separation for high resolution spectroscopy.

It might be expected that the fourth section, dealing with experimental optics, would suffer more than the rest of the book from the effects of compression. Even here it seems that not much has been omitted that is vital to the experiments described, though, perhaps, use as a laboratory manual over an extended period of time would reveal deficiencies.

The book is so good and so well produced that it seems almost ungracious to make adverse criticisms, but the fact that these are few and relatively unimportant is itself a tribute.

There is a misleading diagram, fig. 4.7, on page 46; this correctly illustrates the simple astigmatic image of a star-shaped object described on the previous page, but, as the letterpress immediately above the diagram refers to the use of a test object consisting of concentric circles and radial lines commonly used for examining sagittal and tangential astigmatism, students unfamiliar with the axial symmetry of the aberration naturally inherent in a lens may be confused.

On page 95 the radius of curvature of a spectral line is given, without explanation that the formula quoted is in the simplified form applicable at minimum deviation.

The diagram on page 213, showing a section of the Nicol prism, either should have shown a side elevation or should have been accompanied by an end elevation in order to make it clear that the diagonal cut is from blunt vertex to blunt vertex; students are otherwise apt to confuse the Nicol prism with the Glan-Thompson, which in section only is deceptively similar.

A slip has occurred on page 249, where the units of resistivity (ohms. cms.) are incorrectly given as ohms/cms^2, and a corresponding error is made in the units of conductivity.

The book, like most American scientific publications, is well printed on first quality paper which does justice to the type, the diagrams and the half-tone blocks.

A. M. TAYLOR.

Ultrasonic Physics, by E. G. Richardson. Pp. x + 285. (Amsterdam : Elsevier; London : Cleaver-Hume, 1952.) 30*s*.

This is an opportune moment for the publication of a book on experimental ultrasonic physics. The fact that there have been two international conferences on ultrasonics in the last two years, at Rome in 1950 and at Brussels in 1951, is evidence of growing interest in the subject. On the other hand only two important review articles covering the previous decade can be cited (Richards 1939, Kittel 1946–47). Apart from these articles and a great mass of original papers, Dr. Vigoureux's excellent monograph (1950) and Professor Bergmann's comprehensive treatise (1949) have represented practically the whole extent of the literature.

In writing this new book Dr. Richardson has explicitly set out to deal with the experimental basis of the subject, perhaps taking the view that its theoretical side is not yet well enough established to deserve treatment at length. The practical aspect has been generously treated and many details are given, in particular of the hot-wire technique developed by the author. The numerical results of experiments are rather less fully quoted and, as a result, the overall picture of our present knowledge of propagation in solids, liquids and gases is not always quite as clear as it might be.

The first three chapters deal with sources, methods of detection and techniques of measurement. Ultrasonics owes its existence as a field of study to the thermionic valve, and every advance in electronics has widened its scope; it is a pity, therefore, that this side of the technique is not satisfactorily presented in chapter I. For example, the circuits of figs. 9 and 10 are greatly over-simplified and the relevant passage in the text does not suffice to elucidate them; the circuit of the magnetostriction oscillator shown in fig. 13 shows a direct short between the valve anode and cathode. Chapters II and III are perhaps the best in the book. The various physical effects encountered in ultrasonic measurements are simply and clearly described, and the errors that can be caused by diffraction effects are carefully pointed out. Chapters IV, V and VI describe experimental work on the propagation constants of gases, liquids and solids respectively. Besides pure liquids and mixtures of liquids, chapter V includes references to electrolytic solutions, shear waves in certain liquids and first and second sound in liquid helium. The author has done a useful service by tabulating in chapters IV and V the propagation constants of a variety of liquids and gases. The tables are, however, much condensed and the attenuation is given to single-figure accuracy only; the reader is referred to the original papers for fuller details. Copious references at the end of each chapter facilitate this. An indication could usefully have been given in these chapters of the numerical accuracy of the experimental methods and of the results quoted. The omission from chapter IV of the results of Leonard and of Fricke on dispersion and absorption in carbon dioxide is rather puzzling. Chapter VII gives a very brief account of the relaxation theory of the anomalous absorption and dispersion in gases and liquids, with which the author is evidently not fully in sympathy. A more detailed introduction to this theory will be found in Dr. Vigoureux's book and in Bergmann's *Ultraschall* and the two review articles already mentioned. The final chapter deals with a variety of topics such as propagation in aerosols and suspensions, effects on bubbles, the coagulation of emulsions, and the interaction of ultrasonic waves with liquid jets. Two errors should be pointed out : it is stated on p. 177 that the addition of a CH_3 group to the benzene molecule causes a large *in*crease in absorption; in fact, as is clear from the table on p. 206, it causes a large *de*crease. On p. 174 M. R. Rao is said to have shown for any liquid that the product vc^3 (v molecular volume, c velocity of sound) is independent of temperature, whereas he did, in fact, show $vc^{1/3}$ to be constant (this is not a simple misprint—other equations consistent with the constancy of vc^3 are quoted in the same passage).

The book is well produced and clearly printed in large widely spaced type : there is an index covering the text and the references.

In conclusion, the book is recommended to those whose main interest is in experimental ultrasonic methods.

J. M. M. P.

Bergmann, L., 1949, *Der Ultraschall* (Zürich : Hirzel Verlag, 5th edn.), p. 748.
Kittel, C., 1946–47, *Rep. Prog. Phys.*, **11**, 205 (London : Physical Society).
Richards, W. T., 1939, *Rev. Mod. Phys.*, **11**, 36.
Vigoureux, R., 1950, *Ultrasonics* (London : Chapman and Hall).

Optique physiologique, by Y. LE GRAND. Vol. I.: La dioptrique de l'oeil et sa correction. Pp. 372. 2nd edn. (Paris: Revue d'Optique, 1952). 1.600 fr.

A second edition of this scholarly volume is very welcome. No major changes appear to have been made from the edition reviewed in 1946 (*Proc. Phys. Soc.*, 1946, **58,** 624), but at certain points the material has been brought up to date and amplified. The author is an authority on physiological optics, and this book can be recommended as a sound text on the dioptric aspects of the subject.

W. D. WRIGHT.

Physics of Lubrication (Supplement No. 1 to the *British Journal of Applied Physics*) Pp. viii+96. (London: Institute of Physics, 1951.) 15*s.*

This book is a record of the proceedings of a joint symposium by the British Rheologists Club (now the British Society of Rheology) and the Institute of Physics, held at Manchester in July 1950. During recent years the general interest in friction and lubrication has greatly increased. A measure of this is seen by the fact that the papers submitted come from as many as eleven different British research laboratories. University, Government Establishment, Research Association and Private Industry are all represented. This is not surprising when one considers the many branches of physics and technology which are concerned in lubrication research. For instance among the diverse subjects in the eighteen papers are Investigations of surface damage using radioactive tracers, The lubrication of cotton and Lubrication by metallic soaps. Most papers have a full discussion which in many cases is both critical and constructive.

The papers have been grouped into two parts. Part one concerns Hydrodynamic lubrication and the Rheology of lubricants and part two is on the Boundary layer and Extreme pressure lubrication. The organizers have wisely included in each group a review article which adds perspective to the whole.

The contents of part one provide some interesting evidence to show that hydrodynamic lubrication cannot be described solely in terms of the geometry of the bearing, and the viscosity of the oil. Thus papers by E. W. J. Mardles and by S. M. Neale *et al.* describe rheological properties of oils which depend on the rate of shear and on the pressure. The way in which these vary for different oils and in different parts of the bearing must play an important part in a complete theory of hydrodynamic lubrication.

The papers in part two show that investigations into boundary lubrication have proceeded in two ways. Firstly, information has been sought about the structure and the mode of formation of the boundary films which prevent adhesion between the sliding surfaces. G. I. Finch reviews our present state of knowledge of the detailed structure of the layer and J. W. Menter describes experiments correlating changes in the structure of the oriented boundary layers as shown by electron diffraction, with changes in the coefficient of friction. F. T. Barwell and A. A. Milne, and K. V. Shooter have investigated metallic soaps and other long chain organic compounds and have compared their effectiveness as lubricants with their known surface active properties. A. C. Moore describes a radio tracer technique which detects with great sensitivity surface reactions between the lubricant and the substrate. Secondly, investigations have been carried out on the way the sliding surfaces are affected when the boundary film breaks down. E. Rabinowicz has used a radio tracer technique to measure the amount of metal transferred from one surface to the other, and G. I. Finch and R. T. Spurr describe the combinations of mechanical properties of surface film and underlying metal which will facilitate break-down of the film and welding of the sliding surfaces. C. Clayton and C. H. M. Jenkins show that, under conditions of poor lubrication, profound metallurgical changes may take place on steel surfaces after continual rubbing. Other papers in part two include a description of some possible solid lubricants by F. T. Barwell and A. A. Milne, the spreading behaviour and lubricating properties of mixed liquids by E. W. J. Mardles *et al.* and a discussion of the importance of the electrostatic component in the force of friction by R. Schurmann.

This book can be recommended for those who wish to have a concise account of the work in progress in most of the centres in Britain engaged in friction and lubrication research. Although many of the papers may be rather restricted in scope the whole gives a good general picture. Very complete name and subject indexes are included.

A. J. W. M.

Optical Crystallography, by ERNEST E. WAHLSTROM. Pp. vii+247. 2nd edn. (New York: John Wiley; London: Chapman and Hall, 1951.) 36*s*.

The student's approach to any subject must depend very greatly upon his general experience and equipment. This book, now appearing in its second edition, has been written by a successful teacher whose task it has apparently been to introduce the subject to a very varied range of students. As he remarks, the identification of crystals by optical means is important to chemists, engineers, biologists, medical men and many others in addition to the mineralogists and petrographers who were the pioneers in the field. He does not, however, deal at any great length with the actual procedure in identification since the bulk of the book is devoted to a painstaking discussion of the chief topics and theorems of the main subject.

Apart from the quotation of a few formulae, the treatment is generally non-mathematical, and one of the prominent features of the book is the great number of diagrams, with many clear clino-graphic projections of three-dimensional subjects, so that students possessing good visual imagination ought to find it easy to picture ray-velocity surfaces and the like with its aid. It is rather difficult, perhaps, for a physicist with a preference for a more analytical approach to assess the relative value of verbal and pictorial matter—though the question might be raised whether a student who had occasion to go as deeply into the subject as is suggested would not generally be better advised to acquire a little analytical geometry to help him on his way. He would then avoid the rather 'static' kind of image that even the best diagram may convey, for example in trying to explain the phenomena of the passage of monochromatic light through a crystal plate. The book will, then, probably find its readers mainly outside the ranks of physicists and applied mathematicians.

The text is clearly written, and the whole is most attractively produced. L. C. M.

Advanced Theory of Waveguides, by L. LEWIN. Pp. 192. (London: Iliffe, 1951.) 30*s*.

In this monograph we are given a selection of waveguide problems which, because of their mathematical complexity, have received but brief mention in books attempting a more comprehensive treatment. A number of excellent books on microwave theory have appeared during the past few years, and the reader is assumed to be familiar with the elements of the subject. Problems which present analytical difficulty are those concerned with obstacles in waveguides and discontinuities in cross section and which for the most part can only be solved by approximate methods, calling for advanced analytical techniques. The author is aware that the average microwave engineer will not have sufficient mathematical knowledge for an appreciation of the subject matter of the book, although for most practical purposes the physical concepts are clearly understood and a knowledge of the equivalent lumped impedance of the discontinuity is all that is required by the engineer. The emphasis is on mathematical method and not waveguide practice.

The first chapter presents in condensed form the equations of electromagnetic theory—Maxwell's equations, Hertzian vectors, curvilinear coordinates and field equations in rectangular waveguides. It is unfortunate that the author should adopt what he calls the c.g.s. practical system of units with magnetic fields in oersteds instead of m.k.s. units which have found increasing favour amongst microwave engineers.

For the greater part of the book the mathematical methods are similar but are applied to different problems. Chapters 2, 3 and 4 are concerned with inductive, capacitive and resonant cylindrical posts and diaphragms in waveguides; chapter 5 discusses steps, T-junctions and tapers; chapter 6 is devoted to the aperture impedance of an open-ended waveguide. The problem in each case is effectively to obtain the current distribution on the obstacle or the field distribution across a gap. For the cylindrical post the method adopted is to represent the current by a sum of multipoles and arrange their relative amplitudes to make the field vanish at the surface of the post. For the diaphragm the field distribution is obtained in the form of an integral equation. A great deal of mathematical ingenuity has gone into the solution of these problems and many useful analytical techniques are hidden amongst the complexities of the particular problem in which they are used. Indeed, an earlier chapter devoted to mathematical methods would have served to emphasize the more important theoretical points. Schwinger's variational technique, which is used extensively in later parts of the book, is one of the most powerful methods of modern analysis, but the treatment given on p. 79 is rather sketchy.

The problems discussed in the final chapter differ from those in the earlier parts of the book. Here we are concerned with continuously and periodically loaded waveguides. There is an interesting section on material loaded with small particles. Finally, an account is given of the theory of corrugated waveguides which have been used in recent years for the acceleration of electrons.

The author's style is cryptic at times and there is an impatience to proceed with the mathematical discussion; a brief qualitative discussion of the method to be pursued on each problem would have prepared the reader for the details of the analysis.

The book will appeal to those who are interested in the origin of many theoretical results given without proof in the *Waveguide Handbook*. The student of mathematical method will also find much to interest him. W. WALKINSHAW.

Diélectriques solides, by R. JOUAUST. Pp. 84. (Paris: Editions de la Revue d'Optique, 1949.) 500 fr.

This little book gives an elementary introduction to the physics of dielectrics. It is primarily written for engineers and does not presuppose any extensive knowledge of atomic physics. It starts with an introduction into the atomic and electronic structure of solids, which is followed by simple facts on polarization, conductivity and dielectric loss. Further chapters deal with the influence of surface layers, and with various types of dielectric breakdown. Naturally a book of this length can deal only superficially with such a large subject. Thus, for instance, only seven pages could be allowed for dielectric loss, and the author has not found it possible to go much beyond the phenomenological theories. In other chapters, too, the explanation of the various properties in terms of atomic structure is only indicated.

As a whole, I think, the book will be valuable by showing to electrical engineers the importance of modern physics for the understanding of dielectric phenomena. H. FRÖHLICH.

Elements of Optical Mineralogy: Part II—Description of Minerals (with special reference to their optical and microscopical characters), by A. N. WINCHELL in collaboration with H. WINCHELL. 4th edn. Pp. xvi + 551. (New York: John Wiley; London: Chapman and Hall, 1951.) $12.50, 100*s*.

The third edition of this classic work was published in 1933. The new edition has 92 pages and 66 figures more than the previous edition. The contents page at once reveals the influence of studies of crystal structure in the classification of the minerals. The silicates especially have been divided into six groups according to the scheme largely based on X-ray studies. The new classification is much better than the old, though it seems somewhat doubtful whether the subdivision of some of the groups is really helpful. The dimensions of the unit cell and the space group are given.

The introductory chapter on drawings, projections and variation diagrams is valuable, and there is a good introduction to the silicates in which the main features of the atomic arrangement of the members in this group are described. The first two-fifths of the book is devoted to elements, halides, sulphides, oxides, carbonates, other mineral carbon compounds, borates, sulphates and phosphates. The remaining three-fifths is devoted to the silicates.

So great a wealth of information is contained in these pages that this book is an essential reference work but, unfortunately, the reliability of the information is not as great as could be wished. The number of errors is unduly high (a list of 80 is given by D. Jerome Fisher in the *Journal of Geology*, 1951, **59**, 402). It is a great achievement to have completed the task of bringing out this fourth edition, but its value would have been greatly enhanced if more care had been exercised in the selection of data presented. In conclusion it should be said that the print is pleasant to read and the drawings are well drawn. W. A. WOOSTER.

Introduction to Electronic Circuits, by R. Feinberg. Pp. xiv + 163. (London: Longmans, Green, 1952.) 18*s*.

This book, which is based on a lecture and laboratory course given at the University of Manchester, deals with the general properties of electronic devices and basic circuits rather than with their radio applications. Although much must of necessity be omitted from a book of this size, the author deals with the properties of thermionic valves up to and including the hexode, magnetrons, cathode-ray tubes, photoelectric tubes, and valves of the cold-cathode, gas-filled and mercury-pool types. The circuit effects covered include rectification, amplification, feedback, frequency multiplication, intermodulation, sinusoidal and relaxation oscillation, electronic switching, current control and inversion. The mathematical knowledge required is not beyond that of Honours Physics or Engineering students, for whom the book is primarily intended.

It is well written and concise, giving one an impression that the author has adopted a policy of eliminating superfluous words in order to make the best use of the available printing space. This economy is made possible by the inclusion of simple, clear, well-captioned diagrams, depicting only what is essential to the understanding of the text ; there are nearly 130 of these in the 163 pages of the book. Further, at the end of each major section there is a list of other literature bearing on the section.

The value of the book does not lie merely in the information it imparts and its presentation, for, in addition, instructions are given for performing a series of electronic experiments relating to the subjects covered in preceding pages. Suitable valves and components are suggested for the experiments; numerical examples (with the answers) are also given. The student is thus encouraged to get the feel of the subject in much the same way as many people familiarized themselves with electronic devices and circuits by designing and constructing their own wireless sets in the days when radio sets were less complicated than they are now.

There is an unusual convention in the book. Instead of + and − signs to indicate the polarity of the terminals of a source of e.m.f., the author uses an arrow to indicate in which direction a current would flow in a hypothetical circuit joining the terminals ; this arrow therefore points the opposite way to the direction of current flow *through* the source. The same kind of arrow is also used to indicate actual current flow in other parts of the circuit. It would have been more helpful to the reader if, say, a tailed arrow had been used for one purpose and a plain one for the other; the reader can, of course, easily modify one set of arrows if he desires. A student using the author's convention might lose marks in an examination if the examiner had not had the convention explained to him.

The book will be appreciated not only by students, but also by those who have often felt the need for a simple refresher course on electronics. C. E. W-W.

Industrial Magnetic Testing, by N. F. Astbury. Pp. 132. (London: The Institute of Physics, 1952.) 25*s*.

For some considerable time there has been a real need for an up-to-date account of the methods of magnetic testing which are in use in industrial laboratories. The bridges and permeameters there used are rarely encountered in university physics laboratories, although it is to be hoped that their behaviours would easily be understood by a properly trained physicist.

Professor Astbury obviously possesses considerable mathematical ability and pronounced critical faculty. He brings them to bear in discussing the basic concepts of magnetization phenomena such as induction, hysteresis loops and the various permeabilities which are in use. He deals in a most praiseworthy manner with the laws of closed and open circuits, and is at pains to examine exactly what is meant by energy loss per cycle in terms of measured fields and inductions.

The chapter on instruments, including galvanometer amplifiers, is very good and the reader ought not to be dissuaded from reading it by Professor Astbury's suggestion of ' over-analytical ' treatment. The discussion of permeability and hysteresis measurements is very thorough, although perhaps a few more words on the subject of magnetic reluctance might be helpful to some readers. The critical examination of the sources of error in magnetization measurements is particularly valuable and the reviewer noted many interesting points. For example, it comes as a shock to learn that in 1911 a critical comparison of various methods of testing gave differences in the apparent value of B which could be as high as 5% in the power induction range and as high as 20 or 30% in the low induction region, and that such a critical comparison has not been repeated since 1911.

Industrial laboratories have raised the measurement of power losses to a high pitch of efficiency, and the bridge methods in use seem to be about 100 times as sensitive as the best direct calorimetric methods. While Professor Astbury indicates in his preface that he does not think that technique and ' know-how ' can ever come from reading, his chapters on power loss measurements and on alternating current bridge and potentiometer measurements will certainly be found helpful by most readers, who will also find them worth reading more than once.

The chapter on permanent magnet testing might, it is suggested, be enlarged in a future edition. It is pleasing to note the inclusion of descriptions of nuclear resonance methods for the measurement of magnetic field intensity, and more than pleasing to associate oneself with the author's views on the use of m.k.s. units in magnetic measurements. The author and the Institute of Physics are to be congratulated on a very welcome publication.

L. F. BATES.

CONTENTS FOR SECTION A

PAGE

Prof. H. S. Green and Dr. H. Messel. On the Theory of the Angular and Lateral Spread of the Nucleon Component of the Cosmic Radiation 689

Dr. A. L. Hodson. The Altitude Variation of Penetrating Showers 702

Dr. G. J. Kynch. The Calculation of Scattering Amplitudes 708

Dr. K. J. Le Couteur. Statistical Fluctuations in Nuclear Evaporation . . . 718

Dr. B. H. Bransden. Deuteron Production in the Collision of High Energy Neutrons with Nuclei 738

Mr. D. M. Thomson, Mr. A. V. Cohen, Dr. A. P. French and Dr. G. W. Hutchinson. The Angular Distribution of Long-Range Alpha-Particles from the Bombardment of Boron-11 by Protons 745

Dr. R. Middleton and Dr. C. T. Tai. Angular Distributions of Particle Groups from Deuteron Bombardment of Neon 752

Letters to the Editor :

Prof. C. B. A. McCusker and Dr. D. D. Millar. Local Penetrating Showers from Water and Carbon 758

Dr. D. L. Livesey and Dr. C. L. Smith. Resonance Effects in the Photo-Disintegration of ^{16}O Nuclei into four α-Particles 758

Mr. G. S. Bogle, Mr. H. J. Duffus and Dr. H. E. D. Scovil. The Nuclear Electric Quadrupole Moment of Erbium 167 760

Mr. K. L. Aitken, Mr. D. J. Littler, Mr. E. E. Lockett and Mr. G. H. Palmer. Pile Neutron Absorption Cross Sections of Lead 206 and 207 . 761

Dr. J. H. Fremlin. Artificial Activity Induced in Carbon by Fast ^{3}He Ions . 762

Dr. J. R. Holt and Mr. T. N. Marsham. The Deuteron Stripping Reaction with Aluminium 763

Reviews of Books 765

Contents for Section B 769

Abstracts for Section B 770

ABSTRACTS FOR SECTION A

On the Theory of the Angular and Lateral Spread of the Nucleon Component of the Cosmic Radiation, by H. S. Green and H. Messel.

ABSTRACT. The three-dimensional development of the nucleon component of extensive air showers is investigated. A vectorial diffusion equation is derived for the phase-space distribution of the nucleons, and solved as far as required to determine the mean square angular deviation, and the mean square distance from the shower axis. Account is taken of the variation of density in the atmosphere, and numerical results are obtained for all altitudes. These are exhibited graphically. The lateral spread of the nucleon cascade in lead is also determined, and the results tabulated. A full discussion is given of the significance of the numerical values obtained.

The Altitude Variation of Penetrating Showers, by A. L. Hodson.

ABSTRACT. The altitude variations of local penetrating showers and of extensive penetrating showers have been studied between sea level and 33 500 ft.

The attenuation length in air of the radiation producing local penetrating showers is found to be (129 ± 2) g/cm^2. This value has been corrected for the effect of deviations of the radiation from vertical incidence on the apparatus. Local penetrating showers observed under a transition layer of lead 10 cm thick are about 750 times more frequent at 33 500 ft. and 500 times more frequent at 30 000 ft. than at sea level.

*The Calculation of Scattering Amplitudes**, by G. J. Kynch.

ABSTRACT. In two earlier papers a differential equation was given for the asymptotic phases required in the two-body scattering problem. The method implied a resolution of the wave function into eigenfunctions of the orbital or total angular momentum as the potential was central or non-central. This feature can be avoided and in this paper a integro-differential equation is given for the total scattering amplitude corresponding to a given incident wave. It can be applied to any scattering or ionization problem, single or multiple, where no particles are bound after scattering which were not bound before. The method is applicable to the Schrödinger or Dirac equations.

If used with time-dependent equations the usual time-dependent perturbation theory results, owing to the apparent necessity of adhering to a definite time distinction between initial and final states. The same is true for the quantized field equations in the Heisenberg representation.

Statistical Fluctuations in Nuclear Evaporation by K. J. Le Couteur.

ABSTRACT. Previous treatments of nuclear evaporation have dealt with average values, neglecting fluctuations. In the present paper the fluctuations are considered in detail. The distributions of the number of neutrons and of the total energy associated with evaporation stars of a given size and the size distribution of stars of given total energy, are evaluated explicitly.

Knowledge of the fluctuations is useful for interpretation of data concerning small stars, such as those produced by π-meson capture or by artificially accelerated particles. The fluctuations are not very important in the large stars and do not modify any of the results of the author's previous mean value calculations.

The analysis of the mean evaporation process has also been put into a simplified form, from which numerical results can easily be obtained. The method has been used to compare experimental data with various theoretical energy–temperature relationships ; the Fermi gas law previously used by the author seems to be the most satisfactory connection between the high-energy star data and the observed level density at low energies

---

* This paper forms a continuation of two papers entitled "The Two-Body Scattering Problem with Non-Central Forces" published in *Proc. Phys. Soc.*, 1952, pp. 83, 94.

Deuteron Production in the Collision of High Energy Neutrons with Nuclei, by B. H. BRANSDEN.

ABSTRACT. The production of deuterons in high-energy collisions of neutrons with nuclei has been explained in terms of a direct ' pick-up ' process by Chew and Goldberger and by Heidmann, the reaction being of the form nucleus A + neutron → nucleus B + deuteron. Here it is shown that an alternative reaction, in which the incident neutron interacts with a nucleon in the target nucleus, which in turn ' picks up ' a second nucleon to form a deuteron, is more important at incident energies greater than approximately 200 Mev (nucleus A + neutron → neutron + nucleus B + deuteron).

The total cross section for deuteron production is calculated numerically for energies of the incident neutron in the range 100–300 Mev and comparison is made with the results of the direct ' pick-up ' theory.

*The Angular Distribution of Long-Range Alpha Particles from the Bombardment of Boron-*11 *by Protons*, by D. M. THOMSON, A. V. COHEN, A. P. FRENCH and G. W. HUTCHINSON.

ABSTRACT. The angular distribution of alpha-particles of long range from the reaction $^{11}B(p, \alpha)^{8}Be$ has been studied over the range 130 to 280 kev proton energy. A strong anisotropy varying with energy is observed and can be explained in terms of an interference between states of opposite parity in ^{12}C. The theoretical analysis gives the result that the well-known 16·11 Mev level in ^{12}C formed by resonant capture of 162 kev protons in ^{11}B has spin 2 and even parity.

Angular Distributions of Particle Groups from Deuteron Bombardment of Neon, by R. MIDDLETON and C. T. TAI.

ABSTRACT. The angular distributions of nine proton groups, the elastically scattered deuteron group and an inelastically scattered deuteron group from the 8 Mev deuteron bombardment of neon have been investigated using the photographic plate technique. The absolute differential cross section for the production of the various groups have been calculated and the spins and parities of some of the states of the residual nucleus ^{21}Ne determined.

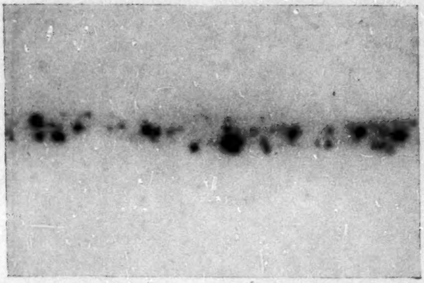

Fig. 1. Autoradiograph of fragments of silver transferred to polyvinyl chloride during sliding. One traversal of track. Fragments are distributed across width of track.

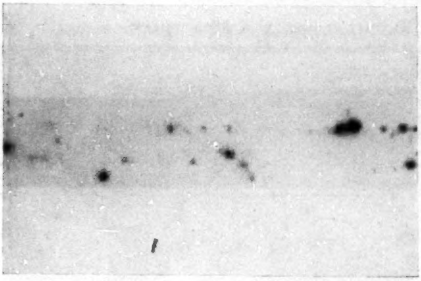

Fig. 2. Autoradiograph of fragments of silver transferred to polyethylene during sliding. One traversal of track. Fragments are concentrated along edges of track.

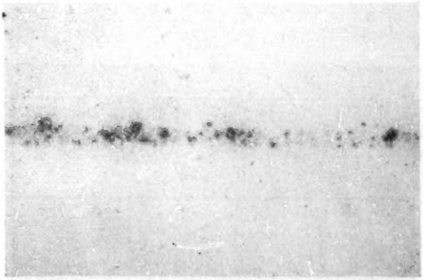

Fig. 3. Autoradiograph of fragments of copper transferred to steel during sliding. One traversal of track.

Fig. 3. Fragments of polyvinyl chloride left adhering to a steel plate after sliding, ×250.

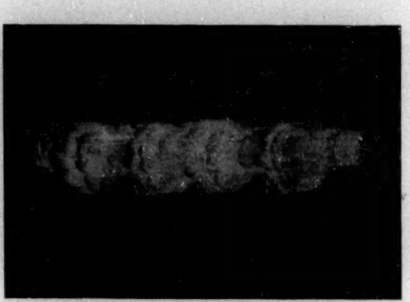

Fig. 4. The heavy surface damage caused by a polyvinyl chloride slider sliding on a block of the plastic, ×32.

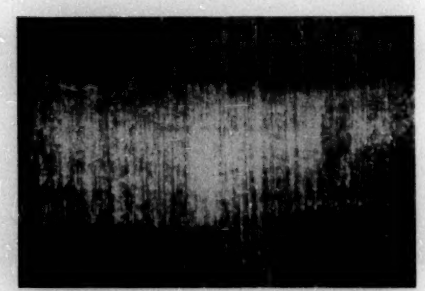

Fig. 5. Fragments of indium left on a block of polyethyleneterephthalate after sliding, ×25.

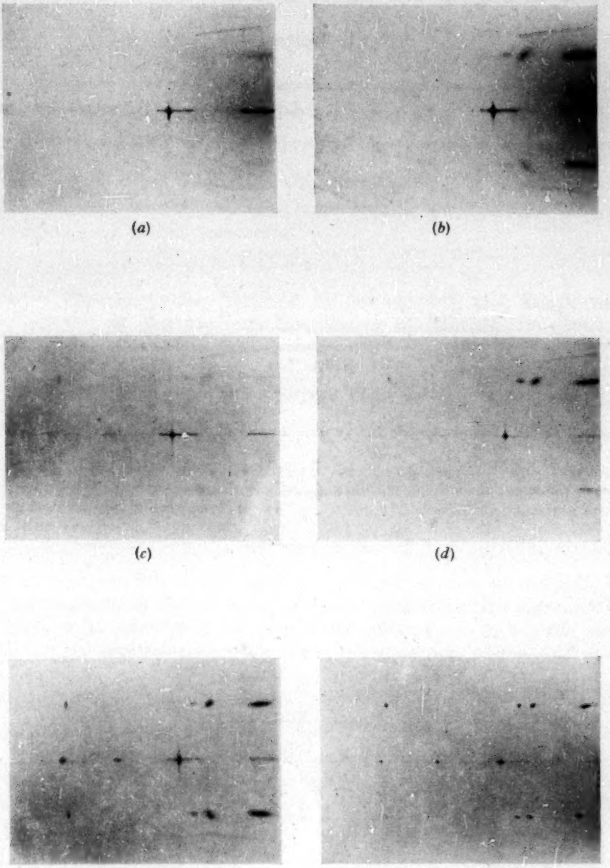

(*a*) (*b*)

(*c*) (*d*)

(*e*) (*f*)

Oscillation photographs of specimens (*a*) to (*d*), table 1. Filtered copper radiation.